AN ABSTRACT OF THE THESIS OF

Benjamin Americus for the degree of Master of Science in Microbiology presented on October 30, 2019.

Title: Investigation of Nematocyst Discharge in Parasitic Cnidarians (Myxozoa)

Abstract approved: _____

Stephen D. Atkinson

Myxozoans are an enigmatic group of obligately parasitic, microscopic cnidarians. They diverged from their free-living relatives over 600 million years ago and have highly reduced genomes. However, they have retained nematocyst stinging cells which characterize the phylum Cnidaria. Free-living cnidarians utilize this cellular weaponry for defense and predation whereas the myxozoans use it to anchor to their hosts as the first step to infection. In this thesis, I explore similarities and differences in the structure and function of nematocysts from myxozoans and free-living cnidarians via a "double-bladed" approach consisting of wet-lab techniques and bioinformatic analyses. In chapter 2, I report my results from two wet-lab assays that I developed to test the effect of chemical treatments on nematocyst discharge and infection, using the model myxozoan *Myxobolus cerebralis*. I found that Na^+ significantly increased discharge and reduced infection to rainbow trout. This finding aligned with prior work using free-living Cnidaria, suggesting divalent cations bound to poly-gamma glutamate inside the nematocyst can be exchanged with monovalent ions from the environment through the capsule wall to promote discharge. In Appendix A, I report my initial results from bioinformatic analyses of proteomic and transcriptomic datasets from the myxozoan *Ceratonova shasta*, in searches for genes for voltage-gated ion channels. In free-living Cnidarians, these channels play a role in signaling nematocyst discharge and exocytosis of Ca^{2+}. I found that in *C. shasta*, genes for these channels were co-expressed with nematocyst-specific genes during sporogenesis in the fish host. Taken together, the results of my wet-lab and computational "double-bladed" approach demonstrate structural and functional homologies between the nematocysts of myxozoans and their free-living cnidarian relatives.

Investigation of Nematocyst Discharge in Parasitic Cnidarians (Myxozoa)

by

Benjamin Americus

A THESIS

submitted to

Oregon State University

in partial fulfillment of
the requirements for the
degree of

Master of Science

Presented October 20, 2019
Commencement June 2020

Master of Science thesis of Benjamin Americus presented on October 30, 2019

APPROVED:

_____

Major Professor, representing Microbiology

_____

Head of the Department of Microbiology

_____

Dean of the Graduate School

I understand that my thesis will become part of the permanent collection of Oregon State University libraries. My signature below authorizes release of my thesis to any reader upon request.

_____

Benjamin Americus, Author

ACKNOWLEDGEMENTS

TABLE OF CONTENTS

TABLE OF CONTENTS (Continued)

LIST OF FIGURES

LIST OF FIGURES (Continued)

LIST OF FIGURES (Continued)

LIST OF FIGURES (Continued)

LIST OF TABLES

DEDICATION

This document is dedicated to Neil Durco, who loved wild salmon and science.

CHAPTER 1

INTRODUCTION

A comparison of the structure and function of cnidarian nematocysts in free-living species and myxozoan parasites

Benjamin Americus, Jerri L. Bartholomew, Tamar Lotan, Stephen D. Atkinson

INTRODUCTION TO FREE-LIVING AND PARASITIC CNIDARIA

Cnidaria is the phylum of animals that contains jellyfish, hydra, anemones, and corals. These organisms have life cycles that begin as asexual polyps and end as sexually reproducing medusae. The fossil record and molecular clock analyses suggest cnidarians branched from their sister taxa, the Bilateria, between 700 and 800 million years ago[1–3] and that much of the subsequent diversification within the phylum occurred 500 million years ago[4]. Cnidarians today retain the hallmarks of their ancient origins. They have simple body plans consisting of only two tissue layers (an endoderm and ectoderm), a single opening which serves as both a mouth and an anus, and predominantly radial symmetry[5]. All cnidarians contain nematocysts, which are specialized stinging cells that contain an evertible, needle-like tubule used for defense, predation, and adhesion[6]. The majority of known cnidarian species are free-living; however, relatively recently a previously ambiguous group of spore-forming parasites has been recognized as belonging in the Cnidaria: the Myxozoa[7].

Myxozoans are a diverse, species-rich group of obligate parasites which have complex life cycles requiring alternate vertebrate and invertebrate hosts, with transmission via microscopic waterborne spores[8]. Their cnidarian affinity is affirmed by their possession of nematocysts (historically called "polar capsules" in myxozoan research). Morphological[8,9] and molecular[10,11] evidence has shown that polar capsules are homologous to nematocysts from free-living Cnidaria. Within the Myxozoa are two primary groups that correlate with known invertebrate hosts: the Malacosporea, which infect bryozoans, and the Myxosporea, which infect annelids.

Most myxosporeans fit within three clades: those whose known invertebrate hosts are oligochaetes, a group with other annelid hosts, and the *Sphaerospora* sensu stricto clade with unknown invertebrate hosts[12,73,7]. While vertebrate hosts of myxosporeans include diverse taxa such as shrews[13], waterbirds[14], reptiles, and amphibians[15] these instances are exceptions that prove the rule, as the majority of Myxosporea have freshwater or marine teleost fish hosts[3,7].

Myxosporean replication within the hosts produces two morphologically distinct forms, actinospores that develop in the invertebrates (then infect fish), and myxospores that develop in the vertebrate host (then infect the invertebrate). Both life stages are microscopic and waterborne, typically 10–50 microns across[7]. And there is a great variety of morphological diversity both between conspecific actinospores and myxospores, and among congeneric or co-familial species[16]. Both spores consist of three cell types: valve cells, sporoplasm, and nematocytes (containing the nematocysts)[3,7].

Actinospores are usually tri-radially symmetric (Fig. 1.1) with valve cells that inflate osmotically after release from the invertebrate host[16]. These structures contribute to the near neutral buoyancy of this life stage, allowing interaction with the fish hosts in the water column. In contrast, myxospores are usually bilaterally symmetric, with more compact valve cells that do not typically inflate, meaning that the spores are negatively buoyant and thus sink and interact with their typically benthic invertebrate hosts. Unlike actinospores, which become inactive in normal environmental conditions in a matter of days[16,17], myxospores can remain viable for months, though not generally surviving freezing or desiccation[18,19].
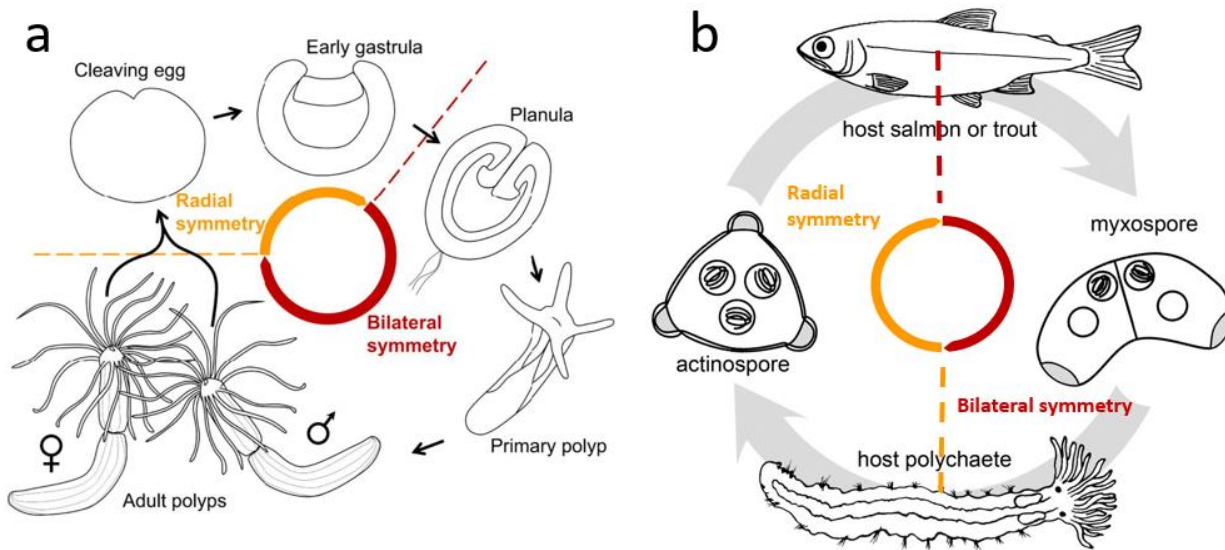
Figure 1.1. Paralogous lifecycles of a: the anemone *Nematostella vectensis*, and b: the myxozoan *Ceratonova shasta*. Both Cnidaria species share life cycles that encompass multiple morphologies and body symmetry. Modified from Dubuc et al. 2018[20].

In Myxozoa, the nematocytes ("capsulogenic cells") and their nematocysts ("polar capsules") lie proximal to the junction of the valve cells, often at one or both ends of the spore (Fig. 1.2). Most actinospore stages have three nematocysts, and most myxospore stages have two, each of which contains an evertable coiled tubule historically called a "polar filament." Electron microscopy [21] has clearly shown that "polar filaments" are not solid filamentous structures, but are hollow eversible tubules as found in free-living cnidarians, hence recent adoption of the term "polar tubule" [21]. Unlike their free-living relatives, myxozoans do not use their nematocysts for feeding or defense; instead they discharge tubules to anchor the spore to the host and facilitate infection.
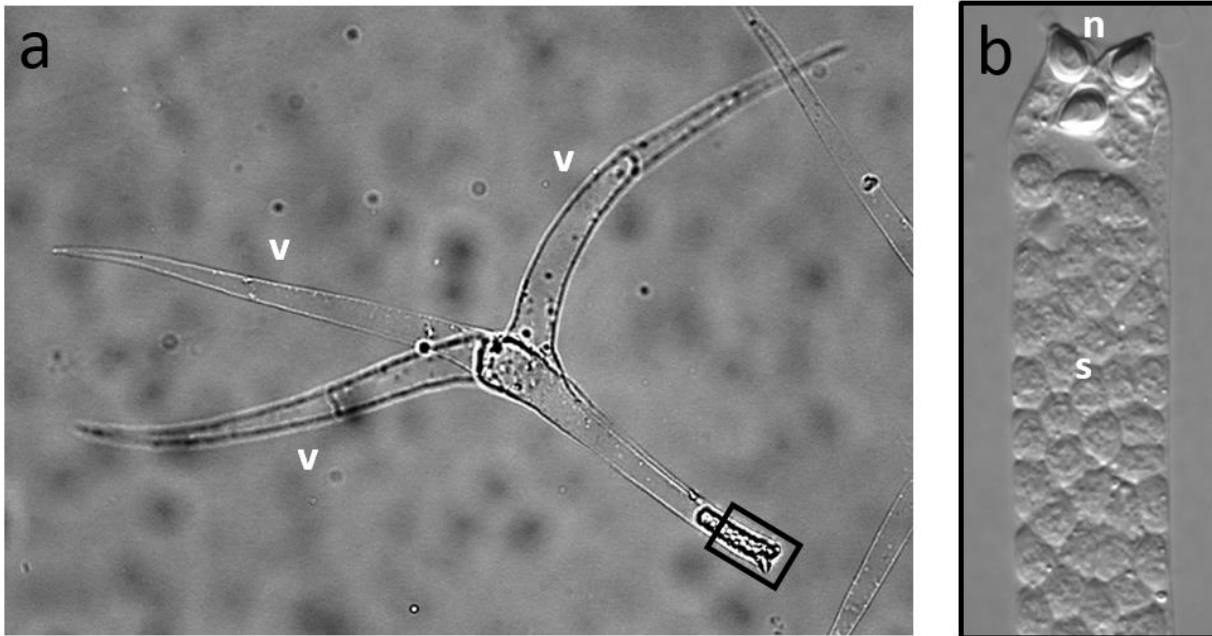
Figure 1.2. Morphological characteristics of myxozoan spores. Actinospores of *Myxobolus cerebralis*, used in this study, showing valve cells (v), sporoplasm and its many germ cells (s) and three nematocysts (n) at the spore apex. a: bright field; b: Nomarski interference contrast of region denoted by black rectangle in a.

MYXOZOAN DISEASE IN WILD AND AQUACULTURE FISHES

Infection of the invertebrate hosts are the least studied part of myxozoan life cycles, but from a few model species they are regarded as being sub-lethal, sometimes resulting in reduced fecundity[22,23] but increased growth[22,24]. These host effects would provide the parasite with increased substrate for proliferation and development into actinospores. Much more is known about myxozoan effects in their vertebrate hosts, where notable cases of species causing severe pathology and lethal infections has led to major concern about these parasites impacting wild and aquaculture fish stocks.

Myxozoan parasites represent a major threat to cultured and wild fish stocks, globally. Aquaculture, which includes the rearing of aquatic animals and marine plants, is the fastest growing sector of agriculture, expanding at a rate of 5.8% average annual global production by volume. In contrast, the production of capture fisheries, which target wild spawned fish, has

remained relatively stagnant since the 1980s as a result of stock depletion and a shift towards more sustainable management[25]. To keep pace with a human population expected to reach 8.5 billion by 2030, global aquaculture production needs to expand by 37% over this timeframe[25]. Currently, aquaculture growth is limited by pathogens and disease at levels that rival impacts to the terrestrial livestock sector[26]. Given the relative nascency of aquaculture as a global food provider, this may suggest major improvements in disease control are possible. Of all pathogens in aquaculture, losses from myxozoan parasites represent a major issue, particularly for finfish[27].

Increases in aquaculture production do not directly result in increases in epizootic events, particularly for diseases caused by myxozoans parasites, which cannot be horizontally transmitted between fish. However, the artificial movement of fish can result in lasting disease problems in native host of the same or closely-related fish species, particularly if the parasite of concern utilizes a widespread invertebrate host like *Tubifex tubifex*[28]. One noteworthy example of this is the spread of *Thelohanellus nikolskii* to native European carp (*Cyprinus carpio*) in Hungary, via the import of wild *C. carpio* from Asia[29]. Myxozoan diseases can also emerge when a new host is introduced to an existing system. For example, when gilthead sea bream (*Sparus auratus*) were moved from the Mediterranean to the Red Sea, outbreaks of the native myxozoan *Kudoa iwatai* occurred[30].

Widespread environmental changes brought about by a warming and more variable climate may also contribute to myxozoan disease outbreaks. Many freshwater systems are projected to experience eutrophication, which can promote proliferation of potential host oligochaetes. For example, in the St. Lawrence River, an increase in the abundance of the oligochaete *Limnodrilus hoffmeisteri* in response to eutrophication has been linked to an increase in the prevalence and diversity of myxozoan infections in spottail shiners (*Notropis hudsonius*)[31,32]. Similarly, warming and eutrophication have been correlated with outbreaks of proliferative kidney disease, which is caused by *Tetracapsuloides bryosalmonae*, which requires a bryozoan host[33]. This parasite is predicted to extend its range into northern latitudes as warming temperatures promote disease development in fish, and warmer and more eutrophic waters enhance bryozoan biomass, similar to annelids[33,34].

Among the most studied disease-causing myxozoans are *Myxobolus cerebralis* and *Ceratonova shasta*, both of which impact wild and cultured salmonid fish. Epizootic outbreaks of whirling disease caused by *M. cerebralis*, and myxozoan-induced enteronecrosis caused by *C. shasta*, have historically been tied to the effectors discussed above. Research efforts into these two organisms has resulted not only in discovery of their two-host life cycles, but their replication in laboratory mesocosm culturing systems. Together with a wealth of literature on the effects of the parasites in both their vertebrate and invertebrate hosts, these two species can be regarded as model myxozoans.

MYXOBOLUS CEREBRALIS

Myxobolus cerebralis was the first myxozoan to have its complete lifecycle described and be shown to require two alternate hosts[35] (Fig. 1.3). The 1984 work by Wolf and Markiw describing its life cycle was also the first to correctly identify myxospores and actinospores as two forms of a single organism rather than separate species.[35] The actinospore stage of *M. cerebralis* develops in the aquatic oligochaete *Tubifex tubifex*, which is found worldwide[36]. Within the gut epithelium of the worm, tri-radially symmetric actinospores, referred to as triactinomyxons or "TAMs" develop and are expelled into the water column with feces. TAMs are able to infect many species of salmonids including anadromous fish from genera *Oncorhynchus* and *Salmo*, and freshwater fishes from *Salvelinus*, *Prosopium*, *Thymallus*, and *Hucho*[37]. Upon contacting the fish host, the actinospores are activated, the nematocysts fire to anchor the spore to the host, and then the sporoplasm enters the fish via mucus excretory pores in the fins, gills, and skin[38]. Parasite stages then travel to the cranium and spine where they replicate to produce myxospores in the cartilage[39]. Parasite growth and destruction of the cartilage constricts the fish nervous tissue and results in the characteristic "whirling" behavior, skeletal deformities, a blackened tail, and death.

The pathogen likely originated in Eurasian brown trout (*Salmo trutta*) [40]. It was first described in rainbow trout (*Onchorhyhnchus mykiss*) transported to Europe from North America for aquaculture in the late 1800s. *Myxobolus cerebralis* was first detected in North America in 1956 in brook trout from Pennsylvania. Its introduction was either from infected fish used as feed or brown trout imported live from Europe. The parasite was likely introduced separately in Nevada,

where it has been present since at least 1957[41,42]. Since its introduction in Pennsylvania and Nevada, the range of *M. cerebralis* has expanded to include most of the western United States including Alaska[43], North Carolina[44], and Alberta in Canada[45]. This expansion was largely driven by the stocking of live infected rainbow trout[40].
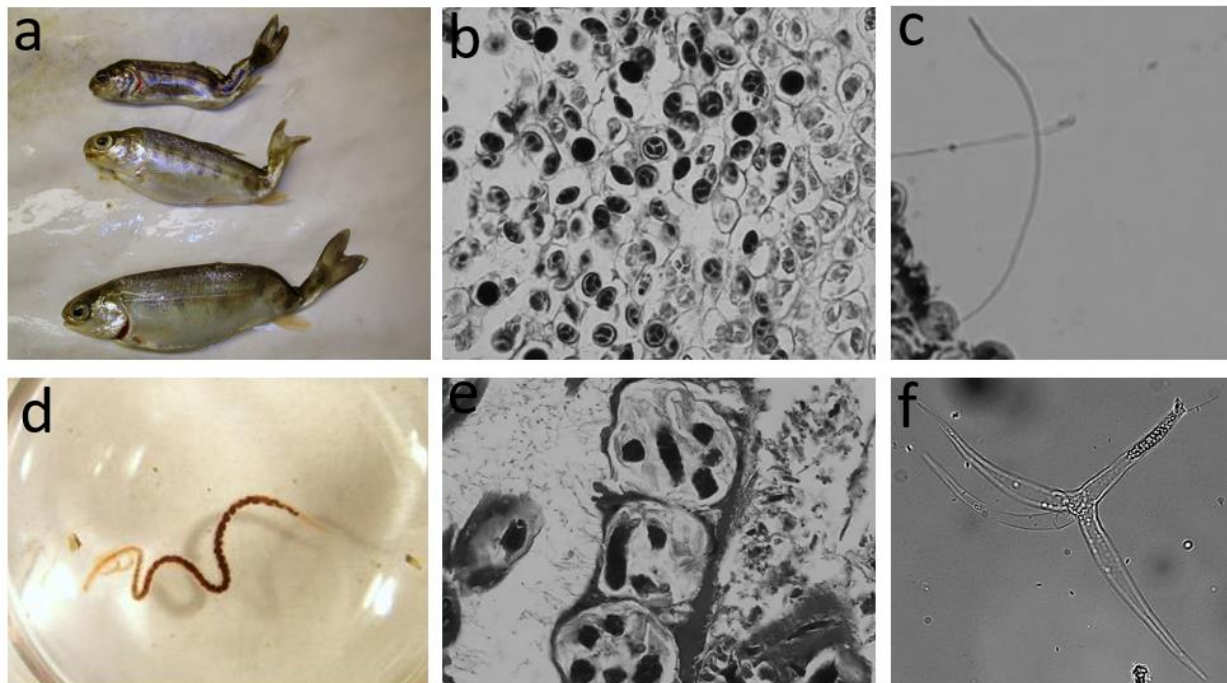
Figure 1.3. *Myxobolus cerebralis* in both of its hosts. a: infected rainbow trout showing characteristic skeletal deformity; b: histological section of myxospores (stained dark) in cartilage; c: mature myxospore (bottom left) with extruded polar tubule; d: infected *Tubifex* oligochaete; e: histological section of pansporocysts developing in the intestinal epithelium of the worm; f: mature actinospore.

CERATONOVA SHASTA

The two-host life cycle of *C. shasta* was first elucidated by Bartholomew et al. in 1997[46] (Fig. 1.4). The myxospore stage is ingested by the aquatic non-clitellate annelid *Manayunkia* sp., which probably filters myxospores from the water during normal feeding. Inside the worm, the spores fire their tubules, attach to the gut wall, then the sporoplasm penetrates the gut mucosa. The parasites migrate to the tegument where they proliferate to produce actinospores, which are

then released into the water column[47]. Actinospores invade the vertebrate host salmonid fishes through the gills and parasite stages migrate through the circulatory system to the gut[48]. The parasite proliferates in the gut tissue and causes swelling, hemorrhaging, and in the most severe cases, necrosis of the intestine[49]. In susceptible rainbow trout, a single infectious spore is capable of causing lethal infection[50].

Ceratonova shasta is native to the Pacific Northwest of North America[51–54]. It was first described in rainbow trout reared at the Crystal Lake Hatchery, California[55]. Today, the Klamath River Basin, 100 km north of Crystal Lake, is one of the areas most heavily affected by *C. shasta*. Despite extensive hatchery enhancement of Chinook and coho stocks, salmon populations have continued to decline in part due to *C. shasta*-related mortalities in returning adults and out-migrating juveniles[56,57]. Southern Oregon/Northern California Coast coho salmon (*Oncorhynchus kisutch*) are federally listed under the Endangered Species Act of 1973, and preservation of this stock has mandated strict flow regimes and monitoring efforts of *C. shasta* on the Klamath River[58]. These efforts have provided extensive, multi-year datasets of salmon and annelid host abundance, parasite density and distribution in the river system, and hydrological conditions by which to model the potential effects of climate change on myxozoan infections[59]. Most climate scenarios predicted by Global Circulation Models[60] are expected to result in increased infection severity of *C. shasta* in coho and Chinook salmon on the Klamath River, mostly due to reduced flow regimes, increase in annelid host abundance, and heavy actinospore production during springtime juvenile salmon migration[59].
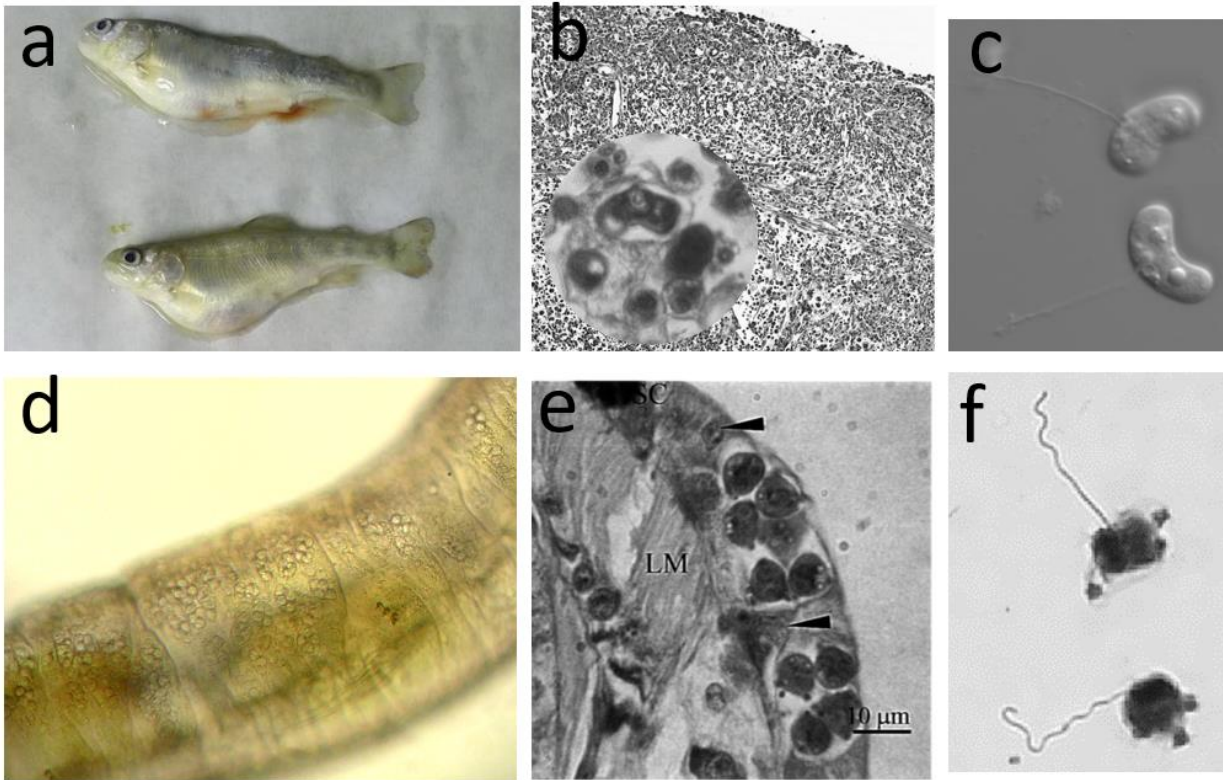
Figure 1.4. *Ceratonova shasta* in its vertebrate and invertebrate hosts: a heavily infected rainbow trout showing abdominal distention due to ascites production; b: histological section of H&E stained infected gut tissue with inset enlarged to show developing bean-shaped myxospore; c: mature myxospores, one with an everted tubule; d: *Manayunkia* annelid host showing spotty tegument characteristic of spore production; e: Giemsa stained histological sections showing developing packets of actinospores in tegument. "LM" indicates longitudinal musculature of the worm. "SC" worm secretory cells. Arrowheads point to host tissue displaced by the developing pansporocysts. Modified from Meaders & Hendrickson, 2009[47]; f: two mature actinospores with fired tubules, stained with DifQuik (RAL Diagnostics).

COMPARISON OF NEMATOCYSTS IN MYXOZOANS AND FREE-LIVING CNIDARIANS

NEMATOCYSTS AS INFECTION TOOLS

The structural affinities between the "polar capsules" of myxozoans and the nematocysts of free-living cnidarians led to early speculation that myxozoans were cnidarians rather than a unique phylum of protists[61]. The advent of DNA sequencing and phylogenetic analyses added strong

support for this hypothesis[39,62,63]. Over the last two decades, this shift in understanding has led to many works comparing the structure, function and more recently, molecular components of nematocysts in both parasitic and free-living Cnidaria[21,64,65].

Whereas in free-living Cnidaria, nematocyst discharge plays a central role in capturing, immobilizing and digesting prey, and deterring invaders[66], in myxozoans it is essential for infection. Yet little work has been done to elucidate the specific stages and chemical components of myxozoan nematocyst discharge in response to its target host; this was the core area of investigation of this thesis. Most of what is known about this process comes from observations of actinospores of a few species interacting with their fish hosts[67,48]. Less is known about interactions between myxospores and the invertebrate hosts, particularly in malacosporeans, which utilize a bryozoan as a definitive host rather than an annelid. Myxozoans probably utilize a multi-step process of sensing, activation, nematocyst discharge, and sporoplasm migration to infect their hosts[39,67].

When an actinospore receives a host-specific signal, either through mechanical or chemical cues[68] the coiled tubule within the nematocyst explosively everts, penetrates host tissue, and then contracts, pulling the myxozoan alongside its target [9] (Fig. 1.5). In *M. cerebralis*, tubules evert in less than 10 milliseconds[67].

Once the spore is anchored and alongside its host, the infectious sporoplasm actively migrates out through a split in the seam (suture) between the valve cells. It migrates between host epithelial cells using pseudopodia and suspected proteolytic activity[48,69]. Once the sporoplasm has migrated inside the host, the primary cell encompassing the infectious package degrades, releasing blood-stages[70,39]. In this thesis, I primarily investigated the first step in infection: nematocyst discharge.
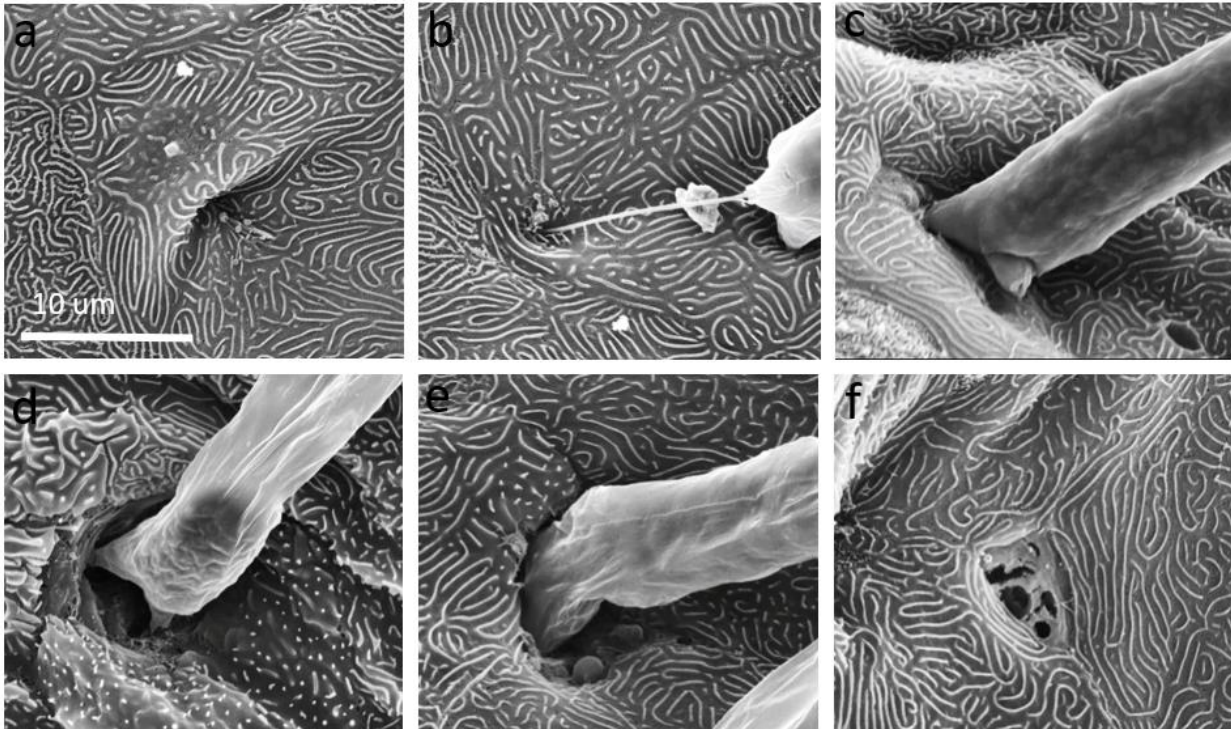
Figure 1.5. Composite set of scanning electron microscopy images detailing stepwise infection of juvenile mountain whitefish by *Myxobolus cerebralis* actinospores: a: normal mucus pore on the fish skin; b: discharged tubule anchoring the spore to the fish; c & d: contracted tubule has brought the spore apex into close contact; e: sporoplasm 'burrowing' into fish epithelium; f: damage to epithelium after passage of the parasite sporoplasm and detachment of the now-empty actinospore. Images courtesy of George Schisler of the Colorado Division of Parks and Wildlife.

NEMATOCYST "STOPPERS"

In free-living cnidarians, nematocysts are organelles within specialized cells called cnidocytes which contain an exterior sensory apparatus, the cnidocil (Fig. 1.6). Nematocysts contain coiled tubules and have a single opening, sometimes occluded by a "stopper". In medusazoan cnidarians, which are sister taxa to Myxozoa[65], nematocysts are capped with an operculum. Myxozoans contain analogous "stoppers" or plugs at the apex of the capsule[71] (Fig. 1.7). When discharge is initiated, the stopper releases or dissociates rapidly, which allows the tubule to evert and elongate[72]. An apparently similar stopper is visible in transmission electron microscopy (TEM) of developmental stages of *M. cerebralis* actinospores[73]. In mature, undischarged *M.*

cerebralis actinospores, this conical plug protrudes from lip-like, junctions of the valve cells[39,73]. However, the exact function and specific homology of the "stoppers" and apical parts of myxozoan nematocysts is poorly understood.
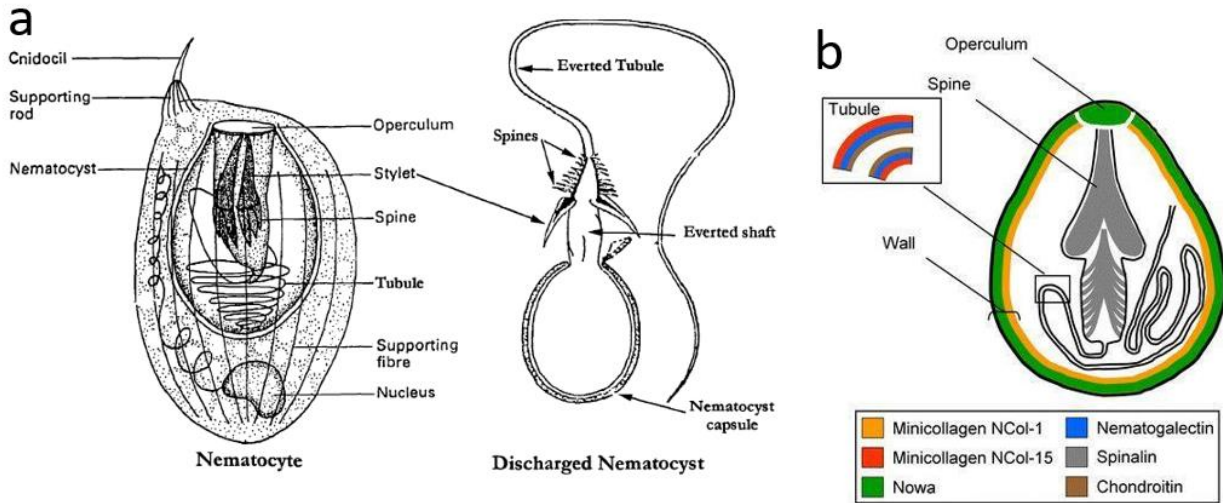
Figure 1.6. Nematocyst structures and morphological features; a: in many free-living Cnidaria. Modified from Cannon & Wagner, 2003.[9]; b: Molecular components of mature nematocysts in *Hydra*. Modified from Shpirer et al., 2014[11].
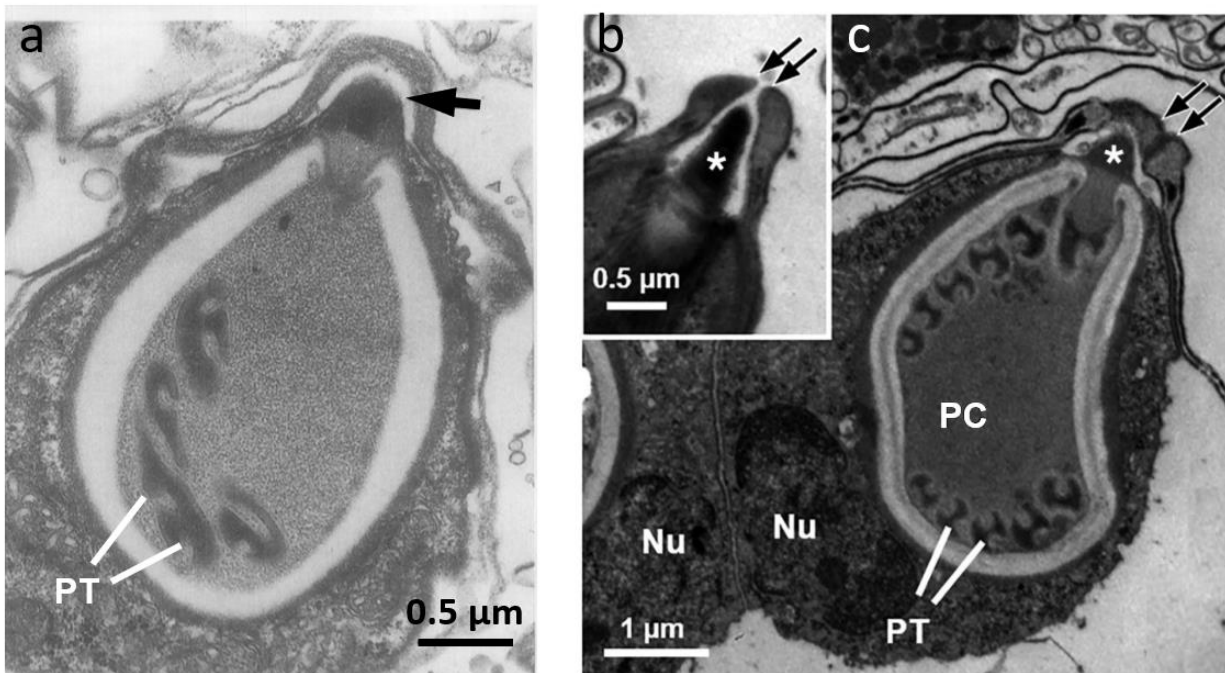
Figure 1.7. Sections detailing "stoppers" in developing myxozoan nematocysts. a: Transmission electron microscopy of a developing nematocyst in the actinospore stage of *Myxobolus cerebralis*. Arrow indicates "stopper" at the mouth of the capsule. "PT" indicates coiled polar tubules, referred to as simply "tubules" in this manuscript. Modified from El-Matbouli & Hoffmann, 1998[73]; b & c: Transmission electron microscopy of developing nematocyst in the actinospore stage of *Paramyxidium* sp. Arrows indicate suture line at the mouth of the capsule; "*" indicates a conical "stopper"; "PC" indicates myxozoan polar capsule, referred to as "nematocysts" in this manuscript; "Nu" indicate nuclei of capsulogenic cells; "PT" indicates coils of the polar tubule. Modified from Rocha et al., 2019[74].

NEMATOCYST PROTEINS AND CHEMISTRY

In free-living Cnidaria, the exterior walls of nematocysts contain two proteins unique to the organelle. (Fig. 1.6b) The outer layer consists of nematocyst outer wall antigen (NOWA) bound to minicollagens. Minicollagens, but not NOWAs, have been identified in molecular datasets of Myxozoa[11,64]. Nematocysts contain high concentrations of metal ions, including Mg^{2+} and Ca^{2+} and/or monovalent K^+ ions[75,76,77], and the anionic polymer poly-gamma glutamate, which likely stabilize each other to form a matrix[76]. Cnidaria are the only metazoans known to synthesize poly-gamma glutamate[76,77]. Nematocyst capsules, isolated from their membrane sheath, are permeable to molecules as large as 600Da, which suggests that cations can move freely in and out of the nematocyst while poly-gamma glutamate chains remain inside[78]. A prey/host signaling event may induce the rapid dissociation of metal cations from this matrix, increasing the osmotic pressure within the nematocysts, and driving tubule discharge. Experiments in manipulating the intracapsular ion contents found that those loaded with K^+ have greater intracapsular pressure[75] and discharge nearly 10 times faster than those loaded with Ca^{2+} [79]. A recent proteomic analysis of nematocysts isolated from *C. shasta* identified a suite of enzymes related to poly-gamma glutamate biosynthesis[64]. This finding, alongside the heavy staining observed when the cationic dye acridine orange is added to capsules, suggests the contents of myxozoan nematocysts may be similar to the nematocysts of their free-living relatives[64].

TUBULES

Cannon and Wagner (2003)[9] describe myxozoan tubules as morphologically similar to "atrichous isorhizae" in some free-living Cnidaria. Unlike holotrichous isorhizae, which have spines throughout, or basitrichous isorhizae with spines only at the base of the tubule, atrichous isorhizae are simple, spine-less tubules thought to be used exclusively for prey attachment. They secrete a sticky mucus which binds to prey rather than injecting venom[80]. It is hypothesized that myxozoan polar tubules, like those of atrichous isorhizae, do not penetrate deeply into host tissue or inject venom and are simply involved in the initial attachment to hosts[81].

Ben-David et al. (2016)[21] investigated the structure and discharge dynamics of polar tubules in myxospores from three myxozoans: *Myxobolus klamathellus*, *Myxobolus shantungensis*, and *M. cerebralis*. Scanning electron microscopy (SEM) of discharged tubules from *M. klamathellus* myxospores revealed double-helical symmetry, consistent with what has been observed in the nematocysts of free living-cnidarians[82], and a sealed tip, which has only been observed in myxozoans[71]. Scanning electron microscopy of *M. cerebralis* tubules show similar morphology (Fig. 1.8). Video of *M. klamathellus* and *M. shantungensis* myxospores loaded with toluidine blue dye show tubule eversion, contraction, and the release of capsule contents through lateral openings in the tubule. Dye-loaded *M. cerebralis* myxospores displayed eversion and contraction but did not release any capsule contents. Tubule contraction, and the discharge of capsule contents solely through lateral openings has not been observed in free-living cnidarians[78,78,83] and may represent unique adaptations for parasitism.
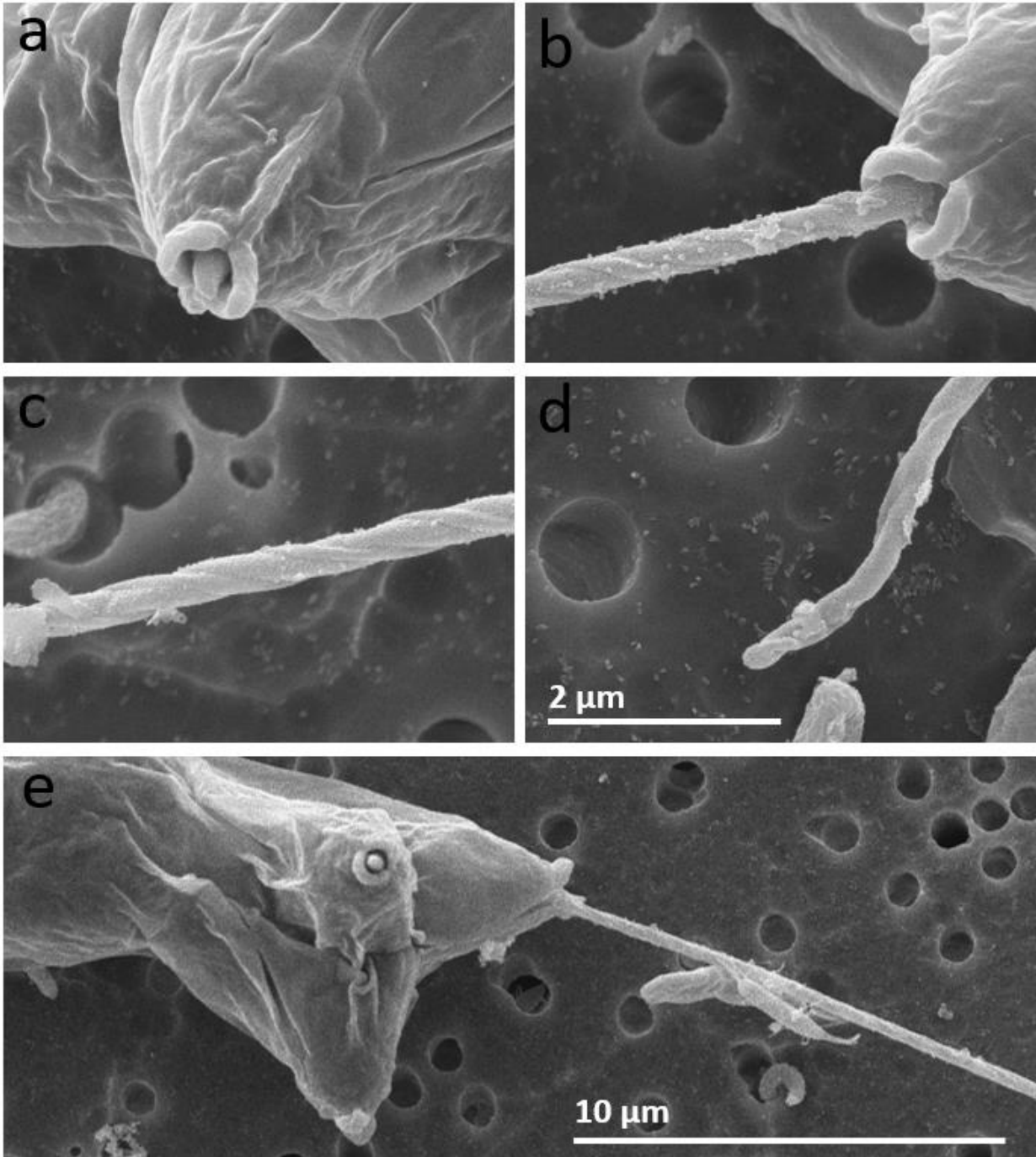
Figure 1.8. Scanning electron microscopy of *Myxobolus cerebralis* nematocysts; a: unfired nematocyst with a "stopper" or tubule tip at the opening; b-d: nematocysts with fired tubules showing helical structure and closed tip. a-d displayed at the same size scale. e: actinospore with a single fired nematocyst. See Appendix F for methods.

SOURCE OF TUBULE DISCHARGE ENERGY

Comparatively little is known about the forces driving nematocyst discharge in myxozoans. Over 100 years ago, Kudo (1918) observed tubule discharge from the now defunct clade Cnidosporidia which contained both Microsporidia and Myxozoa, and proposed "Osmotic pressure is considered in this case to be the cause of filament extrusion"[84]. Despite major taxonomic refinement, this hypothesis is still proposed for both clades[85,86,75].

The source of energy driving tubule discharge in free-living cnidarians has been widely discussed. Our current understanding suggests a combination of intrinsic forces, built into the coiled tubule during cnidogenesis[86,87,88] and intracapsular hydrostatic pressure generated through water entering the capsule to equilibrate an osmotic gradient[75]. Two hypotheses have been proposed to explain the source of this osmotic gradient, and both relate to cations binding to poly-gamma glutamate, a nematocyst-specific protein matrix (Fig. 1.9).

The first proposal suggests that when the discharge is signaled, water flows into the nematocyst and an internal matrix of cations bound to poly-gamma glutamate dissociates, resulting in a rapid increase in Donnan potential, exocytosis and discharge[78]. An alternative, though less accepted hypothesis to the Donnan-potentiated model was proposed by Berking, and Herrmann (2006)[89]. They suggest that nematocysts do not initially contain high concentrations of cations, and that capsule swelling and discharge is driven by an initial release of protons from the carboxyl groups poly-gamma glutamate. This neutralizes the initially acidic content of the capsule and results in electrostatic repulsion and intracapsular pressure. A subsequent influx of water and monovalent cations drives osmotic pressure and tubule discharge. It is possible that both mechanisms exist in nature but drive discharge in different organisms[89]. This increase in internal osmotic pressure may not account for all the driving force behind tubule elongation. When *Rhopilema nomadica* nematocysts were discharged in oil where no osmotic gradients can build up, elongation was orders of magnitude slower than in water. This suggests that in addition to being pushed by the osmotic potential within the nematocyst, tubules are pulled by osmotic potential that develops at their moving fronts[90].
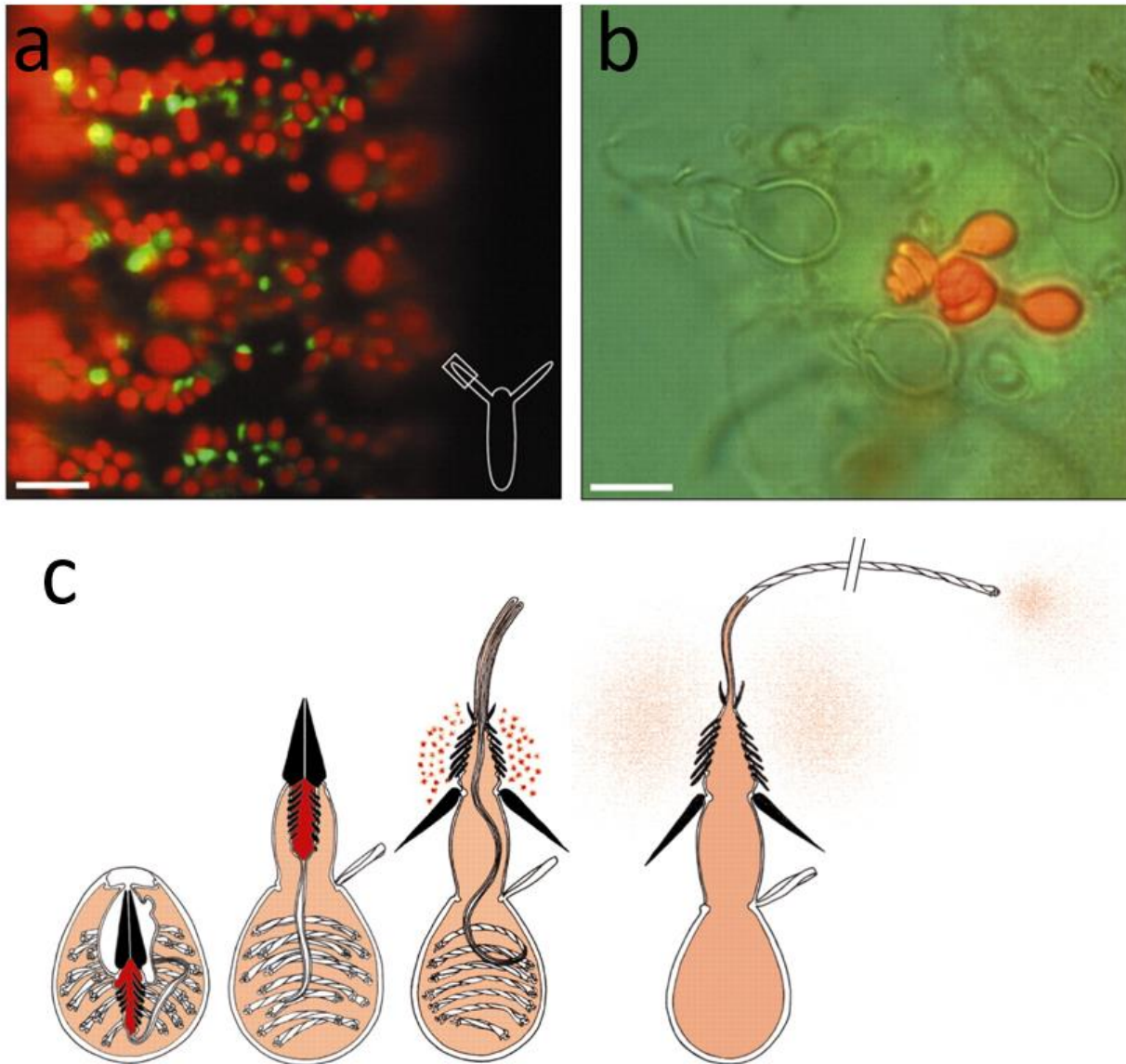
Figure 1.9. Dye staining of poly-gamma glutamate within *Hydra* nematocysts. a: Acridine orange (red) and DAPI (green) stained nematocysts in *Hydra vulgaris* tentacle; b: Acridine orange stained of stenoteles, isorhizas, and desmonemes-type nematocysts. Only the desmonemes are stained, presumably because they lack open-ended tubules. c: Discharge process of a stenotele-type nematocyst of *Hydra vulgaris*. Light red indicates poly-gamma glutamate in the capsule matrix, and dark red indicates of poly-gamma glutamate within the tubule. All figures modified from Szczepanek et al., 2002[77].

TESTING DISCHARGE HYPOTHESIS: EFFECT OF IONS

Studies have explored the effect of metal ions on promoting or inhibiting nematocyst discharge[9]. Early efforts explored the potential for salts to induce discharge in-situ[91,92]. Later works developed methods to study isolated nematocysts in the absence of host tissue[93] and explored the potential of ions to inhibit or promote discharge in response to artificial triggers[94]. These studies have *examined* different ions (anions and cations) and the roles they might play in nematocyst discharge[92].

ANIONS

In the jellyfish *Palagia noctiluca*, eight sodium salts were tested at the same osmolarity for their potential to induce nematocyst discharge[95]. Efficacy proceeded: sulfate > acetate > fluoride > chloride > bromide > nitrate > iodide > perchlorate > thiocyanate, following the Hofmeister series, with less soluble salts inducing more discharge. In *M. cerebralis*, KCl induced greater discharge than KI, and K_3PO_4 (which is even more soluble than KI) at the same concentration, suggesting this principle applies across multiple different cations and in Myxozoa[96].

MONOVALENT CATIONS

In many species of Cnidaria, the addition of potassium ions, and to a lesser extent sodium, to artificial seawater or native media induces nematocysts discharge[91,86,92,97]. Hidaka and Afuso (1993)[98] observed an increase in internal osmotic pressure and swelling in nematocysts bathed in NaCl and KCl and hypothesized that it was caused by an exchange of intracapsular divalent cations with monovalent cations in the environment. To maintain electroneutrality during this exchange, each divalent cation must be replaced with two monovalent cations, which increases the extracapsular pressure within the capsule. In *M. cerebralis*, the addition of K^+ ions via KCl induced nematocyst discharge[96].

DIVALENT CATIONS

The addition of divalent cations inhibits the response of nematocysts to physical and chemical cues, potentially through reducing osmotic gradients[9]. The addition of Ca^{2+} and Mg^{2+} to seawater

with *Aiptasia pallida* nematocysts did not induce discharge. Interestingly, these ions inhibited the discharge normally caused by increasing the concentration of monovalent salts[78,99]. This stabilizing effect of divalent cations has repeatedly been observed. Ca^{2+}, Mg^{2+}, and Ba^{2+} reduced discharge in *Pelagia noctiluca* exposed to iodide[95]. Ca^{2+} but not Mg^{2+} inhibited discharge in *P. noctiluca* exposed to trypsin[95]. The observation of this stabilizing effect, and the hypothesis that divalent cations can decrease the osmotic force necessary for discharge, led to the development of SafeSea, a sunscreen that contains Ca^{2+} and Mg^{2+} and inhibits jellyfish stings[100].

TRIVALENT CATIONS

Similarly, trivalent cations including Gadolinium (Gd^{3+}) and Lanthanum (La^{3+}) inhibit nematocyst discharge, though the proposed mechanism is different than that of divalent cations[101,102]. In *P. noctiluca* stimulated to discharge with a gelatin probe and *Tubularia mesembryanthemum* signaled to stimulated with addition of K^+, the presence of Gd^{3+} and La^{3+} ions in solution reduced the proportion of discharge relative to the controls [101,102]. It was hypothesized that this observed effect was due to interference with ion channels necessary in the exocytosis of calcium. Later work revealed the ability of trivalent cations to interfere with ion transport through both low and high voltage-activated calcium channels via physical occlusion and electrical interference[103]. Voltage gated calcium channels have long been suspected to play a role in nematocyst discharge[104] and have recently been detected in highly specialized forms in nematocysts[105] (Fig. 1.10).
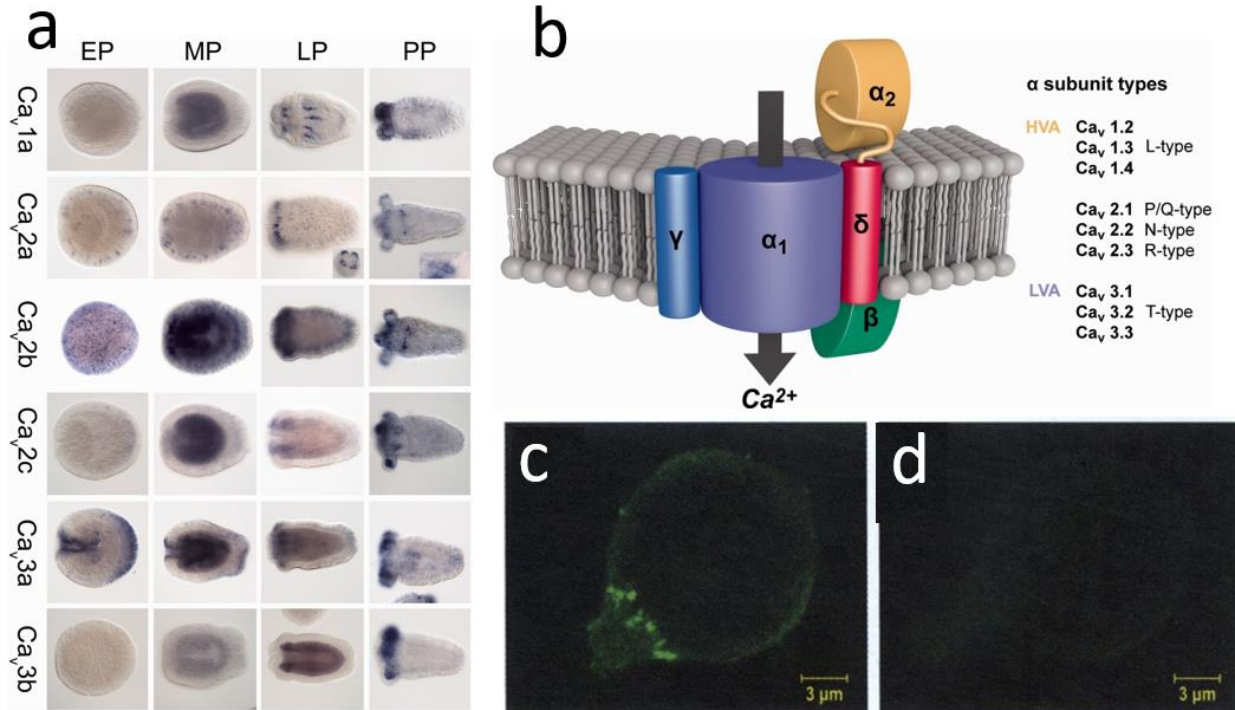
Figure 1.10. Immuno-staining of voltage-gated ion channel components within free-living cnidarian nematocysts. a: Spatiotemporal expression of voltage-gated calcium channel alpha subunits in *Nematostella vectensis*. Developmental stages are abbreviated: EP, early planula; MP, mid-planula; LP, late planula; PP, primary poly. Ca_v2a staining is localized to nematocysts. Modified from Moran & Zakon, 2014[106]; b: Diagram "of voltage-gated calcium channel components; LVA: low-voltage activated channels; HVA: high-voltage activated channels. Modified from Moran & Zakon, 2014[106]; c: Anti-voltage-gated calcium channel beta subunit immunostaining in nematocysts isolated from *Physalia physalis L.* jellyfish. Staining is localized around the mouth of the capsule. Modified from Bouchard & Anderson, 2014[107]; d: Pre-serum stained, negative control nematocysts. Modified from Bouchard & Anderson, 2014[107].

ANTIHISTAMINES

In anemones, a class of chemoreceptors has been identified that initiates nematocyst discharge when bound to amino and imino acids, and histamines[108]. Three antihistamines (diphenhydramine, tripelennamine, and cimetidine) block sensitization and amino acid-induced discharge. This effect was proportional to the concentration of the antihistamine antagonist, and

reversible, suggesting competitive inhibition of receptor sites. The effect of antihistamines on myxozoan nematocyst discharge has not yet been tested.

CHEMICAL AND PHYSICAL SIGNALS FOR DISCHARGE

In the nematocysts of free-living cnidarians, discharge is triggered by a multicellular pathway consisting of a complex of cnidocyte-supporting cell (CSC) and sensory cell/supporting cell (SCSC), neurons, and specialized sensory cells that respond to physical stimulation, light change, specific vibrational frequency or chemical cues[109,110,111]. The organization of this pathway and the specific chemical and vibrational signals vary between species[109]. Broadly, free-living cnidarians contain receptors for N-acetylated sugars, amino acids, or both[112,9,113]. Voltage measurements from inside nematocysts showed synaptically-driven spikes of action potential, which suggested that nematocysts act as individual sensory apparatus and as signal conduits to other nearby cells[115,116]. In animal cells, action potentials are driven by the opening and closing of voltage gated sodium and calcium channels. Recently, molecular approaches have detected components of both types of channels in nematocysts of free-living cnidarians[116,106,107]. It remains uncertain however, whether these proteins are involved in the exocytosis of calcium during discharge or in presynaptic, cell-to cell signaling, however the unsuccessful efforts to induce discharge with microelectrodes[117] or artificially induced action potentials[114] suggests the latter.

Much less is known about the signaling process of myxozoans. Yokoyama et al. (1995)[118] identified fish mucus homogenate as an effective discharge agent for *Myxobolus cultus*. Kallert et al. (2005)[119] further refined the technique, applying rainbow trout mucus to *M. cerebralis* and with an additional mechanostimulation step. The vibrational frequency applied did not significantly influence discharge. The authors compared mucus homogenates from rainbow trout and three non-hosts of *M. cerebralis* to test specificity of the discharge process: common bream (*Abramis brama*), common carp (*Cyprinus carpio*), and edible frog (*Rana esculenta*). Their findings demonstrated that even non-permissive-host mucus can activate myxozoan nematocyst discharge, but that mucus from rainbow trout, a well-established host, is most effective. To better resolve the specific chemical cue, rainbow trout mucus was sub-fractionated by High Performance Liquid Chromatography (HPLC)[120,68]. Fractions were identified by Nuclear

Magnetic Resonance (NMR) and were shown to include several amino and nucleic acids and their degradation products. The most abundant chemical fractions (tryptophan, adenosine, inosine, guanosine, and 2'-deoxyinosine) were tested in a series of in vitro nematocyst discharge assays with three *Myxobolus* spp. Inosine, an ATP-catabolite present in the mucus of live and freshly dead fish was most effective at inducing discharge[68,121].

In another experiment, *Henneguya nuesslini* actinospores were incubated in calcium-free water and exposed to carp and vibrational stimuli[67]. Spores in calcium-free water exhibited significantly less discharge than spores in water with calcium at the same osmolarity. Interestingly, *H. nuesslini* actinospores discharged to an even greater extent in calcium-free waters to which NaCl was added to restore osmolarity. These findings in myxozoans are consistent with the work in free-living cnidarians, and suggest the ionic composition, not only the charge difference of the external environments, can influence nematocyst discharge in all Cnidaria.

The ion-dependent discharge in *H. nuesslini* suggests the involvement of voltage gated calcium or sodium channels, although no voltage gated ion channel component has yet been described in Myxozoa[67]. However, septate junctions, which are the invertebrate equivalent of tight junctions and allow the exchange of ions and small molecules, have been observed by TEM in several myxozoans[122]. In developmental stages of *Myxidium gadi*, these junctions line the barriers between capsulogenic cells and between capsulogenic and sporoplasm cells[123]. It is possible that these regions contain the putative voltage gated ion channels used in nematocyst discharge and/or intracellular signaling.

SUMMARY

The Phylum Cnidaria includes free-living groups like jellyfish and anemones and obligate parasitic myxozoans and is characterized by its member species having nematocyst "stinging cells". Free-living cnidarians utilize this cellular weaponry for defense and predation[66] whereas the myxozoans use it to anchor to their hosts as the first step to infection. Despite these very different functions and the ~650 million years of divergence between free-living cnidarians and myxozoans[3], their nematocyst organelles have many morphological and molecular

commonalities. Both consist of a simple structure of a capsule with a single opening and a coiled tubule inside and are made up of unique nematocyst proteins nematogalectin and minicollagen[11]. Further, both likely contain an internal matrix of metal cations covalently bound to the anionic polymer poly-gamma glutamate[64]. The rapid dissociation of this matrix and the resulting increase in osmotic internal potential is the driving force behind tubule elongation during nematocyst discharge[78]. Our understanding of this mechanism is largely derived from decades of experimentation examining the role of external ions on nematocyst function, particularly from free-living Cnidaria, with little work done with Myxozoa.

RESEARCH QUESTIONS, OBJECTIVES AND HYPOTHESES

In this thesis project, I explored the similarities and differences in the structure and function of nematocysts from myxozoan and free-living cnidarians. I utilized two model myxozoans, *M. cerebralis* and *C. shasta*, which share the same fish hosts, and have known life cycles that are maintained at OSU. The availability of parasites under controlled conditions permitted me to examine and experiment with both organisms at different stages of their life cycles and use them for controlled exposure to susceptible fish. My investigations employed a "double-bladed" approach: First, with *M. cerebralis* I developed novel wet-lab assays to examine how myxozoan tubule discharge, sporoplasm migration, and infection was influenced by chloride salts of different valence and an antihistamine. Secondly, in *C. shasta*, I used bioinformatic methods to search for presence, absence, evolution, and expression of homologues of ion-interacting compounds known from nematocysts of free-living cnidarians. Given the similarities described above, I hypothesize that although overall nematocyst function is different between free-living and parasitic Cnidaria, the actual discharge process in Myxozoans will be homologous to that of free-living species. I hypothesize that given the different life requirements (parasitic rather than free-living), novel innovations have arisen in Myxozoa with respect to sporoplasm migration which is required for successful infection and reproduction.

REFERENCES

1. Van Iten, H., Muir, L. A., Botting, J. P., Zhang, Y. D. & Lin, J. P. Conulariids and Sphenothallus (Cnidaria, Medusozoa) from the Tonggao Formation (Lower Ordovician, China). *Bulletin of Geosciences* 713–722 (2013). doi:10.3140/bull.geosci.1400

2. Dohrmann, M. & Worheide, G. Novel Scenarios of Early Animal Evolution--Is It Time to Rewrite Textbooks? *Integrative and Comparative Biology* **53**, 503–511 (2013).

3. Holzer, A. S., Bartošová-Sojková, P., Born-Torrijos, A., Lövy, A., Hartigan, A., & Fiala, I. The joint evolution of the Myxozoa and their alternate hosts: A cnidarian recipe for success and vast biodiversity. *Mol. Ecol.* **27**, 1651–1666 (2018).

4. Cartwright, P. & Collins, A. Fossils and phylogenies: integrating multiple lines of evidence to investigate the origin of early major metazoan lineages. *Integr. Comp. Biol.* **47**, 744–751 (2007).

5. Technau, U. & Steele, R. E. Evolutionary crossroads in developmental biology: Cnidaria. *Development* **138**, 1447–1458 (2011).

6. Holstein, T. The morphogenesis of nematocytes in Hydra and Forsklia: An ultrastructural study. *Journal of Ultrastructure Research* **75**, 276–290 (1981).

7. Atkinson, S. D., Bartholomew, J. L. & Lotan, T. Myxozoans: Ancient metazoan parasites find a home in phylum Cnidaria. *Zoology* **129**, 66–68 (2018).

8. Kent, M. L., Andree, K. B., Bartholomew, J. L., El-Matbouli, M., Desser, S. S., Devlin, R. H., Feist ,S.W., Hedrick, R.P., Hoffmann R.W., Khattra, J, Hallett, S.L., Lester R. J., Longshaw, M., Palenzeula, O., Siddall, M.E. & Xiao, C. Recent advances in our knowledge of the Myxozoa. *J. Eukaryot. Microbiol.* **48**, 395–413 (2001).

9. Cannon, Q. & Wagner, E. Comparison of Discharge Mechanisms of Cnidarian Cnidae and Myxozoan Polar Capsules. *Reviews in Fisheries Science* **11**, 185–219 (2003).

10. Holland, J. W., Okamura, B., Hartikainen, H. & Secombes, C. J. A novel minicollagen gene links cnidarians and myxozoans. *Proc. Biol. Sci.* **278**, 546–553 (2011).

11. Shpirer, E., Chang, E. S., Diamant, A., Rubinstein, N., Cartwright, P., & Huchon, D. Diversity and evolution of myxozoan minicollagens and nematogalectins. *BMC Evol. Biol.* **14**, 205 (2014).

12. Fiala, I., Bartošová-Sojková, P. & Whipps, C. M. Classification and Phylogenetics of Myxozoa. *Myxozoan Evolution, Ecology and Development* 85–110 (2015). doi:10.1007/978-3-319-14753-6_5

13. Prunescu, C.-C., Prunescu, P., Pucek, Z. & Lom, J. The first finding of myxosporean development from plasmodia to spores in terrestrial mammals: *Soricimyxum fegati* gen. et sp. n. (Myxozoa) from *Sorex araneus* (Soricomorpha). *Folia Parasitol.* **54**, 159–164 (2007).

14. Bartholomew, J. L., Atkinson, S. D., Hallett, S. L., Lowenstine, L. J., Garner, M. M., Gardiner, C. H., Rideout, B. A., Keel M. K. & Brown, J. D. Myxozoan parasitism in waterfowl. *Int. J. Parasitol.* **38**, 1199–1207 (2008).

15. Hartigan, A., Fiala, I., Dyková, I., Rose, K., Phalen, D. N., & Šlapeta, J. New species of Myxosporea from frogs and resurrection of the genus Cystodiscus Lutz, 1889 for species with myxospores in gallbladders of amphibians. *Parasitology* **139**, 478–496 (2012).

16. Okamura, B., Gruhl, A. & Bartholomew, J. L. An Introduction to Myxozoan Evolution, Ecology and Development. *Myxozoan Evolution, Ecology and Development* 1–20 (2015). doi:10.1007/978-3-319-14753-6_1

17. Kallert, D. M. & El-Matbouli, M. Differences in viability and reactivity of actinospores of

three myxozoan species upon ageing. *Folia Parasitol.* **55**, 105–110 (2008).

18. Hedrick, R. P., McDowell, T. S., Mukkatira, K., MacConnell, E. & Petri, B. Effects of freezing, drying, ultraviolet irradiation, chlorine, and quaternary ammonium treatments on the infectivity of myxospores of *Myxobolus cerebralis* for *Tubifex tubifex*. *J. Aquat. Anim. Health* **20**, 116–125 (2008).

19. Barry Nehring, B., Schisler, G., Chiaramonte, L., Horton, A. & Poole, B. Assessment of the Long-Term Viability of the Myxospores of *Myxobolus cerebralis* as Determined by Production of the actinospores by *Tubifex tubifex*. *J. Aquat. Anim. Health* **27**, 50–56 (2015).

20. DuBuc, T. Q., Stephenson, T. B., Rock, A. Q. & Martindale, M. Q. Hox and Wnt pattern the primary body axis of an anthozoan cnidarian before gastrulation. *Nat. Commun.* **9**, 2007 (2018).

21. Ben-David, J., Atkinson, S. D., Pollak, Y., Yossifon, G., Shavit, U., Bartholomew, J. L., & Lotan, T. Myxozoan polar tubules display structural and functional variation. *Parasit. Vectors* **9**, 549 (2016).

22. Elwell, L. C. S., Steinbach Elwell, L. C., Kerans, B. L. & Zickovich, J. Host-parasite interactions and competition between tubificid species in a benthic community. *Freshwater Biology* **54**, 1616–1628 (2009).

23. Bartholomew, J. L., Atkinson, S. D. & Hallett, S. L. Involvement of *Manayunkia speciosa* (Annelida: Polychaeta: Sabellidae) in the life cycle of *Parvicapsula minibicornis*, a myxozoan parasite of Pacific salmon. *J. Parasitol.* **92**, 742–748 (2006).

24. Shirakashi, S. & El-Matbouli, M. Effect of cadmium on the susceptibility of *Tubifex tubifex* to *Myxobolus cerebralis* (Myxozoa), the causative agent of whirling disease. *Dis. Aquat. Organ.* **89**, 63–70 (2010).

25. Food and Agriculture Organization of the United Nations. *2018 The State of World Fisheries and Aquaculture: Meeting the sustainable development goals*. (Food & Agriculture Org., 2018).

26. Stentiford, G. D., Sritunyalucksana, K., Flegel, T. W., Williams, B. A. P., Withyachumnarnkul, B., Itsathitphaisarn, O., & Bass, D. New Paradigms to Help Solve the Global Aquaculture Disease Crisis. *PLoS Pathog.* **13**, e1006160 (2017).

27. Shinn, A. P., Pratoomyot, J., Bron, J. E., Paladini, G., Brooker, E. E., & Brooker, A. J. Economic costs of protistan and metazoan parasites to global mariculture. *Parasitology* **142**, 196–270 (2015).

28. Deedee Kathman, R., Brinkhurst, R. O. & Aquatic Resources Center (College Grove, Tenn.). *Guide to the Freshwater Oligochaetes of North America*. (1998).

29. Molnár, K. Differences between the European carp (*Cyprinus carpio carpio*) and the coloured carp (*Cyprinus carpio haematopterus*) in susceptibility to *Thelohanellus nikolskii* (Myxosporea) infection. *Acta Vet. Hung.* **50**, 51–57 (2002).

30. Diamant, A., Ucko, M., Paperna, I., Colorni, A. & Lipshitz, A. *Kudoa iwatai* (Myxosporea: Multivalvulida) in wild and cultured fish in the Red Sea: redescription and molecular phylogeny. *J. Parasitol.* **91**, 1175–1189 (2005).

31. Marcogliese, D. J. & Cone, D. K. Myxozoan Communities Parasitizing *Notropis hudsonius* (Cyprinidae) at Selected Localities on the St. Lawrence River, Quebec: Possible Effects of Urban Effluents. *The Journal of Parasitology* **87**, 951 (2001).

32. Marcogliese, D. J., Gendron, A. D. & Cone, D. K. Impact of municipal effluents and hydrological regime on myxozoan parasite communities of fish. *Int. J. Parasitol.* **39**, 1345–1351 (2009).

33. Carraro, L., Mari, L., Hartikainen, H., Strepparava, N., Wahli, T., Jokela, J., Gatto, M., Rinaldo, A., Bertuzzo, E. An epidemiological model for proliferative kidney disease in salmonid populations. *Parasit. Vectors* **9**, 487 (2016).

34. Carraro, L., Mari, L., Gatto, M., Rinaldo, A. & Bertuzzo, E. Spread of proliferative kidney disease in fish along stream networks: A spatial metacommunity framework. *Freshwater Biology* **63**, 114–127 (2018).

35. Wolf, K. & Markiw, M. E. Biology contravenes taxonomy in the myxozoa: new discoveries show alternation of invertebrate and vertebrate hosts. *Science* **225**, 1449–1452 (1984).

36. Gilbert, M. A. & Granath, W. O. Persistent Infection of *Myxobolus cerebralis*, the Causative Agent of Salmonid Whirling Disease, in *Tubifex tubifex*. *The Journal of Parasitology* **87**, 101 (2001).

37. American Fisheries Society. Whirling Disease: Reviews and Current Topics : Proceedings of the Seventh Annual Whirling Disease Symposium Held at Salt Lake City, Utah, USA, 8-9 February 2001. *Amer Fisheries Society* (2002).

38. Eszterbauer, E., Sipos, D., Szakály, Á. & Herczeg, D. Distinctive site preference of the fish parasite *Myxobolus cerebralis* (Cnidaria, Myxozoa) during host invasion. *Acta Veterinaria Hungarica* **67**, 212–223 (2019).

39. El-Matbouli, M., Hoffmann, R. W., Schoel, H., McDowell, T. S. & Hedrick, R. P. Whirling disease: host specificity and interaction between the actinosporean stage of *Myxobolus cerebralis* and rainbow trout *Oncorhynchus mykiss*. *Dis. Aquat. Organ.* **35**, 1–12 (1999).

40. Hoffman, G. L. *Myxobolus cerebralis*, a Worldwide Cause of Salmonid Whirling Disease. *Journal of Aquatic Animal Health* **2**, 30–37 (1990).

41. Whirling Disease: Reviews and Current Topics. Based on a symposium held in Salt Lake City, Utah, 8–9 February 2001. American Fisheries Society Symposium, Volume 29. Edited by Jerri L Bartholomew and J Christopher Wilson. *The Quarterly Review of Biology* **78**, 108–108 (2003).

42. J. L. Bartholomew and P. W. Reno. The History and Dissemination of Whirling Disease. in *American Fisheries Society Symposium* 1–22

43. Arsan, E. L., Hallett, S. L. & Bartholomew, J. L. *Tubifex tubifex* from Alaska and their susceptibility to *Myxobolus cerebralis*. *J. Parasitol.* **93**, 1332–1342 (2007).

44. Ruiz, C. F., Rash, J. M., Arias, C. R., Besler, D. A., Orélis-Ribeiro, R., Womble, M. R., Roberts, J. R., Warren, M. B., Ray, C. L., Lafrentz, S., Bullard, S. A., Morphological and molecular confirmation of *Myxobolus cerebralis* myxospores infecting wild-caught and cultured trout in North Carolina (SE USA). *Dis. Aquat. Organ.* **126**, 185–198 (2017).

45. *2017 Whirling Disease Program Report*. (Alberta Environment and Parks, 2017).

46. Bartholomew, J. L., Whipple, M. J., Stevens, D. G. & Fryer, J. L. The life cycle of *Ceratomyxa shasta*, a myxosporean parasite of salmonids, requires a freshwater polychaete as an alternate host. *J. Parasitol.* **83**, 859–868 (1997).

47. Meaders, M. D. & Hendrickson, G. L. Chronological development of *Ceratomyxa shasta* in the polychaete host, *Manayunkia speciosa*. *J. Parasitol.* **95**, 1397–1407 (2009).

48. Bjork, S. J. & Bartholomew, J. L. Invasion of *Ceratomyxa shasta* (Myxozoa) and comparison of migration to the intestine between susceptible and resistant fish hosts. *Int. J. Parasitol.* **40**, 1087–1095 (2010).

49. Bartholomew, J. L., Smith, C. E., Rohovec, J. S. & Fryer, J. L. Characterization of a host response to the myxosporean parasite, *Ceratomyxa shasta* (Noble), by histology, scanning electron microscopy and immunological techniques. *Journal of Fish Diseases* **12**, 509–522

(1989).

50. Bjork, S. J. & Bartholomew, J. L. Effects of *Ceratomyxa shasta* dose on a susceptible strain of rainbow trout and comparatively resistant Chinook and coho salmon. *Dis. Aquat. Organ.* **86**, 29–37 (2009).

51. Ratliff, D. E. *Ceratomyxa shasta*: Longevity, Distribution, Timing, and Abundance of the Infective Stage In Central Oregon. *Canadian Journal of Fisheries and Aquatic Sciences* **40**, 1622–1632 (1983).

52. Ching, H. L. & Munday, D. R. Geographic and seasonal distribution of the infectious stage of *Ceratomyxa shasta* Noble, 1950, a myxozoan salmonid pathogen in the Fraser River system. *Canadian Journal of Zoology* **62**, 1075–1080 (1984).

53. Hoffmaster, J. L., Sanders, J. E., Rohovec, J. S., Fryer, J. L. & Stevens, D. G. Geographic distribution of the myxosporean parasite, *Ceratomyxa shasta* Noble, 1950, in the Columbia River basin, USA. *Journal of Fish Diseases* **11**, 97–100 (1988).

54. Hendrickson, G. L., Carleton, A. & Manzer, D. Geographic and seasonal distribution of the infective stage of *Ceratomyxa shasta* (Myxozoa) in Northern California. *Diseases of Aquatic Organisms* **7**, 165–169 (1989).

55. Noble, E. R. On a Myxosporidian (Protozoan) Parasite of California Trout. *The Journal of Parasitology* **36**, 457 (1950).

56. Stocking, R. W. & Bartholomew, J. L. Distribution and habitat characteristics of *Manayunkia speciosa* and infection prevalence with the parasite *Ceratomyxa shasta* in the Klamath River, Oregon-California. *Journal of Parasitology* **93**, 78–88 (2007).

57. Fujiwara, M., Mohr, M. S., Greenberg, A., Scott Foott, J. & Bartholomew, J. L. Effects of Ceratomyxosis on Population Dynamics of Klamath Fall-Run Chinook Salmon. *Transactions of the American Fisheries Society* **140**, 1380–1391 (2011).

58. U.S. Department of the Interior Bureau of Reclamation. Final Biological Assessment: The Effects of the Proposed Action to Operate the Klamath Project from April 1, 2019 through March 31, 2029 on Federally-Listed Threatened and Endangered Species. (2018).

59. R. Adam Ray, Julie D. Alexander, Patrick De Leenheer, Jerri L. Bartholomew. Modeling the Effects of Climate Change on Disease Severity: A Case Study of *Ceratonova* (syn *Ceratomyxa*) *shasta* in the Klamath River. in *Myxozoan Evolution, Ecology and Development* (ed. Beth Okamura, Alexander Gruhl, Jerri L. Bartholomew) 363–378 (2015).

60. Intergovernmental Panel on Climate Change. *Climate Change 2007 - Mitigation of Climate Change: Working Group III contribution to the Fourth Assessment Report of the IPCC*. (Cambridge University Press, 2007).

61. Weill, R. L'interprétation des Cnidosporidies et la valeur taxonomique de leur cnidome. Leur cycle comparé à la phase larvaire des Narcomeduses cuninides. *Trav Stat Zool Wimer* 727–744 (1938).

62. Siddall, M. E., Martin, D. S., Bridge, D., Desser, S. S. & Cone, D. K. The Demise of a Phylum of Protists: Phylogeny of Myxozoa and Other Parasitic Cnidaria. *The Journal of Parasitology* **81**, 961 (1995).

63. Kent, M. L., Margolis, L. & Corliss, J. O. The demise of a class of protists: taxonomic and nomenclatural revisions proposed for the protest phylum Myxozoa Grassé, 1970. *Canadian Journal of Zoology* **72**, 932–937 (1994).

64. Piriatinskiy, G., Atkinson, S. D., Park, S., Morgenstern, D., Brekhman, V., Yossifon, G., Bartholomew, J. L., & Lotan, T. Functional and proteomic analysis of *Ceratonova shasta* (Cnidaria: Myxozoa) polar capsules reveals adaptations to parasitism. *Sci. Rep.* **7**, 9010

(2017).

65. Chang, E. S., Neuhof, M., Rubinstein, N. D., Diamant, A., Philippe, H., Huchon, D., & Cartwright, P. Genomic insights into the evolutionary origin of Myxozoa within Cnidaria. *Proc. Natl. Acad. Sci. U. S. A.* **112**, 14912–14917 (2015).

66. Holstein, T. & Tardent, P. An ultrahigh-speed analysis of exocytosis: nematocyst discharge. *Science* **223**, 830–833 (1984).

67. Kallert, D. M., Ponader, S., Eszterbauer, E., El-Matbouli, M. & Haas, W. Myxozoan transmission via actinospores: new insights into mechanisms and adaptations for host invasion. *Parasitology* **134**, 1741–1750 (2007).

68. Kallert, D. M., Bauer, W., Haas, W. & El-Matbouli, M. No shot in the dark: myxozoans chemically detect fresh fish. *Int. J. Parasitol.* **41**, 271–276 (2011).

69. Alama-Bermejo, G., Bron, J. E., Raga, J. A. & Holzer, A. S. 3D Morphology, ultrastructure and development of *Ceratomyxa puntazzi* stages: first insights into the mechanisms of motility and budding in the Myxozoa. *PLoS One* **7**, e32679 (2012).

70. Sipos, D., Ursu, K., Dán, Á., Herczeg, D. & Eszterbauer, E. Susceptibility-related differences in the quantity of developmental stages of *Myxobolus* spp. (Myxozoa) in fish blood. *PLoS One* **13**, e0204437 (2018).

71. Lom, J. & Dykova, I. Fine Structure of Triactinomyxon Early Stages and Sporogony: Myxosporean and Actinosporean Features Compared. *The Journal of Protozoology* **39**, 16–27 (1992).

72. Tardent, P. History and current state of knowledge concerning discharge of cnidae. *The Biology of Nematocysts* 309–332 (1988). doi:10.1016/b978-0-12-345320-4.50022-5

73. El-Matbouli, M. & Hoffmann, R. W. Light and electron microscopic studies on the chronological development of *Myxobolus cerebralis* to the actinosporean stage in Tubifex tubifex. *Int. J. Parasitol.* **28**, 195–217 (1998).

74. Rocha, S., Alves, Â., Fernandes, P., Antunes, C., Azevedo, C., & Casal, G. New actinosporean description prompts union of the raabeia and echinactinomyxon collective groups (Cnidaria, Myxozoa). *Dis. Aquat. Organ.* **135**, 175–191 (2019).

75. Weber, J. Nematocysts (stinging capsules of Cnidaria) as Donnan-potential-dominated osmotic systems. *Eur. J. Biochem.* **184**, 465–476 (1989).

76. Weber, J. Poly(gamma-glutamic acid)s are the major constituents of nematocysts in Hydra (Hydrozoa, Cnidaria). *J. Biol. Chem.* **265**, 9664–9669 (1990).

77. Szczepanek, S., Cikala, M. & David, C. N. Poly-gamma-glutamate synthesis during formation of nematocyst capsules in Hydra. *J. Cell Sci.* **115**, 745–751 (2002).

78. Tardent, P. The cnidarian cnidocyte, a hightech cellular weaponry. *BioEssays* **17**, 351–362 (1995).

79. Pangrazzi, R. Untersuchung uber die kausalen Beziehungen zwischen dem Kationengehalt der Nematocysten einerseits und deren Funktionalitat andererseits. (University of Zurich, 1993).

80. Kepner, W. A. The discharge of nematocysts of hydra, with special reference to the penetrant. *J. Morphol.* **88**, 23–47 (1951).

81. Myxozoan Evolution, Ecology and Development. (2015). doi:10.1007/978-3-319-14753-6

82. Lotan, A., Fishman, L., Loya, Y. & Zlotkin, E. Delivery of a nematocyst toxin. *Nature* **375**, 456 (1995).

83. Ayalon, A., Shichor, I., Tal, Y. & Lotan, T. Immediate topical drug delivery by natural submicron injectors. *Int. J. Pharm.* **419**, 147–153 (2011).

84. Kudo, R. Experiments on the Extrusion of Polar Filaments of Cnidosporidian Spores. *The Journal of Parasitology* **4**, 141 (1918).

85. Frixione, E., Ruiz, L., Cerbón, J. & Undeen, A. H. Germination of *Nosema algerae* (Microspora) Spores: Conditional Inhibition by D2O, Ethanol and Hg^{2+} Suggests Dependence of Water Influx upon Membrane Hydration and Specific Transmembrane Pathways. *The Journal of Eukaryotic Microbiology* **44**, 109–116 (1997).

86. Dujardin, F. Mémoire sur le développement des polypes hydraires et méduses. *Ann. Sci. Nat.* 257–281 (1845).

87. Jones, C. S. The control and discharge of nematocysts in hydra. *J. Exp. Zool.* **105**, 25–60 (1947).

88. Carré, D. [Hypothesis on the mechanism of cnidocyst discharge (author's transl)]. *Eur. J. Cell Biol.* **20**, 265–271 (1980).

89. Berking, S. & Herrmann, K. Formation and discharge of nematocysts is controlled by a proton gradient across the cyst membrane. *Helgoland Marine Research* **60**, 180–188 (2006).

90. Park, S., Piriatinskiy, G., Zeevi, D., Ben-David, J., Yossifon, G., Shavit, U., & Lotan, T. The nematocyst's sting is driven by the tubule moving front. *J. R. Soc. Interface* **14**, (2017).

91. Parker, G. H. The reversal of ciliary movement in metazoans. *American Journal of Physiology-Legacy Content* **13**, 1–16 (1905).

92. Yanagita, T. M. Physiological mechanism of nematocyst responses in sea-anemone—IV. Effects of surface-active agents on the cnidae in situ and in isolation. *Comparative Biochemistry and Physiology* **1**, 140–154 (1960).

93. McKay, M. C. & Anderson, P. A. V. Preparation and Properties of Cnidocytes from the Sea Anemone *Anthopleura elegantissima*. *Biol. Bull.* **174**, 47–53 (1988).

94. Russell, T. J. & Watson, G. M. Evidence for intracellular stores of calcium ions involved in regulating nematocyst discharge. *Journal of Experimental Zoology* **273**, 175–185 (1995).

95. Salleo, A. Discharge Mechanism of the Nematocysts of *Pelagia noctiluca*. *Proceedings in Life Sciences* 63–76 (1984).

96. Eric J Wagner, Quinn Cannon, Mark Smith, Ryan Hillyard, Ronney Arndt. Extrusion of Polar Filaments of the *Myxobolus cerebralis* Triactinomyxon by Salts, Electricity, and Other Agents. Am. Fish. Soc. Symp. 61–76 (2002). *Am. Fish. Soc. Symp.* 61–76 (2002).

97. Kawaii, S., Yamashita, K., Nakai, N. & Fusetani, N. Intracellular calcium transients during nematocyst discharge in actinulae of the hydroid,*Tubularia mesembryanthemum. The Journal of Experimental Zoology* **278**, 299–307 (1997).

98. Hidaka, M. & Afuso, K. Effects of Cations on the Volume and Elemental Composition of Nematocysts Isolated from Acontia of the Sea Anemone *Calliactis polypus. Biol. Bull.* **184**, 97–104 (1993).

99. Blanquet, R. Ionic effects on discharge of the isolated and in situ nematocysts of the sea anemone, *Aiptasia pallida*: A possible role of calcium. *Comparative Biochemistry and Physiology* **35**, 451–461 (1970).

100. Lotan, T. Leveraging Nematocysts Toward Human Care. *The Cnidaria, Past, Present and Future* 683–690 (2016). doi:10.1007/978-3-319-31305-4_42

101. Salleo, A., La Spada, G. & Barbera, R. Gadolinium is a powerful blocker of the activation of nematocytes of *Pelagia noctiluca. J. Exp. Biol.* **187**, 201–206 (1994).

102. Kawaii, S., Yamashita, K., Nakai, M., Takahashi, M. & Fusetani, N. Calcium Dependence of Settlement and Nematocyst Discharge in Actinulae of the Hydroid *Tubularia mesembryanthemum. Biol. Bull.* **196**, 45–51 (1999).

103. Beedle, A. M., Hamid, J. & Zamponi, G. W. Inhibition of transiently expressed low- and high-voltage-activated calcium channels by trivalent metal cations. *J. Membr. Biol.* **187**, 225–238 (2002).

104. Gitter, A. H., Oliver, D. & Thurm, U. Calcium- and voltage-dependence of nematocyst discharge in *Hydra vulgaris. Journal of Comparative Physiology A* **175**, (1994).

105. Moran, Y. & Zakon, H. H. The evolution of the four subunits of voltage-gated calcium channels: ancient roots, increasing complexity, and multiple losses. *Genome Biol. Evol.* **6**, 2210–2217 (2014).

106. Moran, Y. & Zakon, H. H. The Evolution of the Four Subunits of Voltage-Gated Calcium Channels: Ancient Roots, Increasing Complexity, and Multiple Losses. *Genome Biology and Evolution* **6**, 2210–2217 (2014).

107. Bouchard, C. & Anderson, P. A. V. Immunolocalization of a voltage-gated calcium channel β subunit in the tentacles and cnidocytes of the Portuguese man-of-war, *Physalia physalis. Biol. Bull.* **227**, 252–262 (2014).

108. Thorington, G. U. & Hessinger, D. A. Control of Cnida Discharge: I. Evidence for Two Classes of Chemoreceptor. *The Biological Bulletin* **174**, 163–171 (1988).

109. Thorington, G. U. & Hessinger, D. A. Control of Cnida Discharge: III. Spirocysts are Regulated by Three Classes of Chemoreceptors. *Biol. Bull.* **178**, 74–83 (1990).

110. Plachetzki, D. C., Fong, C. R. & Oakley, T. H. Cnidocyte discharge is regulated by light and opsin-mediated phototransduction. *BMC Biol.* **10**, 17 (2012).

111. Watson, G. M. & Mire, P. Stereocilia Based Mechanoreceptors of Sea Anemones. *Cell and Molecular Biology of the Ear* 19–39 (2000). doi:10.1007/978-1-4615-4223-0_2

112. Watson, G. M. & Hessinger, D. A. Receptor-mediated endocytosis of a chemoreceptor involved in triggering the discharge of cnidae in a sea anemone tentacle. *Tissue Cell* **19**, 747–755 (1987).

113. Scappaticci, A. A., Jr, Kahn, F. & Kass-Simon, G. Nematocyst discharge in *Hydra vulgaris*: Differential responses of desmonemes and stenoteles to mechanical and chemical stimulation. *Comp. Biochem. Physiol. A Mol. Integr. Physiol.* **157**, 184–191 (2010).

114. Price, R. B. & Anderson, P. A. V. Chemosensory pathways in the capitate tentacles of the hydroid Cladonema. *Invert. Neurosci.* **6**, 23–32 (2006).

115. Oliver, D., Brinkmann, M., Sieger, T. & Thurm, U. Hydrozoan nematocytes send and receive synaptic signals induced by mechano-chemical stimuli. *J. Exp. Biol.* **211**, 2876–2888 (2008).

116. Bouchard, C. Cloning and functional expression of voltage-gated ion channel subunits from cnidocytes of the Portuguese Man O'War *Physalia physalis. Journal of Experimental Biology* **209**, 2979–2989 (2006).

117. Peter A. V. Anderson and M. Craig McKay. The electrophysiology of cnidocytes. *J. Exp. Biol.* 215–230 (1987).

118. Yokoyama, H., Ogawa, K. & Wakabayashi, H. Chemoresponse of actinosporean spores of *Myxobolus cultus* to skin mucus of goldfish *Carassius auratus. Diseases of Aquatic Organisms* **21**, 7–11 (1995).

119. Kallert, D. M., El-Matbouli, M. & Haas, W. Polar filament discharge of *Myxobolus cerebralis* actinospores is triggered by combined non-specific mechanical and chemical cues. *Parasitology* **131**, 609–616 (2005).

120. Kallert, D. M., Ponader, S., Adelt, S., Kaese, P., Geyer, R., Haas, W. & El-Matbouli, M. Analysis of rainbow trout Oncorhynchus mykiss epidermal mucus and evaluation of

semiochemical activity for polar filament discharge in *Myxobolus cerebralis* actinospores. *Journal of Fish Biology* **77**, 1579–1598 (2010).

121. Howgate, P. A review of the kinetics of degradation of inosine monophosphate in some species of fish during chilled storage. *International Journal of Food Science and Technology* **41**, 341–353 (2006).

122. Myxozoan Evolution, Ecology and Development. (2015). doi:10.1007/978-3-319-14753-6

123. Feist, S. W. Ultrastructural aspects of *Myxidium gadi* (Georgévitch, 1916) (myxozoa: Myxosporea). *European Journal of Protistology* **31**, 309–317 (1995).

CHAPTER 2

PAIRED *IN VITRO* AND *IN VIVO* ASSAYS REVEAL THAT SODIUM AFFECTS
NEMATOCYST DISCHARGE BEHAVIOR IN PARASITIC CNIDARIA

Benjamin Americus, Brett Austin, Tamar Lotan, Jerri L. Bartholomew, Stephen D. Atkinson

ABSTRACT

Myxozoans are obligately parasitic, microscopic cnidarians. They possess specialized stinging
cells called nematocysts (historically called "polar capsules" in Myxozoa). Free-living cnidarians
discharge nematocysts for feeding and defense, whereas myxozoans use them to anchor to their
hosts in the first step of infection. Nematocyst discharge is thought to be driven by dissociation
of an internal matrix of cations bound to poly-gamma glutamate, which causes a sudden buildup
of osmotic energy; this hypothesis is based largely on work with free-living cnidarians. Much
less is known about discharge triggers and processes in myxozoan nematocysts. In this
manuscript, we utilized the myxozoan *Myxobolus cerebralis* to develop two novel wet-lab assays
to explore the nature of nematocyst discharge. We developed an *in vitro* assay that utilized
rainbow trout mucus homogenate to stimulate discharge of actinospores in solutions enriched
with metal ions and an antihistamine. In parallel, we used an *in vivo* assay to test the effects of
these treatments on the ability of *M. cerebralis* actinospores to infect fish. The assays revealed
that Na^+ significantly increased nematocyst discharge but reduced infection. This aligns with
prior work in free-living Cnidaria, which suggests that divalent cations bound to poly-gamma
glutamate inside the nematocyst can be exchanged with monovalent ions from environment
through the capsule wall, and promote discharge. In Myxozoa, this may result in a "hair trigger"
state in which nematocysts discharge prematurely or inaccurately when presented with a fish cue.
These finding underlie commonalities between nematocysts in myxozoans and free-living
Cnidaria and suggests a novel approach for controlling myxozoan diseases in aquaculture.

INTRODUCTION

Myxozoans are a speciose group of obligately parasitic cnidarians, with complex life cycles that
involve two hosts and two distinct spore stages (actinospores and myxospores). Both life stages

are microscopic and waterborne, typically 10–100 microns across with a great variety of morphological diversity both between conspecific life stages and among different species[1,2]. Like all cnidarians, both spore stages contain nematocysts (historically called "polar capsules"). In free-living Cnidaria, nematocyst discharge plays a central role in capturing and immobilizing prey, and deterring invaders[9]. In myxozoans, these specialized organelles are crucial to the process of infection; when a spore receives a host detection signal, either through mechanical or chemical cues,[6] a tubule everts explosively, penetrates the host epithelium, then contracts to pull the myxozoan to its target. Once anchored, the valve cells open along their sutures, and the infectious parasite sporoplasm migrates actively out of the spore and into the host, to begin replicating[7,3,8,5].

In free-living Cnidaria, nematocyst discharge is driven by a combination of intrinsic forces. These are built into the coiled tubule during cnidogenesis[10,11] and are generated through hydrostatic pressure that swells the capsule to equilibrate an osmotic gradient[12]. When discharge is signaled, water flows into the nematocyst and an internal matrix of cations bound to poly-gamma glutamate dissociates, resulting in a rapid increase in Donnan potential, exocytosis and discharge of the tubule[13]. Much of our understanding of nematocyst discharge in Myxozoa is inferred from structural similarities to the nematocysts of free-living Cnidaria: proteomic analysis of nematocysts isolated from the myxozoan *C. shasta* identified enzymes related to poly-gamma glutamate biosynthesis[14]. The same study explored dyeing nematocysts with acridine orange, which binds cations, and heavy staining was observed. These observations suggest the contents of myxozoan nematocysts may be similar to the nematocysts of their free-living relatives[14].

To develop treatments[15] against pathogenic myxozoans, or for descriptive purposes, myxozoan nematocysts may be induced to discharge abiotically using strong bases[16, 17], urea[18] and hydrogen peroxide[19]. Drawing upon known stimulants of nematocyst discharge in free-living Cnidaria, Wagner et al. (2002)[20] explored the effect of extreme pH, salts, electricity, and two chemosensitizers (proline, and N-acetylneuraminic acid), and a series of neurochemicals on nematocyst discharge in the model myxozoan *M. cerebralis*. Notably, *M. cerebralis* did not respond to either chemosensitizer or any neurochemical which suggested that the chemical cue for discharge is different in myxozoans. As with the nematocysts of free-living cnidarians, very

low and very high pH, and electrical pulses stimulated discharge; however, more extreme pH levels and much higher voltages were required to discharge the nematocysts of *M. cerebralis* than used in free-living cnidarian nematocysts[23,24]. Similarly, the addition of K^+ ions induced myxozoan nematocyst discharge, as it does in free-living cnidarians[25,22,26,27].

While myxozoan tubule discharge can be induced by chemical activation[4,31], as parasites the spores need to both discharge their tubules and trigger their sporoplasms to migrate, if infection is to occur. This biologically essential function of sporoplasm migration has only been successfully initiated by fish mucus homogenates and isolates[32]. Yokoyama et al. (1995)[33] identified fish mucus homogenate as an effective discharge agent for *Myxobolus cultus.* Kallert et al. (2005)[34] refined the technique, applying rainbow trout mucus to *M. cerebralis* with an additional mechanostimulation step. In a subsequent work[35] Kallert et al. (2007) explored the response of *Myxobolus parviformis* actinospores to calcium: the spores responded to a greater extent to mucus in calcium-free waters to which NaCl was added to restore osmolality, but less in calcium-free waters that were not osmotically restored. This suggested that a threshold of osmolarity, and not simply the endocytosis of environmental Ca^{2+}, is necessary for nematocyst discharge in Myxozoa.

Given that myxozoan spores can be activated under experimental scenarios, we sought to develop assays to test the effects of compounds known to affect free-living Cnidaria on the nematocyst discharge and sporoplasm migration responses of myxozoan spores. Using actinospore stages of *M. cerebralis*, we developed an *in vitro* assay capable of distinguishing the effects of chemical treatments. To validate our *in vitro* observations and to test effects of the compounds on process of infection to hosts, we performed *in vivo* exposures with live fish and quantified parasite load in host tissues with qPCR. Results from the paired *in vitro* and *in vivo* tests suggest that myxozoan nematocysts respond to cationic treatments very similarly to the nematocysts of free-living cnidarians, with Na^+ having the greatest effect in both assays.

METHODS

SOURCE OF FISH

Rainbow trout hatched at the Roaring River Fish Hatchery and reared at the Oregon State University's Aquatic Animal Health Laboratory (AAHL) in Corvallis, Oregon were used for all experiments. Fish hatched in spring 2017 (90-100 mm) were used to isolate mucus for the *in vitro* assay. Fish hatched in spring 2018 (60-70 mm) were used in the subsequent *in vivo* assay. All procedures involving fish were conducted at the AAHL in accordance with OSU institutional animal welfare guidelines under permit #5040.

SOURCE OF FISH MUCUS

Individual Roaring River rainbow trout were euthanized by overdose with MS-222 (tricaine methosulfonate, Argent, Redmond, WA). A mucus homogenate solution was prepared using modified methods of Kallert et al. 2005. We pipetted 100 µL deionized water onto the fish and scraped the mucus off the lateral surfaces using the broad end of a flat spatula. Scrapings were collected in a 1.7 mL tube and vortexed for 30 s with garnet beads to promote transfer of soluble compounds from mucus to water. The mucus homogenate was then centrifuged for 10 min at $2200 \times G$ and any pellet was discarded. The supernatant was held on ice until use (within 2 h).

SOURCE OF *M. CEREBRALIS* ACTINOSPORES

Oligochaetes (*Tubifex tubifex*) infected with *M. cerebralis* were provided for this study by George Schisler at the Colorado Parks and Wildlife, Parvin Lakes Research Laboratory. Identity of the parasite had been verified previously by PCR and Sanger sequencing. Oligochaete cultures were kept in two 3-L static tanks with aerators, in an incubator at 15°C. Water over the oligochaetes was periodically replaced with dechlorinated tap water and the worms fed one algae pellet monthly (Hikari Algae Wafers Fish Food). For harvest, approximately 150 oligochaetes were removed from each tank and placed in 200-mL cups with clean mineral sand under 100 mL dechlorinated tap water. After 48 h they were moved to 157-mL glass petri dishes. After 36 h, 125 mL from each dish was collected, pre-filtered through a 180 µm wire mesh to catch worms

and large debris, then the spore solution was reduced in volume with a 20 µm Nitex screen which retained the actinospores. Spores were held on ice and used within 3 h of collection.

SOURCES AND PREPARATION OF CHEMICAL COMPOUNDS

Per OSU ACUP guidelines, all chemicals were pharmaceutical grade (Table 2.1) and diluted with deionized water.

Table 2.1. Compounds, sources, and final concentrations used in the *in vitro* and *in vivo* trials.

Test Compound	Supplier	Concentration *in vitro* (mM)	Concentration *in vivo* (mM)
NaCl	Consolidated Midland Corporation	100	100
KCl	Lab Alley	100	15
Diphenhydramine	WinCo Foods LLC (banded capsules)	0.1	0.05
$CaCl_2$	Research Products International	50	50
$FeCl_2$	Lab Alley	5	10
$GdCl_3$	Alfa Aesar	0.1	0.1

IN VITRO EXPERIMENTS

Fresh actinospores were divided evenly among 8 x 0.5 mL tubes (2 control, 6 treatment groups). To each treatment tube, 6 µL of the corresponding chemical solution was added to achieve the desired concentration (Table 2.1). Experiments were performed over ~45 min at 13 °C. Compounds were added to the tubes sequentially and in the same order to standardize incubation times, while pipetting the discharging the full contents each tube once to mix. Each compound was added to a solution of *M. cerebralis* actinospores at T = 0, then subsampled at T = 15 min, prior to addition of mucus at T = 16 min, with a final subsampling at T= 46 min. Each subsample was immediately fixed by addition of an equal volume of 10% formalin to lock in the state of the nematocysts and sporoplasm.
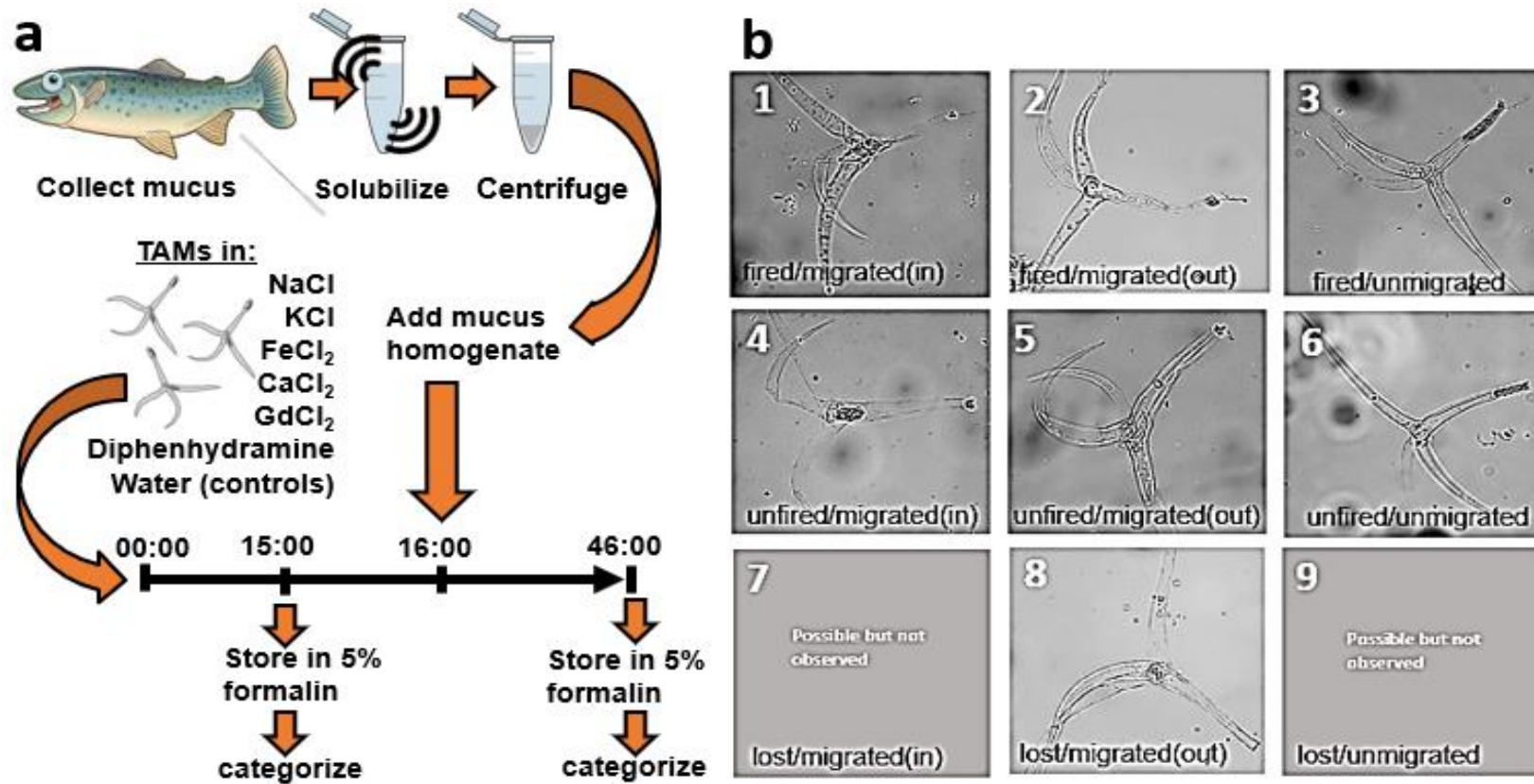
Figure 2.1: Experimental design and measured spore characteristics for the *in vitro* assay. a: flowchart showing method overview and timings; samples were collected and fixed at 0, 15, and 31 minutes; b: the 9 discrete categories of actinospore appearance. Labels signify the status of the nematocysts: fired vs. unfired vs not present (lost), and the status of the sporoplasm: migrated inside the valve cells vs. migrated outside of the valve cells vs. unmigrated.

Counting and categorizing actinospores

From each subsample, 3×2 µL aliquots (with additional replicates if needed to enumerate 50-100 actinospores) were taken and streaked widthwise across a glass microscope slide, and left uncovered. Actinospores were enumerated, and nematocyst and sporoplasm conditions assessed by examining spores visually with brightfield microscopy at 200× and with the field diaphragm mostly closed to enhance contrast. From each timepoint, we counted 50-100 spores from each of 3 replicate subsamples. Individual actinospores were assigned to one of 9 categories (Fig. 2.1b). Actinospores were not counted if the nematocyst or sporoplasm were obscured, or if obviously malformed e.g. miniaturism/incomplete inflation.

Statistics and Data Processing

The proportion of discharged actinospores was calculated from three replicates of each treatment at both timepoints. Designation of actinospores into discrete, comprehensive categories (Fig. 2.1b) allowed a variety of analyses. Treatments were assessed in two biologically informative ways: 1) "tubule firing", which included categories 1-3, and "tubule firing and migration (out)", which included only category 2. Both polar tubule discharge and sporoplasm migration out of the valve cells are necessary for infection, so this second descriptive category is our closest proxy for spores that represent a successful infection to fish.

To examine the impact of the treatments on normal discharge, mean discharge proportions from the first timepoint were subtracted from the replicates from the second timepoint. This allowed us to distinguish discharge caused by the treatment alone from effects related to the addition of mucus. Normality of data was checked by the Shapiro-Wilk Test and Normal variance was tested by the Bartlett's test. Significant differences among groups were tested by one-way ANOVA and Tukey's honestly significant difference (HSD) multiple t-test was employed to compare treatments. Significance was noted at a p threshold of $p<0.05$.

If data lacked a normal distribution and normal variance and one could not be established by arcsine transformation, the Kruskal Wallis Test was performed as an alternative to one-way

ANOVA. In these instances, we used Dunn's Test with Holm multiple testing correction to examine pairwise differences between treatments.

IN VIVO EXPERIMENTS

Chemical tolerance of fish to compounds

To test what concentration of the nominated compounds was tolerated by the fish under the experimental conditions, we pre-assessed fish and lowered the compound concentration if necessary. 5 juvenile Roaring River rainbow trout were held in each of 8×1-L containers with 250 mL aerated 16 °C well water that contained each compound. Fish were monitored for stress (rapid movement, jumping, gasping for air, loss of equilibrium) for 30 min. Fish exhibiting signs of stress were removed and immediately euthanized by an overdose of MS-222. In those cases, the compound concentration was reduced by half, and the exposure was repeated. Final concentrations that were tolerated by the fish are given in Table 2.1.
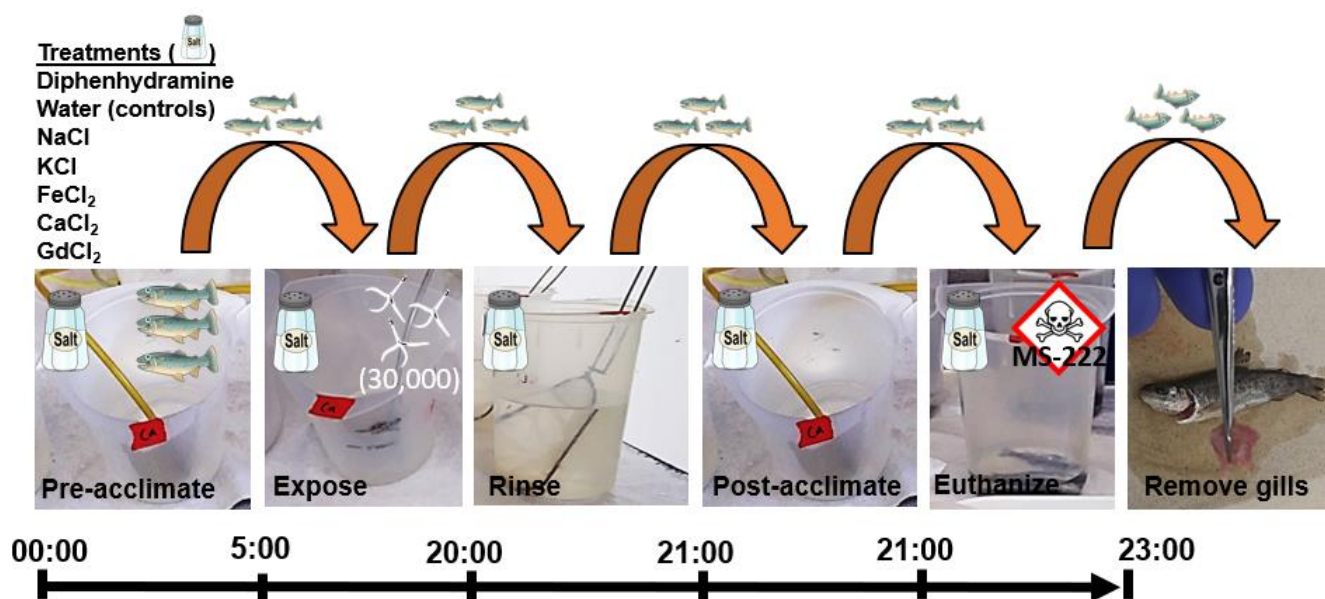
Figure 2.2 Experimental design for *in vivo* assay showing the transfers of fish to different solutions at the corresponding timepoints (minutes after experiment start).

In vivo exposures to actinospores plus compounds

To a set of 1-L containers, we added 30,000 *M. cerebralis* actinospores in 50 mL well water plus 50 mL of 2× salt solution to make 100 mL of solution at the desired salt concentration. Solutions were equilibrated for ~15 min prior to the addition of fish. The temperature of all solutions was 16-20 °C. In parallel, 3 juvenile rainbow trout were pre-acclimated in 1-L aerated containers with 100 mL of each salt solution for 5 min in the absence of parasites, then netted and transferred to the corresponding 1-L container that contained the equilibrated 100 mL salt solution with actinospores. Fish were exposed to the spores for 15 min, netted and dipped three times in spore-free solutions of their respective compounds to rinse off poorly adhered actinospores, then returned to the parasite-free solutions used in the original acclimation. After 5 min, fish were netted and euthanized by an overdose of buffered MS-222 at each respective salt concentration. Fish were then necropsied with gills removed and frozen in 2-mL tubes for downstream processing, decontaminating forceps and scissors with hydrogen peroxide between samples. Bodies were frozen separately. The experiment was conducted twice, with different batches of spores but the same compound solutions and fish stock.

We extracted total DNA from each gill sample using a Qiagen DNeasy Blood and Tissue kit following the manufacturer's recommendations, with DNA eluted from the column with two washes of 100 µL buffer AE. Total DNA concentration was measured with a Nanodrop spectrometer (Thermo Scientific), and total DNA concentration was normalized by dilution with molecular grade water to 150 ng/µL. *M. cerebralis* DNA concentration was measured by the standard quantitative polymerase chain reaction (qPCR)[37].

Statistics and Data Processing

Three replicates of each treatment from two qPCR runs are included in the analysis. A positive standard containing DNA extracted from 1000 *M. cerebralis* actinospores was included in both qPCR runs to control for inter-plate variance. The difference in Cq between the first and the second run of the standard was subtracted from all data in the second run. Prior to binning samples, to test for inter-repeat variation, we performed Dunn's pairwise tests between the same treatment groups from the two repetitions of the experiment. Normality of data was checked by

the Shapiro-Wilk Test. Normal variance was tested by the Bartlett's test. As a non-parametric alternative to one-way ANOVA, the Kruskal-Wallis test was used to examine differences between all treatments. We used Dunn's Test with Holm multiple testing correction to examine pairwise differences between treatments.

RESULTS

IN VITRO ASSAY

The effect of treatment on tubule firing

The effect of treatments on inducing polar filament discharge are displayed in Fig. 2.3. Note that the pH of all salt and actinospore mixtures ranged from 5.3-6.6, which was outside the reported range that could cause pH-induced discharge of tubules in *M. cerebralis*[20]. At T = 15 min, the proportion of actinospores with fired tubules did not diverge between the control groups in water (PC and NC). Both Na^+ and K^+ increased the proportion of fired tubules relative to the control, however there were no significant differences present between the controls and any treatment group. Figure 2.3b.

Panel b:

	NC	Na	K	Ca	Fe	Gd
PC	0.9956					
Na	0.4245					
K	0.2681	1.0000				
Ca	0.9999	0.2542	0.1491			
Fe	0.3998	1.0000	1.0000	0.2366		
Gd	0.8343	0.0403	0.0214	0.9573	0.0369	
D	1.0000	0.3641	0.2240	1.0000	0.3416	0.8839

Panel d:

	PC	Na	K	Ca	Fe	Gd
NC	0.0471					
Na	0.0392					
K	0.1460	0.9947				
Ca	0.1522	0.0002	0.0007			
Fe	0.6233	0.0012	0.0048	0.9623		
Gd	1.0000	0.0409	0.1518	0.1465	0.6098	
D	0.9995	0.0974	0.3168	0.0635	0.3490	0.9997
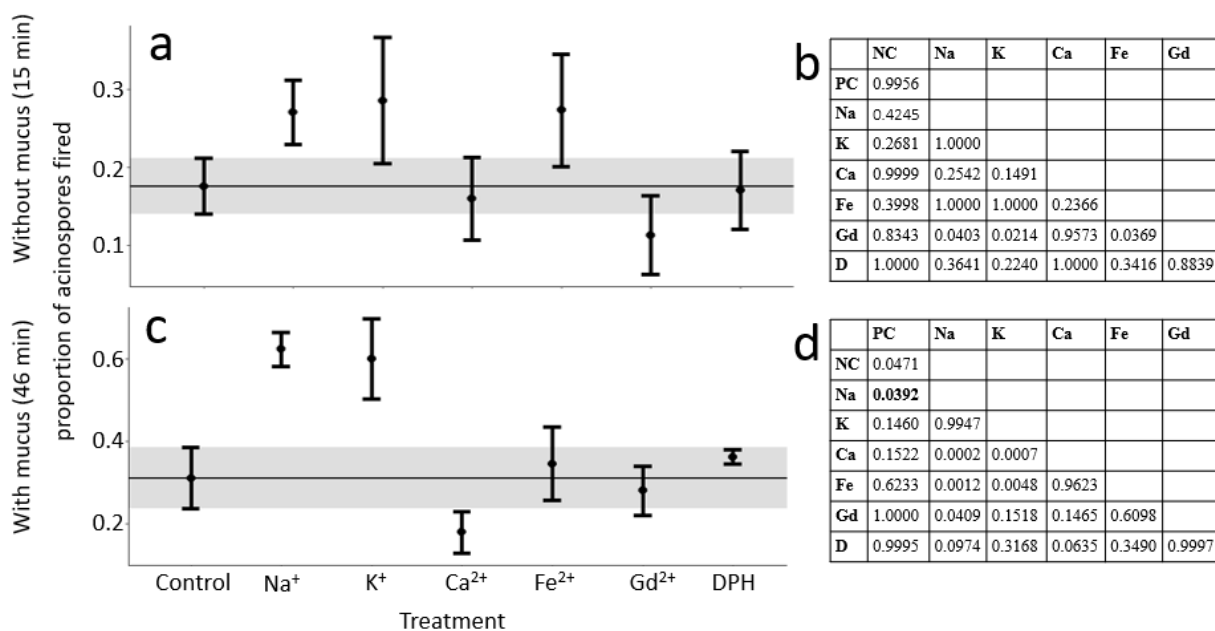
Figure 2.3. *In vitro* effect of chemical treatment on polar filament discharge in *M. cerebralis* at 15 minutes (before addition of mucus; a-b), and at 46 minutes (after addition of mucus; c-d). The y-axis displays the proportion of actinospores with at least one discharged nematocyst. All values have been normalized to the water controls. b and d show the corresponding matrices of P-values from Tukey HSD test comparing treatments.

At T = 46 min, 30 min after addition of mucus, many significant or appreciable differences were detected between treatment groups, and the negative control (NC: water control, no mucus), and positive control (PC: water control, with mucus applied). P-values are given in Fig. 2.3d. The PC had significantly more actinospores with fired tubules than the NC (p=0.047). The NaCl treatment had significantly more actinospores fired than the PC, even after the baseline (pre-mucus) proportion of actinospores with fired nematocysts was subtracted. The CaCl$_2$ treatment had fewer tubules fired than the PC (p=0.152), and the group in KCl had more tubules fired than the PC (p=0.1460).

The effect of treatment on tubule firing and *migration*

When we narrowed our analysis to the rate of actinospores which had fired tubules *and* sporoplasms migrated outside of the valve cells, we found no significant differences between the groups at T = 15 min (Kruskal-Wallis p=0.1615). At T = 30 min, there was no significant difference between the NC and PC (Tukey HSD p=0.7683). The group in KCl however, had significantly more actinospores with discharged tubules than PC (Tukey HSD p=0.0165).
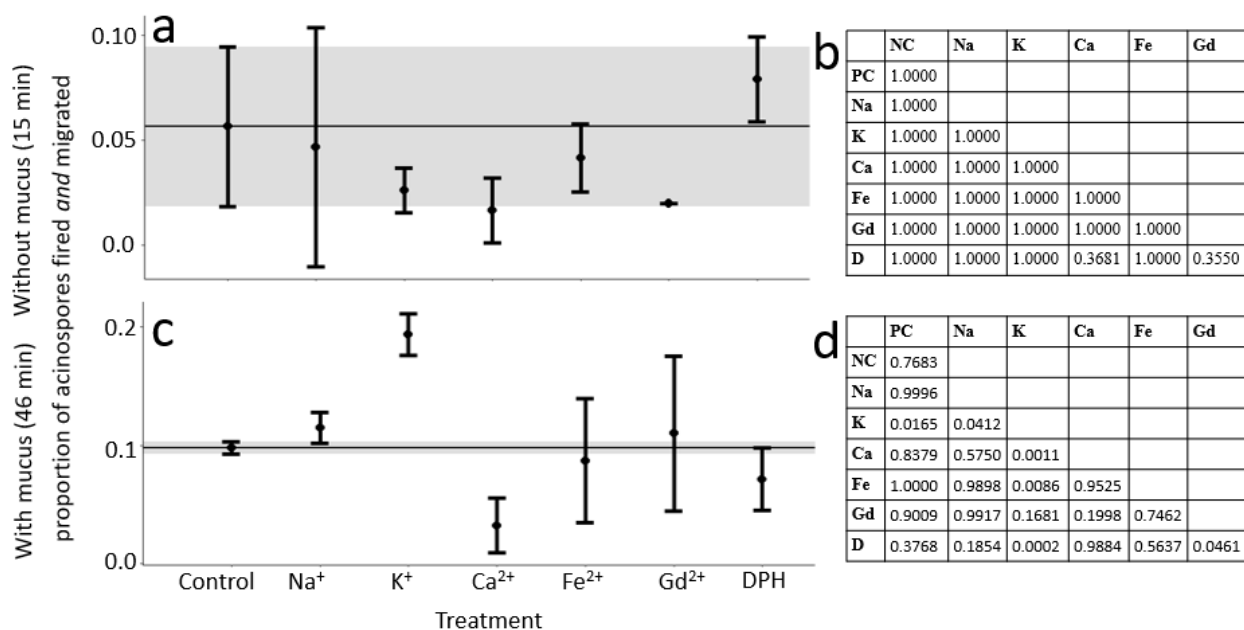
Figure 2.4. *In vitro* effect of chemical treatment on polar filament discharge *and* sporoplasm migration out of the valve cells in *M. cerebralis* at (a) T = 15 minutes (before addition of mucus), and (c) T = 46 minutes (after addition of mucus). The y-axis displays the proportion of actinospores with at least one discharged nematocyst, *and* sporoplasm at least partially migrated out of the valve cells. All values have been normalized to the water controls. (b) Corresponding matrices of P-values from Dunn's test with Holm adjustment comparing treatments. (d) Corresponding matrices of P-values from Tukey HSD test comparing treatments.

IN VIVO ASSAY

Pre-test of chemical tolerance

After 15 min, fish in 0.1 mM diphenhydramine were sedated and lying on their sides. The exposure was repeated at 0.05 mM and 0.025 mM. A similar effect was observed after 20 min at 0.05mM, but not for 30 min at 0.025 mM. No stress was observed in fish treated with the initial concentration of any other compound; hence these concentrations were used.

Fish exposures to spores during chemical treatments

qPCR detection levels of *M. cerebralis* DNA are shown in Fig. 2.5. No significant differences existed between repeated data, thus each of the two sets of three replicates were combined. The PC fish (water control with spores) had the highest mean Cq, signifying the greatest parasite concentration in the gills. A Kruskal-Wallis test on the transformed data suggested significant differences between treatment groups (p=0.0009). The PC fish had significantly lower Cq than the NC (water control, without spores; Dunn's test with Holm correction, p=0.0001). Likewise, the NaCl treatment group had significantly higher log-Cq values (Dunn's test with Holm correction, p=0.0458).

a: (box-and-whisker plot of Cq vs Treatment; y-axis Cq with values 26, 29, 32, 36, 38; x-axis treatments NC, PC, Na$^+$, K$^+$, Ca^{2+}, Fe^{2+}, Gd^{2+})

b:

	PC	Na	K	Ca	Fe
NC	0.0002				
Na	0.0458				
K	0.9423	1.0000			
Ca	0.9271	1.0000	0.9812		
Fe	1.0000	1.0000	1.0000	1.0000	
Gd	1.0000	1.0000	1.0000	1.0000	1.0000
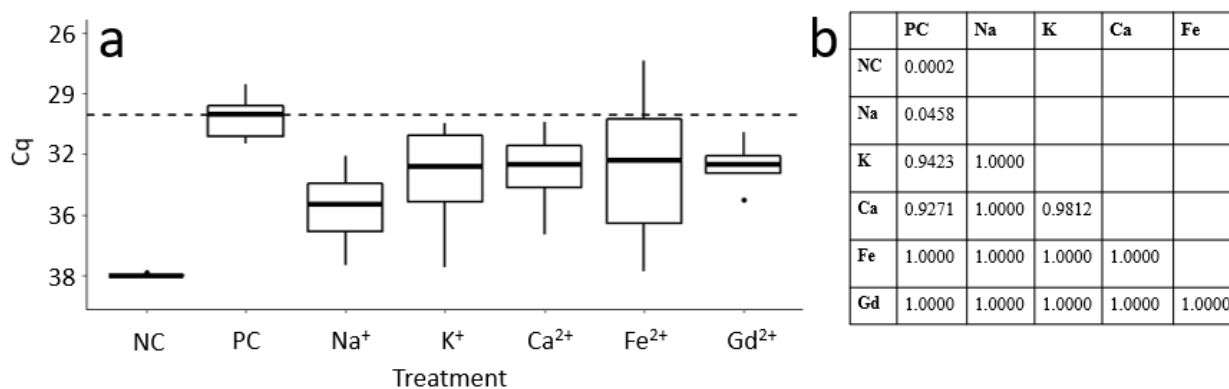
Figure 2.5. Results of *in vivo* exposure of rainbow trout to *Myxobolus cerebralis* actinospores in solutions containing different salts; a: *M. cerebralis* DNA detected on gills of treated fish measured by parasite-specific qPCR, expressed as quantitation cycle (Cq). Each box-and-whisker plot represents 6 fish, 3 from each replication of the experiment. NC = negative control fish not exposed to the parasite. PC = positive control fish exposed to the parasite in water alone; b: Adjusted P-values from Dunn's test with Holm correction comparing Cq between each treatment and the positive control.

Appreciable, but not significant differences existed between the PC fish and the CaCl$_2$ and KCl treatment groups (Dunn's test with Holm correction, p=0.149 and 0.152 respectively). Fish exposed to parasites in 0.025 mM diphenhydramine displayed sedation and slowed swimming not observed in the chemical tolerance test. Because of these signs and that their respiration rates were depressed, making the test likely invalid, these fish were not included in the qPCR analysis.

Table 2.2. Summary of results from the *in vitro* and *in vivo* experiments, with data from literature sources (in parentheses) of the responses of Cnidarians to the compounds. + indicates treatment increased discharge relative to an untreated control. - indicates treatment decreased discharge relative to an untreated control. 0 indicates no effect, and NA indicates data not available. * Indicates a significant (p<0.05) result in our trials.

Test Compound	Results *in vitro* trials	Results *in vivo* trials	Literature data on responses of Myxozoa	Literature data on responses of free-living Cnidaria
NaCl	+*	-*	+ (20)	+ (24)
KCl	+	-	+ (20)	+ (25, 26, 27, 38)
Diphenhydramine	0	NA	NA	- (39, 40)
$CaCl_2$	-	-	+/- (20, 4)	- (41, 42, 24)
$FeCl_2$	0	-	NA	- (12)
$GdCl_3$	0	-	NA	- (43)

DISCUSSION

In Myxozoa, unlike free-living Cnidaria, spore response includes both nematocyst discharge and sporoplasm migration, which are the necessary first steps in the host infection process. The timeframes for these processes only partially overlap. Tubule discharge in response to chemical addition occurs nearly instantaneously (less than 10 ms for *M. cerebralis* actinospores activated by 30% ammonia)[4], while sporoplasm migration occurs over several minutes (5.4 minutes for *Henneguya nuesslini* actinospores activated with carp mucus homogenate)[4]. Literature studies that examined ion-exchange in nematocysts of free-living Cnidaria, changes in nematocyst volume, indicative of changes in intracapsular osmotic pressure, were observed and ceased in < 10 minutes.[36] The practical goal of the *in vitro* assay was to screen a variety of compounds for their ability to promote or inhibit tubule discharge and sporoplasm migration. Accordingly, we

added the compounds to each treatment group, and waited 15 minutes (50% more time to account for possible variation) before sub-sampling and fixing actinospores. The purpose of sampling at this time point was to assess the effect of the chemical compounds on the actinospores in the absence of a fish signal. Immediately afterwards, we added the fish mucus homogenate and waited an additional 30 minutes before fixing the final, "post mucus" sample. This second sample allowed us to assess the effect of the chemicals on the "natural" infection processes. Comparison between pre-mucus samples taken at 15 minutes, and the post-mucus samples allowed us to determine whether each treatment chemically induced discharge or enhanced or diminished the actinospores' ability to respond to mucus stimuli.

To better mimic parasite response to live fish, we employed rainbow trout mucus homogenate rather than inosine-arginine, which has shown similar activation properties[32], and we wanted the *in vitro* tests to mimic the subsequent *in vivo* assay with live fish. We assumed, given the limited possible timeframe for attachment in the wild, that actinospores activated with a "natural" mucus stimulus will respond as quickly as those activated with a chemical stimulus, and that sporoplasm migration in *M. cerebralis* would occur at a similar rate as that in *H. nuesslini*, a parasite studied with inosine-arginine stimulation, and which shares actinospore morphology and fish hosts with *M. cerebralis*[4]. However, the use of complete mucus made it impossible for us to accurately determine and administer homogenous, quantifiable doses of inosine, the signaling compound in fish mucus. Similarly, the use of rainbow trout mucus may have given results that were specific to the fish we extracted mucus from, with its own particular combination of compounds. A practical disadvantage of using complete mucus was the homogenate often obscured actinospores during microscopy, which made categorization difficult and required more spores to be observed.

In previous studies that employed mucus homogenate as an activator, tubule discharge did not always coincide with sporoplasm migration, and vise versa[44]. With this is mind, we designed an *in vitro* assay that could quantify both processes independently. We found that rainbow trout mucus was an effective activator of nematocysts, resulting in almost double the proportion of actinospores with fired tubules than a negative control maintained in the same conditions over the 46 minute experiment.

In our *in vivo* assay, we observed unanticipated variability between replicate fish from the same exposure container, as much as 100-fold difference in DNA quantity. This may be due to differences in individual fish behavior during infection, for example movement, stress level, respiration rate, and position in the exposure cup. Gills were examined rather than other target organs like the fins or skin, because we expected respiration rate to be more similar between fish than swimming speed or fin movement. Despite this precaution, fish movement during the experiment was limited, and may have stratified exposure to actinospores. Some fish were observed to be stationary beside the pipette tip bubblers, where they likely received different actinospore exposures. In future work we would consider an alternative method of aeration, the use of individual fish per trial, or modifications to the size or configuration of the exposure vessel to ensure equal fish movement/exposure to reduce the variation. A future study comparing tissue types for consistent parasite infection under varying behavioral conditions could suggest a more suitable organ for detection.

For chemical treatments, we used concentrations at the upper limit of what was either known to be effective in Cnidarians (Table 2.2), or that we demonstrated were non-lethal to fish in preliminary tolerance trials.

ENHANCERS OF NEMATOCYST DISCHARGE

NaCl was the only compound to have a significant effect in either test and did so in both the *in vitro* and *in vivo* tests (see Table 5). In the *in vitro* assay, for subsamples taken both prior to and after addition of mucus, NaCl enhanced polar tubule discharge, even after those initially "pre-fired" actinospores were subtracted from the total proportion of discharged actinospores. In both the *in vitro* and *in vivo* tests, KCl behaved similarly to NaCl, but it had less of an effect in the *in vivo* assay (but where it was tested at a much lower concentration).

Observation from the *in vitro* assay show effects analogous to studies with free-living Cnidaria[45,25,23,24,38,27], thus we propose that the NaCl and KCl-induced discharge we observed in *M. cerebralis* actinospores (before addition of fish mucus) was likely caused by exchange of divalent cations bound to poly-gamma glutamate during sporogenesis, with two monovalent cations. This increases the intracapsular pressure and promotes discharge of the nematocysts,

either through dislodgement of the nematocysts' "stopper," or disruption of the poly-gamma glutamate matrix. For spores that did not discharge immediately in NaCl and KCl, the osmotic pressure likely remained enhanced, in a hypersensitized "hair trigger" state, which made the actinospores more likely to discharge upon the addition of mucus. These *in vitro* observations led us to predict that NaCl-enhanced tubule discharge would equate to increased infectivity of the spores in the *in vivo* trials.

Intriguingly, our *in vivo* results demonstrated the opposite, with exposure to NaCl significantly reducing parasite DNA detection on fish gills (our proxy for infection). This may have been due to tubule pre-discharge (as seen in the *in vitro* test) rendering many spores non-viable for infection and resulting in reduced attachment. Yet our own *in vitro* data do not support this supposition, as they showed that when mucus was added, a greater proportion of actinospores reacted *even after* the pre-mucus proportion was subtracted. If spores reacted to fish the same as mucus, then more would have been expected to attach and be detected, not fewer. Accordingly, we propose an alternate hypothesis that is consistent with both *in vitro* and *in vivo* observations: that actinospores in the "hair trigger" state discharged prematurely in the water column when fish were present, due to the strong fish mucus signal possibly in combination with the additional mechanical stimulation from proximity to living fish. Regardless of the mechanism, the role of NaCl in enhancing tubule discharge in the *in vitro* assay, and the reduced infection observed in the *in vivo* assay suggests that spores with discharged tubules are less viable for infection than unfired spores.

We observed an interesting difference between NaCl and KCl when considering both polar tubule discharge *and* outward migration of the sporoplasm. After addition of mucus, actinospores in KCl were significantly more likely than the PC to be in a discharged and migrated out state (Tukey HSD p=0.0165). This effect was not observed for NaCl (Tukey HSD p=0.9996) or any other treatment. No chemical treatment in the absence of a mucus stimulus was able to induce sporoplasm migration. The motility of the sporoplasm involves pseudopodia[5,46], and we have possibly shown that motility is mediated in some way by KCl exchange, rather than NaCl.

INHIBITORS OF NEMATOCYST DISCHARGE

Calcium was the only treatment to appreciably inhibit discharge in the *in vitro* test (p=0.152). This was consistent with data from experiments with free-living Cnidaria[24,36,41]. In some species, calcium is thought to be bound to or crosslink the anionic poly-gamma glutamate in the unfired nematocyst, thereby reducing the osmotic potential of the nematocyst[45,47,48]. The addition of external Ca^{2+} has been shown to decrease the internal osmotic pressure within nematocysts, possible by reducing the differential between the interior of undischarged nematocysts and the environment. In the presence of high external ion concentrations, e.g. Na^+, the divalent cations covalently bound to a matrix of anionic poly-gamma glutamate are exchanged through the capsule wall with monovalent cations that can only be more loosely bound to the internal matrix. In free-living cnidarians, this exchange increases the internal osmotic pressure, leading to tubule discharge[45]. Given that we observed discharge induced by monovalent salts (potentially through ion exchange as discussed above), we propose that *M. cerebralis* nematocysts contain Ca^{2+} or another divalent salt in their native state. This concurs with the cationic staining of myxozoan nematocyst contents observed by Piriatinsky et al. 2017.

In both the *in vitro* and *in vivo* experiments, we included $FeCl_2$ as an alternative divalent cation treatment to Ca^{2+}. In both cases, the compound appeared to be oxidized over the course of the experiment, with the solution shifting from a translucent green to murky brown. This was more apparent in the *in vivo* assay, which lasted longer and had aeration applied. We propose future trials should use stable iron salts, such as $FeCl_3$, or an alternate divalent cation such as strontium.

SIGNAL BLOCKERS

We tested the antihistamine diphenhydramine as it has been shown to inhibit nematocyst firing in free-living Cnidaria by competitively inhibiting the imino acid receptors involved in sensing[49]. In our *in vitro* trials, a similar concentration of diphenhydramine showed neither inhibition nor promotion of nematocyst discharge. We interpret this to mean that either the concentration was insufficient to saturate the putative receptors, or the host receptors are very different in myxozoans than free-living Cnidaria, despite both reacting to fish. Differences in sensory machinery might be the result of evolution towards host specificity in Myxozoa[2]. We were

unable to test diphenhydramine *in vivo* as the tested concentration sedated the animals and suppressed respiration.

Similar to our results with diphehydramine, we observed no effect on spores from GdCl₃. Based on published data, we expected Gd^{3+} to inhibit tubule discharge (and thus transmission to fish). It is hypothesized that in free-living Cnidaria, the Gd^{3+} interferes with voltage-gated calcium channels, known to be a component of the initial signal transduction step of nematocyst discharge particularly concerted discharge of multiple nematocysts[50,43,51]. From our results with *M. cerebralis*, we propose that the observed null effect makes biological sense in an organism that has few nematocysts that it fires individually: it may have lost the now-redundant mechanism (voltage-gated ion channels) needed to fire many nematocysts simultaneously.

CONCLUDING REMARKS

The discovery of poly-gamma glutamate, nematogalectins, and calreticulin in the nematocysts of *C. shasta*[14] suggest the molecular makeup of nematocysts in Myxozoa is similar to that of free-living Cnidaria. Further bioinformatic analyses may uncover specific ion channel components and signaling complexes whose roles could be confirmed by testing their interaction with proteins using our treatment assays. The parallel assays that we developed should facilitate continued exploration of myxozoan nematocyst discharge and infection in the presence of different compounds, chosen to probe specific interactions with proteins and structures identified in the 'omics studies. One exciting enhancement to *in vitro* testing would be to design a microfluidics flow cell, similar to the 'Traptasia' employed by Treuren et al. (2019)[55] to visualize coral larvae. We envision a flow cell that could capture and enable temporal imaging of individual myxozoan spores as they respond to test compounds streamed through the flowcell. This would reveal fine-scale temporal and physical effects of different compounds to different myxozoan spores, potentially even myxospores which are much smaller (10-20 µm) than the *M. cerebralis* actinospores that we used with our *in vitro* setup (~150 µm across).

Collectively, the results of the *in vitro* and *in vivo* experiments suggest that like many free-living cnidarians, *M. cerebralis* actinospores contain nematocysts with divalent cations bound to poly-gamma glutamate complexes which can be passively exchanged with ions in the environment.

Further, the increase in osmotic pressure that occurs when external monovalent cations are exchanged for internal divalent cations, hypersensitizes spores to fish stimuli but makes them less viable for infection. While it was not the goal of these experiments, these results suggest that NaCl, and to a lesser extent, $CaCl_2$ may show promise as a novel treatments for myxozoan parasites in aquaculture, particularly for fish which can withstand high salt concentrations. NaCl is already employed in aquaculture to treat infections from external parasites[52] and minimize osmoregulatory stress[53,54]. Furthermore, seawater applied as a treatment may be used to examine the nature of ocean-dwelling myxozoans and provide insight into the ability of freshwater myxozoans like *C. shasta*, to infect fish within the halocline of river mouths.

ACKNOWLEDGMENTS

REFERENCES

1. Atkinson, S. D., Bartholomew, J. L. & Lotan, T. Myxozoans: Ancient metazoan parasites find a home in phylum Cnidaria. *Zoology* **129**, 66–68 (2018).
2. Holzer, A. S., Bartošová-Sojková, P., Born-Torrijos, A., Lövy, A., Hartigan, A., & Fiala, I. The joint evolution of the Myxozoa and their alternate hosts: A cnidarian recipe for success and vast biodiversity. *Mol. Ecol.* **27**, 1651–1666 (2018).
3. El-Matbouli, M., Hoffmann, R. W., Schoel, H., McDowell, T. S. & Hedrick, R. P. Whirling disease: host specificity and interaction between the actinosporean stage of *Myxobolus cerebralis* and rainbow trout *Oncorhynchus mykiss*. *Diseases of Aquatic Organisms* **35**, 1–12 (1999).
4. Kallert, D. M., Ponader, S., Eszterbauer, E., El-Matbouli, M. & Haas, W. Myxozoan transmission via actinospores: new insights into mechanisms and adaptations for host invasion. *Parasitology* **134**, 1741–1750 (2007).
5. Bjork, S. J. & Bartholomew, J. L. Invasion of *Ceratomyxa shasta* (Myxozoa) and comparison of migration to the intestine between susceptible and resistant fish hosts. *Int. J. Parasitol.* **40**, 1087–1095 (2010).
6. Kallert, D. M., Bauer, W., Haas, W. & El-Matbouli, M. No shot in the dark: myxozoans chemically detect fresh fish. *Int. J. Parasitol.* **41**, 271–276 (2011).
7. Sipos, D., Ursu, K., Dán, Á., Herczeg, D. & Eszterbauer, E. Susceptibility-related differences in the quantity of developmental stages of *Myxobolus* spp. (Myxozoa) in fish blood. *PLoS One* **13**, e0204437 (2018).
8. Adkison MA, H. R. P. Purification of the serine protease from the triactinomyxon stage of

Myxobolus cerebralis. *Proceedings of the 7th annual symposium on whirling disease, Salt Lake City, 8–9 Feb 2001* (2001).

9. Orts, D. J. B., Moran, Y., Cologna, C. T., Peigneur, S., Madio, B., Praher, D., Quinton, L., De Pauw, E., Bicudo, J. E., Tytgat, J., & de Freitas, J. C. BcsTx3 is a founder of a novel sea anemone toxin family of potassium channel blocker. *FEBS J.* **280**, 4839–4852 (2013).

10. Jones, C. S. The control and discharge of nematocysts in hydra. *J. Exp. Zool.* **105**, 25–60 (1947).

11. Carré, D. [Hypothesis on the mechanism of cnidocyst discharge (author's transl)]. *Eur. J. Cell Biol.* **20**, 265–271 (1980).

12. Weber, J. Nematocysts (stinging capsules of Cnidaria) as Donnan-potential-dominated osmotic systems. *Eur. J. Biochem.* **184**, 465–476 (1989).

13. Tardent, P. The cnidarian cnidocyte, a hightech cellular weaponry. *BioEssays* **17**, 351–362 (1995).

14. Piriatinskiy, G., Atkinson, S. D., Park, S., Morgenstern, D., Brekhman, V., Yossifon, G., Bartholomew, J. L., & Lotan, T. Functional and proteomic analysis of *Ceratonova shasta* (Cnidaria: Myxozoa) polar capsules reveals adaptations to parasitism. *Sci. Rep.* **7**, 9010 (2017).

15. Hoffman, G. L., Putz, R. E. & Dunbar, C. E. Studies on *Myxosoma cartilaginisn* sp. (Protozoa: Myxosporidea) of Centrarchid Fish and a Synopsis of the Myxosoma of North American Freshwater Fishes. *The Journal of Protozoology* **12**, 319–332 (1965).

16. Yasutake, W. T. & Wood, E. M. Some Myxosporidia Found in Pacific Northwest Salmonids. *The Journal of Parasitology* **43**, 633 (1957).

17. Lewis, W. M. & Summerfelt, R. C. A Myxosporidian, Myxobolus notemigoni sp. n., Parasite of the Golden Shiner. *The Journal of Parasitology* **50**, 386 (1964).

18. Lom, J. Notes on the extrusion and some other features of myxosporidian spores. *Acta Protozool.* 321–327 (1964).

19. Kudo, R. Experiments on the Extrusion of Polar Filaments of Cnidosporidian Spores. *The Journal of Parasitology* **4**, 141 (1918).

20. Eric J Wagner, Quinn Cannon, Mark Smith, Ryan Hillyard, Ronney Arndt. Extrusion of Polar Filaments of the *Myxobolus cerebralis* Triactinomyxon by Salts, Electricity, and Other Agents. *Am. Fish. Soc. Symp.* 61–76 (2002).

21. Jones, K. H. & Senft, J. A. An improved method to determine cell viability by simultaneous staining with fluorescein diacetate-propidium iodide. *J. Histochem. Cytochem.* **33**, 77–79 (1985).

22. Dujardin, F. Mémoire sur le développement des polypes hydraires et méduses. *Ann. Sci. Nat.* 257–281 (1845).

23. Yanagita, T. M. Physiological mechanism of nematocyst responses in sea-anemone—III excitation and anaesthetization of the nettling response system. *Comparative Biochemistry and Physiology* **1**, 123–139 (1960).

24. Blanquet, R. Ionic effects on discharge of the isolated and in situ nematocysts of the sea anemone, *Aiptasia pallida*: A possible role of calcium. *Comparative Biochemistry and Physiology* **35**, 451–461 (1970).

25. Parker, G. H. The reversal of ciliary movement in metazoans. *American Journal of Physiology-Legacy Content* **13**, 1–16 (1905).

26. Yanagita, T. M. Physiological mechanism of nematocyst responses in sea-anemone—IV. Effects of surface-active agents on the cnidae in situ and in isolation. *Comparative*

Biochemistry and Physiology **1**, 140–154 (1960).

27. Kawaii, S., Yamashita, K., Nakai, N. & Fusetani, N. Intracellular calcium transients during nematocyst discharge in actinulae of the hydroid,*Tubularia mesembryanthemum. The Journal of Experimental Zoology* **278**, 299–307 (1997).

28. Mátyus, L., Szabó, G., Jr, Resli, I., Gáspár, R., Jr & Damjanovich, S. Flow cytometric analysis of viability of bull sperm cells. *Acta Biochim. Biophys. Acad. Sci. Hung.* **19**, 209–214 (1984).

29. Markiw, M. E. Experimentally Induced Whirling Disease II. Determination of Longevity of the Infective Triactinomyxon Stage of *Myxobolus cerebralis* by Vital Staining. *Journal of Aquatic Animal Health* **4**, 44–47 (1992).

30. Kallert, D. M. & El-Matbouli, M. Differences in viability and reactivity of actinospores of three myxozoan species upon ageing. *Folia Parasitol.* **55**, 105–110 (2008).

31. Cannon, Q. & Wagner, E. Comparison of Discharge Mechanisms of Cnidarian Cnidae and Myxozoan Polar Capsules. *Reviews in Fisheries Science* **11**, 185–219 (2003).

32. Kallert, D. M., Forró, B. & Eszterbauer, E. Inosine-arginine salt as a promising agent for in vitro activation of waterborne fish-pathogenic myxozoan actinospores. *Diseases of Aquatic Organisms* **109**, 149–154 (2014).

33. Yokoyama, H., Ogawa, K. & Wakabayashi, H. Chemoresponse of actinosporean spores of *Myxobolus cultus* to skin mucus of goldfish Carassius auratus. *Diseases of Aquatic Organisms* **21**, 7–11 (1995).

34. Kallert, D. M., El-Matbouli, M. & Haas, W. Polar filament discharge of *Myxobolus cerebralis* actinospores is triggered by combined non-specific mechanical and chemical cues. *Parasitology* **131**, 609–616 (2005).

35. Kallert, D. M., Ponader, S., Eszterbauer, E., El-Matbouli, M. & Haas, W. Myxozoan transmission via actinospores: new insights into mechanisms and adaptations for host invasion. *Parasitology* **134**, 1741–1750 (2007).

36. Hidaka, M. Effects of Ca^{2+} on the volume of nematocysts isolated from acontia of the sea anemone *Calliactis tricolor. Comparative Biochemistry and Physiology Part A: Physiology* **101**, 737–741 (1992).

37. Kelley, G. O., Zagmutt-Vergara, F. J., Leutenegger, C. M., Myklebust, K. A., Adkison, M. A., McDowell, T. S., Marty, G. D., Kahler, A. L., Bush, A. L., Gardner, I. A. & Hedrick, R. P. Evaluation of Five Diagnostic Methods for the Detection and Quantification of *Myxobolus cerebralis. Journal of Veterinary Diagnostic Investigation* **16**, 202–211 (2004)

38. McKay, M. C. & Anderson, P. A. V. Preparation and Properties of Cnidocytes from the Sea Anemone *Anthopleura elegantissima. Biol. Bull.* **174**, 47–53 (1988).

39. Thorington, G. U. & Hessinger, D. A. Control of Cnida Discharge: I. Evidence for Two Classes of Chemoreceptor. *The Biological Bulletin* **174**, 163–171 (1988).

40. Lotan, A. Compositions and methods for inhibiting nematocyst discharge. *US Patent* (2002).

41. Salleo, A. Discharge Mechanism of the Nematocysts of *Pelagia noctiluca. Proceedings in Life Sciences* 63–76 (1984). doi:10.1007/978-3-642-69903-0_6

42. Tardent, P. The cnidarian cnidocyte, a hightech cellular weaponry. *BioEssays* **17**, 351–362 (1995).

43. Salleo, A., La Spada, G. & Barbera, R. Gadolinium is a powerful blocker of the activation of nematocytes of Pelagia noctiluca. *J. Exp. Biol.* **187**, 201–206 (1994).

44. Kallert, D. M., Ponader, S., Eszterbauer, E., El-Matbouli, M. & Haas, W. Myxozoan transmission via actinospores: new insights into mechanisms and adaptations for host

invasion. *Parasitology* **134**, 1741–1750 (2007).

45. Hidaka, M. & Afuso, K. Effects of Cations on the Volume and Elemental Composition of Nematocysts Isolated from Acontia of the Sea Anemone *Calliactis polypus*. *Biol. Bull.* **184**, 97–104 (1993).

46. Alama-Bermejo, G., Bron, J. E., Raga, J. A. & Holzer, A. S. 3D Morphology, ultrastructure and development of *Ceratomyxa puntazzi* stages: first insights into the mechanisms of motility and budding in the Myxozoa. *PLoS One* **7**, e32679 (2012).

47. Lubbock, R. & Amos, W. B. Removal of bound calcium from nematocyst contents causes discharge. *Nature* **290**, 500–501 (1981).

48. Lubbock, R., Gupta, B. L. & Hall, T. A. Novel role of calcium in exocytosis: mechanism of nematocyst discharge as shown by x-ray microanalysis. *Proc. Natl. Acad. Sci. U. S. A.* **78**, 3624–3628 (1981).

49. Thorington, G. U. & Hessinger, D. A. Controls of discharge: factors affecting discharge of cnidae. *The Biology of Nematocysts* 233–253 (1988). doi:10.1016/b978-0-12-345320-4.50018-3

50. Gitter, A. H., Oliver, D. & Thurm, U. Calcium- and voltage-dependence of nematocyst discharge in *Hydra vulgaris*. *Journal of Comparative Physiology A* **175**, (1994).

51. Kawaii, S., Yamashita, K., Nakai, M., Takahashi, M. & Fusetani, N. Calcium Dependence of Settlement and Nematocyst Discharge in Actinulae of the Hydroid *Tubularia mesembryanthemum*. *Biol. Bull.* **196**, 45–51 (1999).

52. Dewi, R. R. The Efficacy of Sodium Chloride Application in the Control of Fish Lice (*Argulus* sp) infection on Tilapia (*Oreochromis niloticus*). *Acta Aquatica: Aquatic Sciences Journal* **5**, (2018).

53. Mifsud, C. & Rowland, S. J. Use of salt to control ichthyophthiriosis and prevent saprolegniosis in silver perch,*Bidyanus bidyanus*. *Aquaculture Research* **39**, 1175–1180 (2008).

54. Tacchi, L., Lowrey, L., Musharrafieh, R., Crossey, K., Larragoite, E. T., & Salinas, I. Effects of transportation stress and addition of salt to transport water on the skin mucosal homeostasis of rainbow trout. *Aquaculture* **435**, 120–127 (2015).

55. Van Treuren, W., Brower, K. K., Labanieh, L., Hunt, D., Lensch, S., Cruz, B., Cartwright, H. N., Tran, C., & Fordyce, P. M. Live imaging of Aiptasia larvae, a model system for coral and anemone bleaching, using a simple microfluidic device. *Sci. Rep.* **9**, 9275 (2019).

CONCLUDING SUMMARY

Benjamin Americus, Stephen D. Atkinson

In this thesis project, I explored similarities and differences in the structure and function of Cnidarian nematocysts – specialized organelles that consist of a capsule with a single opening and coiled tubule "stinger" inside. Free-living cnidarians utilize this cellular weaponry for defense and predation[1] whereas parasitic cnidarians, the myxozoans, use it to anchor to their hosts as the first step of infection[2]. Myxozoans are a diverse and speciose group of cnidarians that have complex life cycles involving two hosts (vertebrate and invertebrate) and two distinct spore stages (actinospores and myxospores). In my comparisons, I utilized two model myxozoans, *Myxobolus cerebralis* and *Ceratonova shasta*, which share the same fish hosts, and have life cycles that are maintained in the John L. Fryer Aquatic Animal Health Laboratory at OSU. The availability of parasites under controlled conditions permitted me to examine and experiment with both organisms at different stages of their life cycles and use them for functional studies with susceptible fish. My investigations consisted of wet-lab techniques and bioinformatic analyses.

First, with *M. cerebralis* I developed two novel wet-lab assays to examine how myxozoan tubule discharge, sporoplasm migration, and infection were influenced by a range of metal ions with different valences, and an antihistamine. I devised an *in vitro* procedure that utilized rainbow trout mucus homogenate as a proxy for live fish and parasite actinospores from my worm cultures. Under the microscope, I examined how each chemical treatment affected the ability of *M. cerebralis* actinospores to react to the host signal. I found that two monovalent cations, Na^+ and K^+ acted similarly, inducing tubule discharge in the absence of mucus and enhancing the actinospores response to the mucus stimulus (Na^+ to a statistically significant extent relative to a water control). In contrast, Ca^{2+} reduced tubule discharge in response to mucus.

In follow-up *in vivo* tests, I exposed juvenile rainbow trout to high concentrations of *M. cerebralis* actinospores in baths of the same cations. As a proxy for "infection" to the fish, I used a sensitive and specific qPCR assay to quantify the amount of parasite DNA extracted from the gills after the different treatments. I found that Na^+ significantly reduced the parasite load relative to positive control fish exposed to the same parasite dose in the absence of chemical

treatment. When considered together, the results from *in vitro* and *in vivo* assays suggest the addition of Na^+ ions to the external environment of the nematocyst induces a hypersensitizing effect, shifting actinospores towards a "hair trigger" state in which they may discharge prematurely, or inaccurately when presented with host signals.

My findings with myxozoan nematocysts correlate with a body of published work on behavior of nematocysts from free-living cnidarians, which suggests the walls of nematocysts are permeable to cations[3]. In the presence of high external ion concentrations, e.g. Na^+, the divalent cations covalently bound to a matrix of anionic poly-gamma glutamate inside the nematocyst are exchanged through the capsule wall with monovalent cations that can only be more loosely bound to the internal matrix. In free-living cnidarians, this exchange increases the internal osmotic pressure, leading to tubule discharge[4]. I consider this as the underlying cause of the nematocysts entering a "hair trigger" state.

Normal nematocyst discharge has been shown to coincide with rapid exocytosis of calcium[1,4]. Taken together with observations that there are spikes in action potential in nematocysts prior to discharge, these features suggest that voltage-gated ion channels play a role in the discharge process. The presence of ion channels is also suggested by the ability of trivalent cations Gd^{3+} and La^{3+} to inhibit nematocyst discharge[5]. These compounds exhibit signal inhibition/blocking effects as they are large enough to physically occlude voltage-gated channels[6].

In Appendix A, I present my preliminary data using bioinformatics approaches to investigate the presence and expression of myxozoan genes homologous to those known in free-living Cnidaria to code for voltage-gated ion channel components. I used existing proteomic and transcriptomic data from *C. shasta* and developed novel datasets of time-series gene expression within the host. I analyzed the expression of voltage-gated ion channel components and nematocyst-specific genes in the time-course data, and found that homologs of L- and T-type voltage-gated calcium channels were present in the *C. shasta* libraries and were co-expressed with genes related to nematogalectin, a protein found exclusively in nematocysts. The detection of the genetic signatures of ion channels in *C. shasta* further exemplifies the molecular and mechanistic similarities among divergent Cnidaria. The role of these channels in myxozoan nematocyst discharge remains unknown and will be the subject of future studies.

In combination, these results support the hypothesis that despite ~650 million years of divergence[10], genome reduction [11] and an evolution to parasitism, myxozoans maintain nematocysts that are structurally and functionally homologous to those from their free-living cnidarian relatives.

REFERENCES

1. Holstein, T. & Tardent, P. An ultrahigh-speed analysis of exocytosis: nematocyst discharge. *Science* **223**, 830–833 (1984).
2. El-Matbouli, M., Hoffmann, R. W., Schoel, H., McDowell, T. S. & Hedrick, R. P. Whirling disease:host specificity and interaction between the actinosporean stage of *Myxobolus cerebralis* and rainbow trout Oncorhynchus mykiss. *Diseases of Aquatic Organisms* **35**, 1–12 (1999).
3. Tardent, P. The cnidarian cnidocyte, a hightech cellular weaponry. *BioEssays* **17**, 351–362 (1995).
4. Hidaka, M. & Afuso, K. Effects of Cations on the Volume and Elemental Composition of Nematocysts Isolated from Acontia of the Sea Anemone *Calliactis polypus*. *Biol. Bull.* **184**, 97–104 (1993).
5. Salleo, A., La Spada, G. & Barbera, R. Gadolinium is a powerful blocker of the activation of nematocytes of *Pelagia noctiluca*. *J. Exp. Biol.* **187**, 201–206 (1994).
6. Beedle, A. M., Hamid, J. & Zamponi, G. W. Inhibition of transiently expressed low- and high-voltage-activated calcium channels by trivalent metal cations. *J. Membr. Biol.* **187**, 225–238 (2002).
7. Moran, Y. & Zakon, H. H. The evolution of the four subunits of voltage-gated calcium channels: ancient roots, increasing complexity, and multiple losses. *Genome Biol. Evol.* **6**, 2210–2217 (2014).
8. Bouchard, C. & Anderson, P. A. V. Immunolocalization of a voltage-gated calcium channel β subunit in the tentacles and cnidocytes of the Portuguese man-of-war, *Physalia physalis*. *Biol. Bull.* **227**, 252–262 (2014).
9. Bouchard, C. Cloning and functional expression of voltage-gated ion channel subunits from cnidocytes of the Portuguese Man O'War *Physalia physalis*. *Journal of Experimental Biology* **209**, 2979–2989 (2006).
10. Holzer, A. S., Bartošová-Sojková, P., Born-Torrijos, A., Lövy, A., Hartigan, A., & Fiala, I. The joint evolution of the Myxozoa and their alternate hosts: A cnidarian recipe for success and vast biodiversity. *Mol. Ecol.* **27**, 1651–1666 (2018).
11. Chang, E. S., Neuhof, M., Rubinstein, N. D., Diamant, A., Philippe, H., Huchon, D., & Cartwright, P. Genomic insights into the evolutionary origin of Myxozoa within Cnidaria. Proc. Natl. Acad. Sci. U. S. A. 112, 14912–14917 (2015).

APPENDICES

APPENDIX A:

INITIAL DEVELOPMENT OF BIOINFORMATIC METHODS FOR A MULTI- 'OMICS INVESTIGATION OF VOLTAGE-GATED ION CHANNELS IN THE MYXOZOAN CERATONOVA SHASTA

The energy that drives cnidarian nematocyst discharge is thought to be the combination of intrinsic forces, built into a coiled tubule during cnidogenesis[2,3,4,5,6] and intracapsular hydrostatic pressure generated through water swelling the nematocyst to equilibrate an osmotic gradient[7]. Undischarged nematocysts contain high concentrations (500–600 mmol per kg by wet weight) of Ca^{2+} which rapidly dissociates via exocytosis during discharge[3]. In Chapter 2, I identified Na^+ dependent discharge, which suggested interference with the exocytosis of a divalent cation stored within the nematocyst. These observations support the hypothesis that voltage-gated ion channels are a component of the discharge machinery of nematocysts in both myxozoans and free-living cnidarians.

Our lab collaborated on the description of the *C. shasta* nematocyst proteome[18] which provides the most definitive insight into the molecular makeup of nematocysts in a myxozoan. The proteome comprises 114 sequences that includes homologs of many of the hallmark proteins of nematocysts in free-living cnidarians. This dataset also included proteins containing domains for a type-A von-Willebrand factor. While not directly tied to nematocyst discharge, these domains have been consistently identified in proteomic datasets from nematocysts[21]. In other metazoans systems, von-Willebrand factors are involved in Ca^{2+} homeostasis, potentially through regulating Ca^{2+} transport through sarco/endoplasmic reticulum Ca^{2+}-ATPases (SERCAs). These are ATP-driven calcium channels ion channels that actively transport calcium from the cytoplasm into the sarcoendoplasmic reticulum[22].

Here I outline my initial exploration of the co-expression between genes related to voltage-gated ion channels and those related to nematocyst development in *C. shasta*. Co-expression analysis of RNA-seq data is emerging as a bioinformatic technique that can provide insight into the functional roles and temporal expression patterns of genes through organismal development[29]. In well characterized model systems, genes that are co-expressed (sharing similar expressional profiles) are often functionally related[30] and expressed within the same cell type[31].

I used co-expression analyses to test the hypothesis that voltage-gated ion channels are involved in the buildup and exocytation of calcium in myxozoan nematocysts, as they are suspected to do in free-living Cnidaria[3,11,29]. This hypothesis would be supported if I found that these two sets of genes are co-expressed during sporogenesis and nematocyst development in *C. shasta* transcriptome datasets. I analyze time-course RNA-Seq data from an infected fish by three methods for co-expression analysis: Short Time Series Expression Miner (STEM)[32] profiling, clustering of differentially expressed (DE) genes using DESeq2[33], and a co-expression clustering of DE genes using coseq[34].

METHODS AND RESULTS

Proteomics analysis

I obtained protein sequences for the six isoforms of the voltage-gated ion channel α-subunits described in Moran et al. 2014[10] from Genbank, and directly from authors of previous studies. The *C. shasta* nematocyst proteome was described previously by collaborative work involving our lab (Piriatinskiy et al. 2017[14]). As an initial screen, I used BLASTp to search for *C. shasta* homologs of the six isoforms of the voltage-gated ion channel α-subunits from among the 114 protein *C. shasta* nematocyst proteome. This did not yield any highly homologous (e-value <1e-6) sequences

Source of Time Series data

I used timeseries RNA-seq data and de novo *C. shasta* transcriptome assemblies from studies being undertaken by other lab members (Alama-Bermejo in preparation, Barrett et al. in preparation). These data came from sequential sampling of a group of juvenile rainbow trout exposed to *C. shasta*. Three fish were removed from the group at 7, 14, and 21 days post-exposure; these timepoints represent different stages of parasite development: pre-sporogony, during sporogony, and post-sporogony. Each fish was euthanized, and a portion of large intestine sampled for RNA that was then sequenced on an Illumina HiSeq3000 with 100 bp single-end reads. Two datasets were produced: a combined *C. shasta* transcriptome and separate read libraries for each timepoint.

Transcriptome analysis

Gene names were assigned to transcripts by comparisons using BLASTx to the UniProt database (Release 2015), with a cut-off e-value of 1e-6. A keyword search for genes whose annotations matched included "voltage," "channel," "nemat," and "gamma-glut", and "minicollagen" yielded 54 results (Fig. A1). The "voltage" category contained 19 genes annotated as voltage-dependent and voltage-gated potassium and calcium channel subunits. Genes which included both "channel" and "voltage" in their annotations were assigned to the "voltage" group. The 27 genes remaining were sodium and chloride channels, calcium-activated potassium channels, potassium-activated chloride channels, and non-specific transmembrane channels. This group is hereafter referred to as "non-voltage." The "nemat" category contained three isomers of putative nematogalecin. The "poly-gamma" category contained one gamma-glutamyltranspeptidase-like gene and four genes for glutamine-gamma-glutamyltransferase. No genes included "minicollagen" in their annotations.

Gene — Annotation

Gene	Annotation
TRINITY_DN25892_c0_g1	Putative_calcium_channel_voltage-dependent_alpha2/delta_subunit_1_
TRINITY_DN31757_c0_g1	Putative_calcium_channel_voltage-dependent_alpha2/delta_subunit_1_
TRINITY_DN32077_c0_g1	potassium_voltage-gated_channel_subfamily_H_member_8-like_
TRINITY_DN34957_c0_g1	potassium_voltage-gated_channel_subfamily_KQT_member_4_isoform_X6_
TRINITY_DN36287_c2_g2	Putative_calcium_channel_voltage-dependent_alpha2/delta_subunit_1_
TRINITY_DN3897_c0_g1	Putative_calcium_channel_voltage-dependent_alpha2/delta_subunit_1_
TRINITY_DN39078_c1_g1	Potassium_voltage-gated_channel_subfamily_H_member_4_
TRINITY_DN39199_c0_g1	Potassium_voltage-gated_channel_subfamily_KQT_member_4_
TRINITY_DN39604_c6_g1	Putative_calcium_channel_voltage-dependent_alpha2/delta_subunit_1_
TRINITY_DN39812_c0_g1	potassium_voltage-gated_channel_subfamily_C_member_1-like_
TRINITY_DN39860_c0_g1	Potassium_voltage-gated_channel_subfamily_KQT_member_4_
TRINITY_DN39946_c0_g1	voltage-dependent_calcium_channel_subunit_alpha-2/delta-2-like_isoform_X3_
TRINITY_DN43789_c0_g1	voltage-dependent_T-type_calcium_channel_subunit_alpha-1H-like_
TRINITY_DN6256_c0_g1	voltage-dependent_T-type_calcium_channel_subunit_alpha-1H-like_
TRINITY_DN10381_c0_g1	Voltage-dependent_T-type_calcium_channel_subunit_alpha-1H_
TRINITY_DN22527_c0_g1	Voltage-dependent_calcium_channel_type_A_subunit_alpha-1_
TRINITY_DN35508_c0_g1	Voltage-dependent_L-type_calcium_channel_subunit_alpha-1F_(Fragment)_
TRINITY_DN3857_c0_g1	Voltage-dependent_L-type_calcium_channel_subunit_alpha_
TRINITY_DN38672_c0_g1	Voltage-dependent_L-type_calcium_channel_subunit_alpha_
TRINITY_DN13242_c0_g1	Sodium_leak_channel_non-selective_protein_
TRINITY_DN22013_c0_g1	transient_receptor_potential_cation_channel_subfamily_V_member_4_isoform_X1_
TRINITY_DN28033_c0_g1	Calcium_load-activated_calcium_channel_
TRINITY_DN30961_c0_g1	Chloride_channel_protein_(Fragment)_
TRINITY_DN32141_c0_g1	Transmembrane_channel-like_protein_
TRINITY_DN3339_c0_g1	Small_conductance_calcium-activated_potassium_channel_protein_
TRINITY_DN34189_c0_g1	Potassium_channel_subfamily_T_member_2_
TRINITY_DN36620_c1_g1	Chloride_intracellular_channel_protein_(Fragment)_
TRINITY_DN36706_c0_g1	Potassium_channel_tetramerization_domain_containing_6a_
TRINITY_DN36732_c0_g1	Chloride_channel_protein_
TRINITY_DN37592_c2_g1	Transmembrane_channel-like_protein_
TRINITY_DN37614_c0_g1	Transmembrane_channel-like_protein_
TRINITY_DN37974_c5_g4	epithelial_chloride_channel_protein-like_
TRINITY_DN38222_c0_g1	Chloride_channel_protein_
TRINITY_DN38222_c0_g2	Chloride_channel_protein_
TRINITY_DN38421_c2_g2	Putative_calcium_activated_chlorine_channel_
TRINITY_DN38702_c4_g1	Transmembrane_channel-like_protein_
TRINITY_DN39026_c1_g1	Trimeric_intracellular_cation_channel_type_1B.2_
TRINITY_DN39765_c3_g1	Sodium_channel_epithelial_1_alpha_subunit_
TRINITY_DN39800_c0_g1	Transient_receptor_potential_cation_channel_subfamily_A_member_1_
TRINITY_DN39905_c3_g1	Chloride_channel_protein_
TRINITY_DN40038_c2_g1	Chloride_channel_protein_
TRINITY_DN40088_c0_g1	Potassium_channel_tetramerization_domain-containing_17_
TRINITY_DN40174_c0_g1	Chloride_channel_protein_
TRINITY_DN40502_c2_g6	epithelial_chloride_channel_protein-like_
TRINITY_DN41099_c0_g1	potassium_channel_subfamily_K_member_5-like_
TRINITY_DN43569_c0_g1	calcium-activated_potassium_channel_subunit_beta-4_
TRINITY_DN2910_c0_g1	Putative_nematogalectin_(Fragment)_
TRINITY_DN29333_c0_g1	Putative_nematogalectin_
TRINITY_DN38658_c3_g1	Putative_nematogalectin_
TRINITY_DN36771_c0_g1	Protein-glutamine_gamma-glutamyltransferase_E_(Fragment)_
TRINITY_DN39014_c0_g1	Protein-glutamine_gamma-glutamyltransferase_K_
TRINITY_DN39549_c1_g1	gamma-glutamyltranspeptidase_1-like_
TRINITY_DN40419_c0_g1	Protein-glutamine_gamma-glutamyltransferase_K_
TRINITY_DN41353_c0_g1	protein-glutamine_gamma-glutamyltransferase_E-like_

Annotation
- voltage
- non-voltage
- nemat
- gamma-glut

Figure A1. Gene names and full annotations for 55 genes from the *Ceratonovoa shasta* annotated time-series transcriptome that matched keywords "voltage," "channel"(detailed as "non-voltage,") "nemat," and "gamma-glut"

Phylogenetic Analysis

The best tBLASTn hits in the time series transcriptome were converted to amino acid sequences using NCBI's ORFfinder[35], aligned via ClustalW[36] and trimmed in BioEdit[37] for the regions of highest amino acid conservation. MEGA X 10.1[38] was used to create and visualize a Maximum likelihood tree. The tBLASTn search for the best homologs to voltage-gated calcium channel alpha-subunit protein sequences yielded two transcripts (Figure A.2). When both transcripts were converted to protein sequences, the second, shorter hit was only 46 amino acids long. In the ClustalW alignment, no homologous sections were present between it and all other sequences, thus it was removed from the phylogenetic analysis.

a

Query	Query Channel type	tblasn hit	% identity	e value	bit score
NveCaV1	L-type	TRINITY_DN35508 (L-type subunit)	21.154	3.77e-12	68.6
NveCaV2a	P/Q type	TRINITY_DN35508 (L-type subunit)	25.652	3.22e-20	92.0
NveCaV2b	N-type	TRINITY_DN35508 (L-type subunit)	23.529	8.86e-13	70.1
NveCav2c	R-type	TRINITY_DN35508 (L-type subunit)	21.371	1.23e-11	66.6
NveCaV3a	T-type	TRINITY_DN43789 (T-type subunit)	50.769	4.42e-17	77.0
NveCaV3b	T-type	No hits found	ND	ND	ND

b

NveCav2c
NveCaV3b
NveCaV2b
NveCaV2a
TRINITY DN35508
NveCaV1
NveCaV3a

Figure A2. tBLASTn results: a: comparing protein sequences for voltage-gated calcium channel alpha subunits from from *Nematostella vectensis*[10] to a *Ceratonova shasta* transcriptome assembled from the time-series data; b: Maximum likelihood tree of voltage-gated calcium channel alpha subunit variants and the best homolog from the *Ceratonova shasta* transcriptome. The *C. shasta* transcript is in a single clade with NveCaV1 and NveCaV3b, apart from the CaV2 sequences.

Times Series Analyses

To generate time series expression data for the parasite, I used the tool Salmon[39] to index the *C. shasta* time-series transcriptome assembly and quasi-map raw reads from each of the timepoints to produce quantification files that were used in downstream analysis (three replicates from 7, 14, and 21 dpe each). Count data from Salmon was normalized for increasing parasite load by dividing all counts in each sample by a scaling factor specific to that sample. The scaling factor was calculated by averaging the salmon count data of all isoforms of three known parasite

single-copy genes: glyceraldehyde 3-phosphate dehydrogenase, NADH dehydrogenase [ubiquinone] iron-sulfur protein 2, and Hypoxanthine phosphoribosyltransferase, (Alama-Bermejo, personal correspondence) and dividing it by 100,000 to ensure that this transformation did not result in genes being rounded down to 0 counts.

I examined the temporal expression of two sets of genes. The first "voltage-gated ion channel" set contained transcripts from the time-series transcriptome with annotations containing the keyword "voltage." The second "nematocyst" group contained transcripts with annotations containing "nemat" "gamma-glut" and "minicollagen." The "non-voltage" group was included for contrast and was hypothesized to not be co-expressed with the two "nematocyst" group.

STEM Co-expression Analysis

The parasite-normalized quantification files were reformatted for input into Short Time Series Expression Miner (STEM)[32]. Genes with zero estimated reads at certain time points were artificially transformed to 1e-20 to allow the program to perform log transformations. Data was log-normalized prior to profile analysis. Only those profiles which had p-values <0.05 were included in the analyses. The profile output was parsed for members of our annotated gene list, and profile membership was counted.

I found five statistically significant gene profiles within three clusters (Fig. A3a). For the list annotated as "channel," 14/20 genes were placed in the cluster containing profiles 2, 3 and 0 which have high expression early which decreases over time (Fig. A3b). For list annotated as "voltage," 12/13 fell within profiles 8 and 11 which have expression increasing over the time-series. All three "nemat" genes also were assigned to the profiles with expression increasing across the time-series, whereas the "gamma-glut" genes were split between the increasing and decreasing profiles.
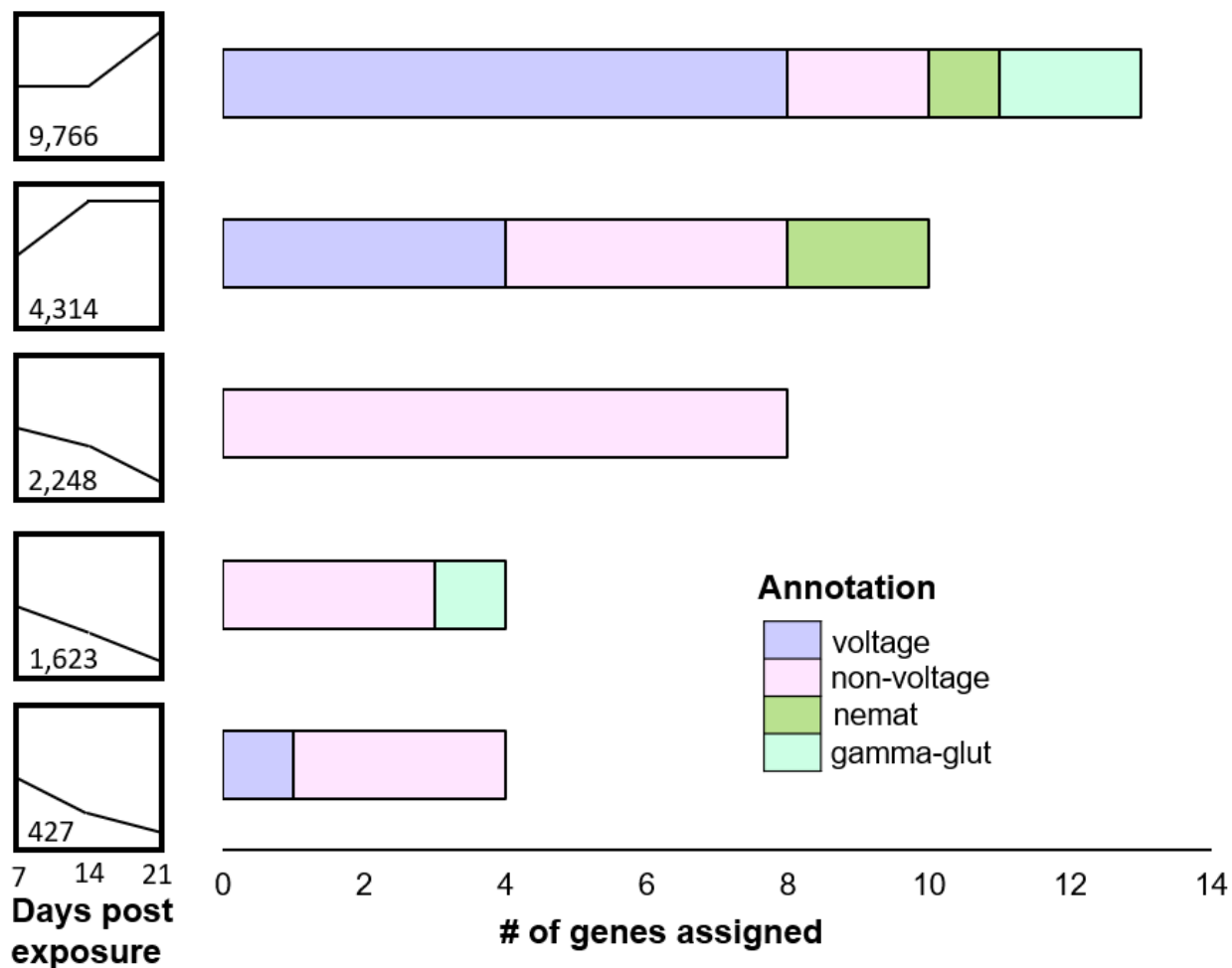
Figure A3. a: Short Time Series Expression Miner profile and cluster assignment of *Ceratonova shasta* gene counts from 7, 14, and 21 days post exposure rainbow trout; b: Cluster membership of the annotated gene list.

Differential Expression Analysis

Separately, the parasite-normalized quantification files were imported into DESeq2 using the tximport package.[40] Each time point contained three replicates, however these were from separate fish, thus only time, and not replicates were included in the DESeq2 experimental design. A likelihood ratio test (LRT) was used to examine genes which were differentially expressed across the three timepoints, with Benjamini-Hochberg multiple testing correction applied.

The LRT test identified 10,253 differentially expressed genes (49%) out of 20,824 genes with nonzero total read counts. From my 54 genes of interest, 28 were differentially expressed. These

included 10/19 labeled "voltage," 12/27 labeled "non-voltage," 3/3 "nemat," and 3/5 "gamma-glut". The pheatmap package clustered samples according to the similarities of their expression across all genes (Fig. A4). For the variance stabilized data, the most similar samples were from the same time points. Samples from days 7 and 21 were more similar to those from 14 days than one another. Significantly expressed genes from the annotated list clustered into three primary clades. All six genes assigned to the first clade were annotated as "channel." The second clade contained one each of "gamma-glut," "non-voltage," and "voltage," and the third composed of 9/19 "voltage" genes. This third group also contained all three "nemat" genes.
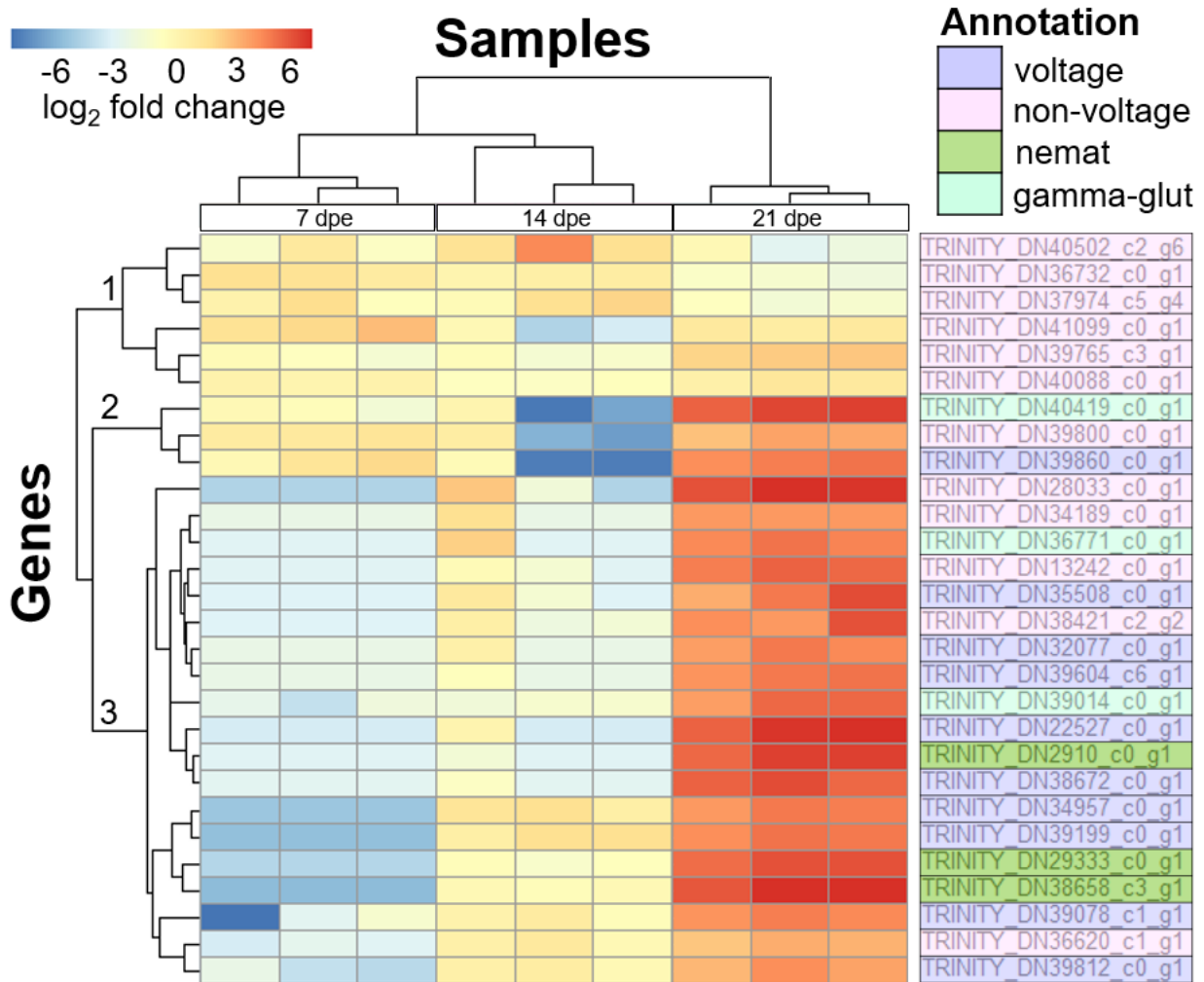
Figure A4. Heatmap with similarity clustered samples and differentially-expressed genes from our annotated gene list. Three gene clusters are denoted.

Coseq Differential Co-expression Analysis

The output from the LRT in DeSeq2 was directly input into the coseq package [34] "coseq" function. Genes with an adjusted p-value of <0.05 from the LRT test were included in a k-means test comparing gene count across all nine samples. The clustering output was parsed for members of our annotated gene list, and cluster membership was counted.

This analysis produced 13 independent gene clusters, many of which had highly similar expression profiles (Fig. A5a). The 28 genes from my list that were differentially expressed fell into nine clusters which were highly similar, except for Cluster 5. This cluster showed similar expression between the three timepoints, in contrast to the rest which showed heavy upregulation between 14 and 21 days. Cluster 5 consisted entirely of genes labeled "non-voltage" (Fig. A5b).
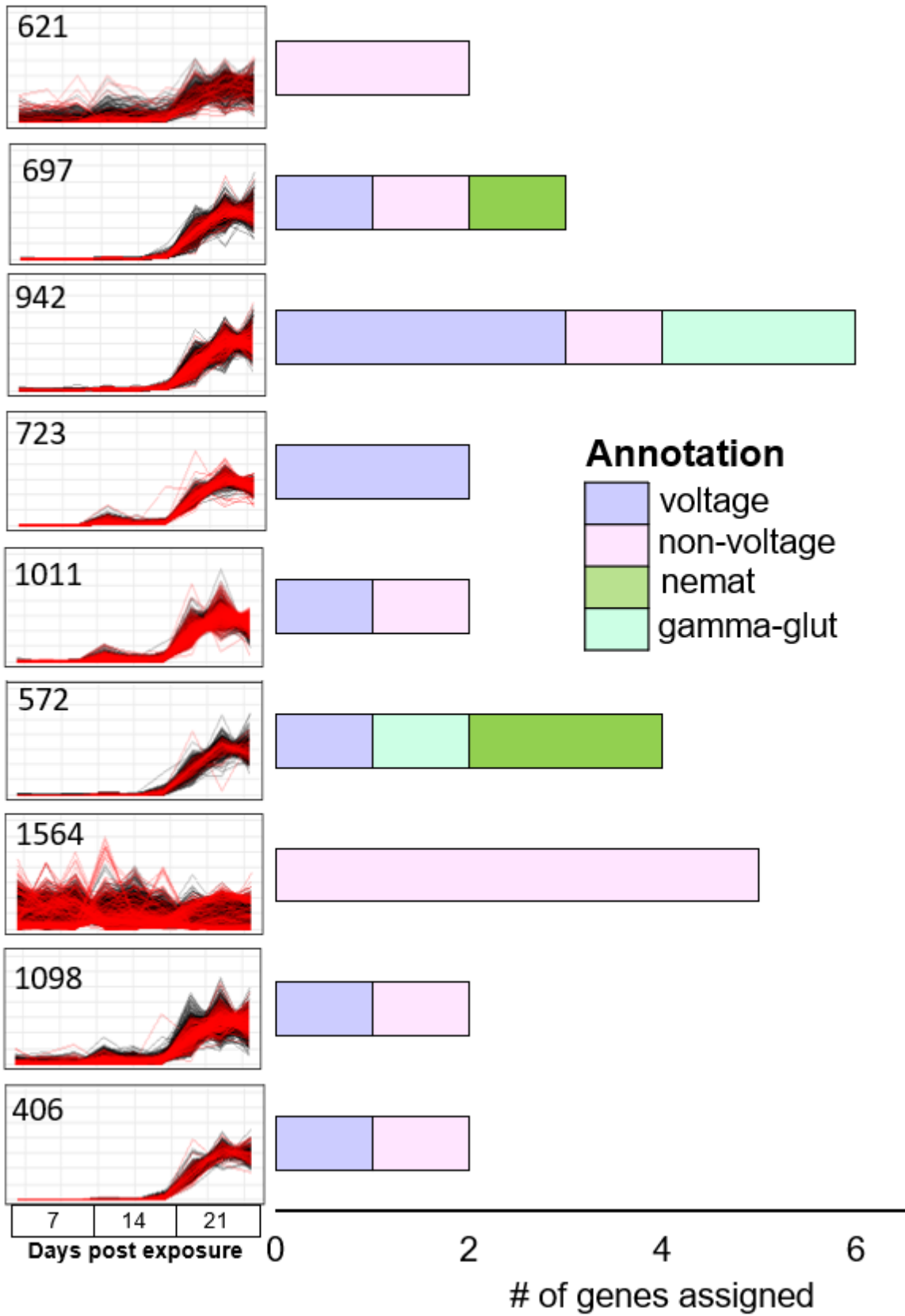
Figure A5. a coseq profiles for differentially-expressed *Ceratonova shasta* genes from three timepoints (7, 14, and 21) each with 3 replicates. Profile membership of the annotated gene list.

DISCUSSION

Among the known types of voltage-gated calcium channels identified in nematocysts of free-living cnidarians, L-type CaVs are regarded as high-voltage-activated channels and T-type CaVs are regarded as low-voltage-activated channels[10] (see Fig. 1.10). In my analyses, I identified both types in the *C. shasta* transcriptome sequences in the "voltage" category (voltage-gated calcium channels). In concordance with this, my phylogenetic analysis showed a single myxozoan sequence clustered with NveCaV1 and NveCaV3a, which are known to be L and T type respectively. My clustering analysis with STEM suggested that the two types are co-expressed, however only the L-type were differentially expressed across the time series. All four of the CaV genes clustered in a single clade in the heatmap. This may suggest that L and T type alpha subunits in Myxozoa are having different roles to those in free-living Cnidaria.

Similarly, I noticed differences in the expression patterns of genes in the "voltage" group and those in the "non-voltage" group. This is most evident in the STEM results in which 14 /20 "non-voltage" were assigned to the cluster containing profiles 2, 3 and 0, whereas only 1/13 genes in the "voltage" group was assigned to this cluster. Of differentially expressed genes, members of the "voltage" group belong solely to the latter two gene clusters in the heatmap, while the first cluster is made up of 5/6 "non-voltage" genes (Fig. A4). It may be possible that voltage-gated channels play a conserved role in the development of nematocysts, whereas chloride channels and are other types are expressed more broadly in development.

Contrary to what I expected, the two sets of nematocyst specific genes, the "nemat" and "gamma-glut" groups, showed disparate expression patterns. Both were most heavily expressed at day 21, however the "nemat" group was assigned only to the first two STEM profiles, and was present in only the third gene cluster in the heatmap. The "gamma-glut" genes, in contrast, were assigned to three STEM profiles, and are present in all three gene clusters in the heatmap. From these results, it was difficult to determine whether genes related to poly-gamma glutamate synthesis or nematogalectin, are more indicative of nematocyst development as a whole. In Cnidaria, these compounds are found exclusively in nematocysts and no other cell type[41,42], thus we can infer that gene expression for nematocyst development is an asynchronous process. Our

clustering approaches demonstrated however, that genes for voltage-gated ion channels and nematogalectin are co-expressed during myxozoan development.

Unexpectedly, I found that many other genes followed the "nemat" and "voltage" expression profiles, with constant expression between days 7 and 14, and then heavy upregulation at day 21. This pattern was consistent across all three analyses, even after normalizing counts for parasite replication. In the STEM co-expression analyses, 9,766 of the 20,825 genes examined were assigned to the first cluster in Fig. A3. In the Coseq analysis of differentially expressed genes, this pattern manifested as many clusters with similar profiles. In the differential expression analysis with Deseq2, almost half (49%) of the total reads with non-zero counts were differentially expressed between the three timepoints, and the heatmap suggests many of these are upregulated at day 21. In future analyses with different biological questions, it may be informative to examine genes that are constitutively expressed or assigned to less densely populated expression profiles.

These consistent expression profiles, and the presence of morphologically "mature" spores with nematocysts at day 21, suggest two possible modes of development and guide future approaches: 1.) The bulk of *C. shasta*'s genetic repertoire is employed between 14 and 21 days, in which case finer time-series data from this period is needed; 2.) The myxospores observable at day 21 are not yet mature, and time-series data from later points is needed. Regardless, this work introduces co-expression analyses of myxozoan infections a potentially useful tool in understanding the parasite's development within hosts.

The detection of the genetic signatures of voltage-gated ion channels in *C. shasta* further exemplifies the molecular and mechanistic similarities among divergent Cnidaria. The role of these channels in myxozoan nematocyst discharge remains unknown and will be the subject of future studies.

REFERENCES

1. Holstein, T. & Tardent, P. An ultrahigh-speed analysis of exocytosis: nematocyst discharge. *Science* **223**, 830–833 (1984).
2. Dujardin, F. Mémoire sur le dévelopement des polypes hydraires et méduses. *Ann. Sci. Nat.* 257–281 (1845).
3. Lubbock, R., Gupta, B. L. & Hall, T. A. Novel role of calcium in exocytosis: mechanism of

nematocyst discharge as shown by x-ray microanalysis. *Proc. Natl. Acad. Sci. U. S. A.* **78**, 3624–3628 (1981).

4. Gitter, A. H., Oliver, D. & Thurm, U. Calcium- and voltage-dependence of nematocyst discharge in *Hydra vulgaris*. *Journal of Comparative Physiology A* **175**, (1994).

5. Jones, C. S. The control and discharge of nematocysts in hydra. *J. Exp. Zool.* **105**, 25–60 (1947).

6. Carré, D. [Hypothesis on the mechanism of cnidocyst discharge (author's transl)]. *Eur. J. Cell Biol.* **20**, 265–271 (1980).

7. Weber, J. Nematocysts (stinging capsules of Cnidaria) as Donnan-potential-dominated osmotic systems. *Eur. J. Biochem.* **184**, 465–476 (1989).

8. Salleo, A., La Spada, G. & Barbera, R. Gadolinium is a powerful blocker of the activation of nematocytes of *Pelagia noctiluca*. *J. Exp. Biol.* **187**, 201–206 (1994).

9. Beedle, A. M., Hamid, J. & Zamponi, G. W. Inhibition of transiently expressed low- and high-voltage-activated calcium channels by trivalent metal cations. *J. Membr. Biol.* **187**, 225–238 (2002).

10. Moran, Y. & Zakon, H. H. The Evolution of the Four Subunits of Voltage-Gated Calcium Channels: Ancient Roots, Increasing Complexity, and Multiple Losses. *Genome Biology and Evolution* **6**, 2210–2217 (2014).

11. Bouchard, C. Cloning and functional expression of voltage-gated ion channel subunits from cnidocytes of the Portuguese Man O'War *Physalia physalis*. *Journal of Experimental Biology* **209**, 2979–2989 (2006).

12. Bouchard, C. & Anderson, P. A. V. Immunolocalization of a voltage-gated calcium channel β subunit in the tentacles and cnidocytes of the Portuguese man-of-war, *Physalia physalis*. *Biol. Bull.* **227**, 252–262 (2014).

13. Oliver, D., Brinkmann, M., Sieger, T. & Thurm, U. Hydrozoan nematocytes send and receive synaptic signals induced by mechano-chemical stimuli. *J. Exp. Biol.* **211**, 2876–2888 (2008).

14. Price, R. B. and Anderson, P. A. V. Chemosensory pathways in the capitate tentacles of the hydroid *Cladonema*. *Invert. Neurosci.* **6**, 23–32 (2006).

15. Peter A. V. Anderson and M. Craig McKay. The electrophysiology of cnidocytes. *J. Exp. Biol.* 215–230 (1987).

16. Kent, M. L., Andree, K. B., Bartholomew, J. L., El-Matbouli, M., Desser, S. S., Devlin, R. H., Feist ,S.W., Hedrick, R.P., Hoffmann R.W., Khattra, J, Hallett, S.L., Lester R. J., Longshaw, M., Palenzeula, O., Siddall, M.E. & Xiao, C. Recent advances in our knowledge of the Myxozoa. *J. Eukaryot. Microbiol.* **48**, 395–413 (2001).

17. Cannon, Q. & Wagner, E. Comparison of Discharge Mechanisms of Cnidarian Cnidae and Myxozoan Polar Capsules. *Reviews in Fisheries Science* **11**, 185–219 (2003).

18. Piriatinskiy, G., Atkinson, S. D., Park, S., Morgenstern, D., Brekhman, V., Yossifon, G., Bartholomew, J. L., & Lotan, T. Functional and proteomic analysis of *Ceratonova shasta* (Cnidaria: Myxozoa) polar capsules reveals adaptations to parasitism. *Sci. Rep.* **7**, 9010 (2017).

19. Ben-David, J., Atkinson, S. D., Pollak, Y., Yossifon, G., Shavit, U., Bartholomew, J. L., & Lotan, T. Myxozoan polar tubules display structural and functional variation. *Parasit. Vectors* **9**, 549 (2016).

20. Chang, E. S., Neuhof, M., Rubinstein, N. D., Diamant, A., Philippe, H., Huchon, D., & Cartwright, P. Genomic insights into the evolutionary origin of Myxozoa within Cnidaria.

Proc. Natl. Acad. Sci. U. S. A. **112**, 14912–14917 (2015).

21. Rachamim, T., Morgenstern, D., Aharonovich, D., Brekhman, V., Lotan, T., & Sher, D. The Dynamically Evolving Nematocyst Content of an Anthozoan, a Scyphozoan, and a Hydrozoan. *Molecular Biology and Evolution* **32**, 740–753 (2015).

22. Michalak, M., Corbett, E. F., Mesaeli, N., Nakamura, K. & Opas, M. Calreticulin: one protein, one gene, many functions. *Biochem. J* **344 Pt 2**, 281–292 (1999).

23. Friedberg, F. & Rhoads, A. R. Evolutionary aspects of calmodulin. *IUBMB Life* **51**, 215–221 (2001).

24. Sunagar, K., Columbus-Shenkar, Y. Y., Fridrich, A., Gutkovich, N., Aharoni, R., & Moran, Y. Cell type-specific expression profiling unravels the development and evolution of stinging cells in sea anemone. *BMC Biol.* **16**, 108 (2018).

25. Shpirer, E., Diamant, A., Cartwright, P. & Huchon, D. A genome wide survey reveals multiple nematocyst-specific genes in Myxozoa. *BMC Evol. Biol.* **18**, 138 (2018).

26. Wolenski, F. S., Layden, M. J., Martindale, M. Q., Gilmore, T. D. & Finnerty, J. R. Characterizing the spatiotemporal expression of RNAs and proteins in the starlet sea anemone, *Nematostella vectensis*. *Nat. Protoc.* **8**, 900–915 (2013).

27. Columbus-Shenkar, Y. Y., Sachkova, M. Y., Fridrich, A., Modepalli, V., Sunagar, K., & Moran, Y. Dynamics of venom composition across a complex life cycle are revealed by the study of a model sea anemone. *Toxicon* **149**, 101 (2018).

28. DuBuc, T. Q., Stephenson, T. B., Rock, A. Q. & Martindale, M. Q. Hox and Wnt pattern the primary body axis of an anthozoan cnidarian before gastrulation. *Nat. Commun.* **9**, 2007 (2018).

29. van Dam, S., Võsa, U., van der Graaf, A., Franke, L. & de Magalhães, J. P. Gene co-expression analysis for functional classification and gene–disease predictions. *Briefings in Bioinformatics* bbw139 (2017). doi:10.1093/bib/bbw139

30. Eisen, M. B., Spellman, P. T., Brown, P. O. & Botstein, D. Cluster analysis and display of genome-wide expression patterns. *Proc. Natl. Acad. Sci. U. S. A.* **95**, 14863–14868 (1998).

31. Boutanaev, A. M., Kalmykova, A. I., Shevelyov, Y. Y. & Nurminsky, D. I. Large clusters of co-expressed genes in the *Drosophila* genome. *Nature* **420**, 666–669 (2002).

32. Ernst, J. & Bar-Joseph, Z. STEM: a tool for the analysis of short time series gene expression data. *BMC Bioinformatics* **7**, 191 (2006).

33. Love, M. I., Huber, W. & Anders, S. Moderated estimation of fold change and dispersion for RNA-seq data with DESeq2. *Genome Biol.* **15**, 550 (2014).

34. Rau, A. & Maugis-Rabusseau, C. Transformation and model choice for RNA-seq co-expression analysis. *Brief. Bioinform.* **19**, 425–436 (2018).

35. Jenuth, J. P. The NCBI. Publicly available tools and resources on the Web. *Methods Mol. Biol.* **132**, 301–312 (2000).

36. Higgins, D. G. & Sharp, P. M. CLUSTAL: a package for performing multiple sequence alignment on a microcomputer. *Gene* **73**, 237–244 (1988).

37. Hall, T. A. BioEdit: a user-friendly biological sequence alignment editor and analysis program for Windows 95/98/NT. *Nucleic Acids Symp. Ser.* (1999).

38. Kumar, S., Stecher, G., Li, M., Knyaz, C. & Tamura, K. MEGA X: Molecular Evolutionary Genetics Analysis across Computing Platforms. *Mol. Biol. Evol.* **35**, 1547–1549 (2018).

39. Patro, R., Duggal, G., Love, M. I., Irizarry, R. A. & Kingsford, C. Salmon provides fast and bias-aware quantification of transcript expression. *Nat. Methods* **14**, 417–419 (2017).

40. Soneson, C., Love, M. I. & Robinson, M. D. Differential analyses for RNA-seq: transcript-

level estimates improve gene-level inferences. *F1000Res.* **4**, 1521 (2015).

41. Shpirer, E., Chang, E. S., Diamant, A., Rubinstein, N., Cartwright, P., & Huchon, D. Diversity and evolution of myxozoan minicollagens and nematogalectins. *BMC Evol. Biol.* **14**, 205 (2014).

42. Szczepanek, S., Cikala, M. & David, C. N. Poly-gamma-glutamate synthesis during formation of nematocyst capsules in Hydra. *J. Cell Sci.* **115**, 745–751 (2002).

43. Kallert, D. M., El-Matbouli, M. & Haas, W. Polar filament discharge of *Myxobolus cerebralis* actinospores is triggered by combined non-specific mechanical and chemical cues. *Parasitology* **131**, 609–616 (2005).

APPENDIX B

TEST OF THE REQUIREMENT OF MECHANOSTIMULATION FOR NEMATOCYST DISCHARGE IN *MYXOBOLUS CEREBRALIS*

In developing the *in vitro* assay described in Chapter 2, I explored means of reliably inducing nematocyst discharge in *Myxobolus cerebralis* actinospores. Kallert et al. (2005)[1] employed rainbow trout mucus homogenate as a chemostimulus and applied a second, mechanostimulation step by mixing actinospores and the mucus homogenate on microscope slides and shaking them for 3 seconds at 50 Hz (0.5 mm amplitude)[1]. In testing this method, I observed that adding the mucus homogenate to tubes and fully pipetting the contents once to mix was adequate to induce discharge. Simultaneously, I was concerned that the mechanostimulation step might induce non-specific discharge in actinospores that were not also activated by the mucus signal. To test this, I compared the effect of mechnostimulation on nematocyst discharge with and without the mucus homogenate chemostimulus.

Test of mechanostimulation

For no-treatment controls, 4 µL of dechlorinated water was added to 16 µL of actinospore solution (see Chapter 2: Source of *M. cerebralis* actinospores). In treatment groups, 4 µL of mucus homogenate was added to 16 µL actinospore solution. Each sample was vortexed for 3 s at 3000 rpm (50 Hz) using an adjustable-speed shaker and placed on ice. Actinospores were visualized immediately afterwards by streaking 3 x 2 µL spore solution onto a glass slide and counting actinospores with and without discharged nematocysts.

The results from this preliminary test are detailed in Fig A6. The addition of mucus, in the absence of an intentional mechanostimulation step, was effective at inducing discharge of an equivalent magnitude. The mechanostimulation step induced minor discharge in the absence of mucus. Therefore, we used mucus alone in all subsequent experiments.
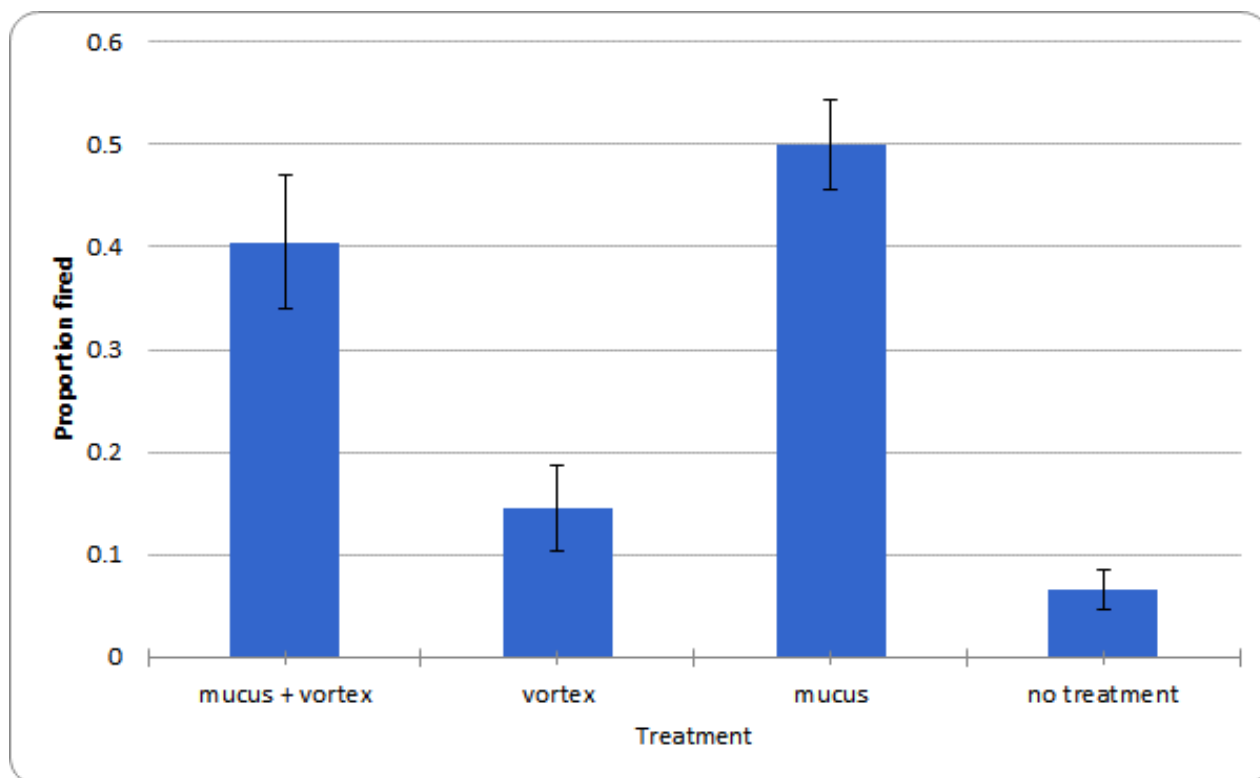
Figure A6. Effect of the addition of mucus homogenate and mechanostimulation by vortexing on nematocyst discharge. The y-axis displays the proportion of actinospores with at least one discharged nematocyst. Error bars show the standard deviation of three replicates.

REFERENCES

1. Kallert, D. M., El-Matbouli, M. & Haas, W. Polar filament discharge of *Myxobolus cerebralis* actinospores is triggered by combined non-specific mechanical and chemical cues. *Parasitology* **131**, 609–616 (2005).

APPENDIX C

TEST OF FISH SKIN AS A SUBSTRATE FOR ACTINOSPORE ATTACHMENT

INTRODUCTION

Prior to adopting mucus homogenate as a stimulator of nematocyst discharge in Myxozoa, we explored alternative proxies for live fish. Our goal was to develop an assay that would allow us to test multiple treatments for nematocyst action while killing minimal fish. Such an assay would utilize multiple replicates of signaling substrate isolated from a single fish. *Myxobolus cerebralis* discharges tubules to attach to goldfish *Carassius auratus*, carp *Cyprinus carpio*, guppy *Poecilia reticulata*, and tadpole *Rana pipiens*, despite none of these organisms being viable hosts [1]. This implies that the parasite reacts to general excreted compounds on fish skin and not species-specific cues. Understanding this, we tested the response of *M. cerebralis* actinospores to sections of rainbow trout skin.

Multiple studies have stained myxozoan actinospores with fluorescein dye to enhance visibility while maintaining viability[2-4]. Before introducing the fish skin, we fluorescently stained *M. cerebralis* actinospores with carboxyfluorescein succinimidyl ester (CFSE).

METHODS

Preparation of fluorescently stained spores

A stock solution of CFSE (Molecular Probes, Inc) was prepared at 10 mM in 100% DMSO and stored at 5 °C, allowing 30 minutes to defrost prior to experimentation. *M. cerebralis* actinspores were filtered from infected worms (see Chapter 2: Source of *M. cerebralis* actinospores) using a 20 μm nylon mesh in a funnel to concentrate the spores. We added 10 μL CFSE per mL spore solution and incubated for 15 minutes at room temperature. The spore suspension was rinsed of unbound dye by pipetting the solution into a funnel consisting of two nested 0.5-mL tubes with bottoms cut off and 20 μL nitex mesh in between them. We collected flow through in a separate 2-mL tube. When the filter became clogged, we resuspend spores with minimal dechlorinated tap water. The stained spore solution was rinsed with two times its volume of dechlorinated tap water. Stained actinospores were visualized using under fluorescence illumination at 200×

magnification using a Leica compound microscope with a 450-490 nm wavelength filter. Half the spores were then deactivated by taking an aliquot and adding to an equivalent volume of 10% formalin and allowing them to fix for 1 hour at room temperature.

Attachment assay

One juvenile rainbow trout (60 mm) was killed via overdose of MS-222. Using a clean scalpel, we removed nine ~1 cm^2 skin pieces from the lateral sides of the fish. Each skin square was added to a 2-mL microcentrifuge tube containing an aliquot of the stained spore solution. The tissue was submerged completely using forceps, and three replicates each were incubated at room temperature for 1, 10, and 30 minutes with mild agitation on a plate rocker. After incubation, equivolume 10% formalin was added to each tube to fix the contents overnight.

Visualization of attached actinospores

We removed the liquid contents of each tube and washed the fixed skin squares several times with reverse-osmosis (RO) water to remove poorly adhered actinospores Using forceps, we removed the tissue from the tubes and placed the three replicates from each timepoint and treatment on glass microscope slides (Fig. A7 a). The tissue was encircled with Permount® (Fischer Scientific). Coverslips were added and the slides were allowed to dry overnight. We examined the slides using a Leica compound microscope with fluorescence illumination and a 450-490nm wavelength filter, a Leica DC 500 camera, and IM50 software. With each skin piece, we counted the number of adhered fluorescently-stained actinospores.
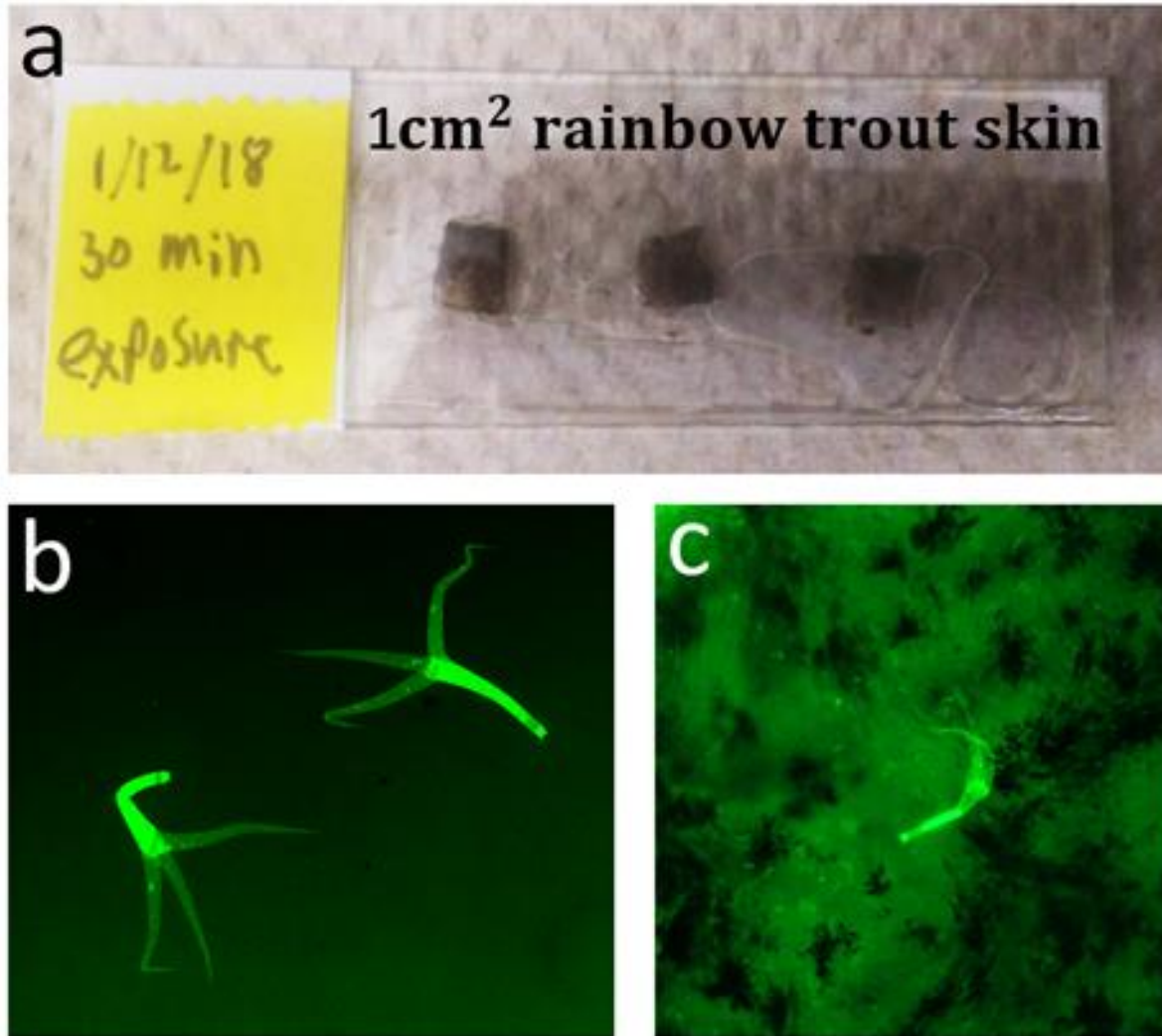
Figure A7. a. Microscope slide mounted with formalin-fixed Rainbow trout skin sections. b. *Myxobolus cerebralis* actinospores stained with carboxyfluorescein succinimidyl ester (CFSE). c. Rainbow trout fish skin with single stained, *M. cerebralis* actinospore.
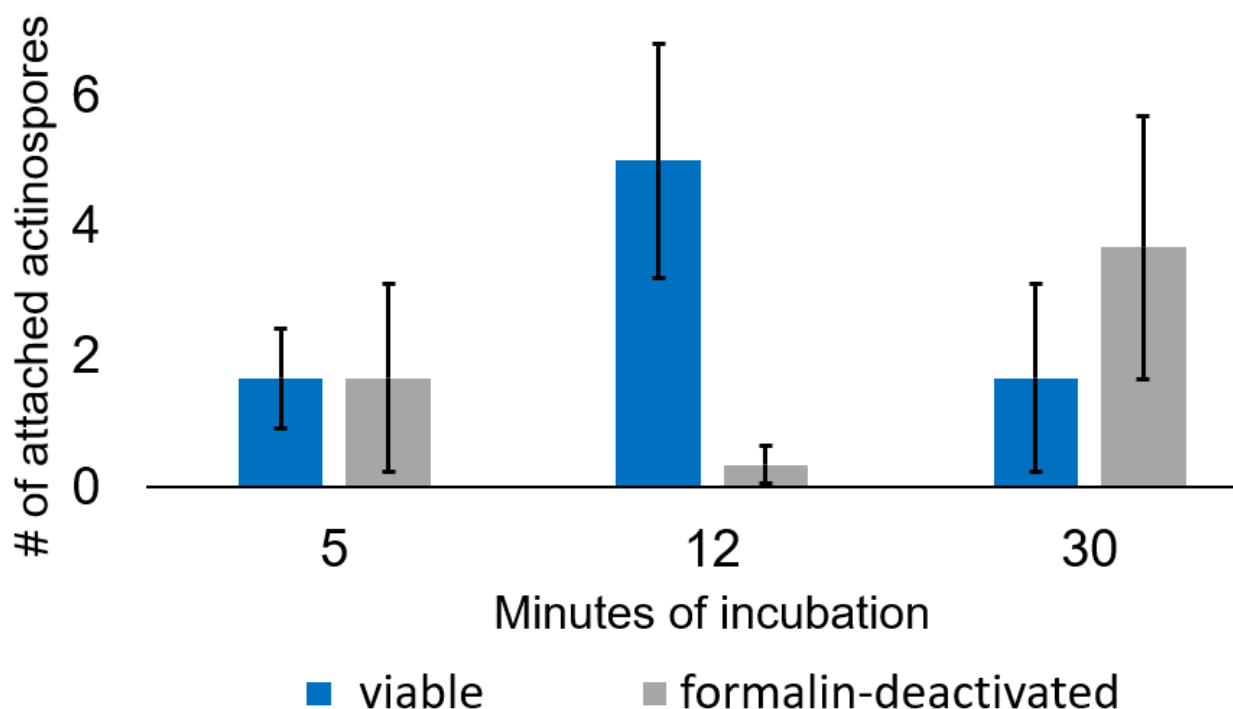
Figure A8. Bar chart comparing the number of viable and deactivated *Myxobolus cerebralis* actinospores attached to fish skin after 5, 12, and 30 minutes of incubation.

RESULTS AND DISCUSSION

Figure A8 displays the results of the attachment assay. When including all replicates from the three timepoints, more actinospores attached to the skin from the viable group than formalin-deactivated group. The greatest difference was for tubes incubated for 12 minutes, however this difference was not statistically significant (T-test, p=0.0913). More viable actinospores attached to the fish skin incubated for 12 minutes vs. 5 or 30 minutes, whereas the formalin deactivated spores showed more attachment at 5 and 30 minutes. This difference coincides with our understanding of the process of myxozoan infection. In *Henneguya nuesslini*, which shares actinospore morphology and host range with *M. cerebralis*, sporoplasm migration takes an average of 5.4 minutes, and the empty valve cells detach from the fish afterwards [5]. If *M. cerebralis* infects in a similar timeframe, the sample incubated for 12 minutes may have the maximum number of spores attached, whereas the 5 minute-incubated sample may have some not yet adhered and the 30 minute incubated sample may have lost some spores which detached after sporoplasm migration.

This time effect coincides with our understanding of myxozoan biology, however several phenomena were observed during this experiment that made us question the validity of the assay. We observed no migrated sporoplasms embedded in the fish skin or actinospores with fired tubules, despite these components uptaking the fluorescent dye (Fig. A7 b and c). Likewise, the presence of many adhered, formalin-deactivated spores makes us question whether "attached" spores had reacted to the fish skin and attached via tubules, or if they had coincidentally become stuck in the fish's mucus without reacting to the stimuli. These unknowns were compounded by difficulty observing actinospores in fish rainbow trout skin, which autofluoresces and has many melanocytes that inhibit visualization. We abandoned experiments with fish skin as a substrate for actinospores attachment assay in favor of assays with rainbow trout mucus homogenate, drawing from the work of Kallert et al. (2005)[6].

REFERENCES

1. El-Matbouli, M., Hoffmann, R. W., Schoel, H., McDowell, T. S. & Hedrick, R. P. Whirling disease: host specificity and interaction between the actinosporean stage of *Myxobolus cerebralis* and rainbow trout *Oncorhynchus mykiss*. *Diseases of Aquatic Organisms* **35**, 1–12 (1999).
2. Bjork, S. J. & Bartholomew, J. L. Invasion of *Ceratomyxa shasta* (Myxozoa) and comparison of migration to the intestine between susceptible and resistant fish hosts. *Int. J. Parasitol.* **40**, 1087–1095 (2010).
3. Kallert, D. M., Eszterbauer, E., Grabner, D. & El-Matbouli, M. In vivo exposure of susceptible and non-susceptible fish species to *Myxobolus cerebralis* actinospores reveals non-specific invasion behaviour. *Dis. Aquat. Organ.* **84**, 123–130 (2009).
4. Markiw, M. E. Experimentally Induced Whirling Disease II. Determination of Longevity of the Infective Triactinomyxon Stage of *Myxobolus cerebralis* by Vital Staining. *Journal of Aquatic Animal Health* **4**, 44–47 (1992).
5. Kallert, D. M., Ponader, S., Eszterbauer, E., El-Matbouli, M. & Haas, W. Myxozoan transmission via actinospores: new insights into mechanisms and adaptations for host invasion. *Parasitology* **134**, 1741–1750 (2007).
6. Kallert, D. M., El-Matbouli, M. & Haas, W. Polar filament discharge of *Myxobolus cerebralis* actinospores is triggered by combined non-specific mechanical and chemical cues. *Parasitology* **131**, 609–616 (2005).

APPENDIX D

COMPARISON OF MYXOZOAN INFECTION IN MIXED-SPECIES EXPOSURES

INTRODUCTION

The specificity with which myxozoan parasites detect and infect fishes has been widely discussed. Actinospores from many species exhibit nematocyst discharge and sporoplasm migration when presented with mucus from non-susceptible fishes in which they cannot replicated or induce disease[1–5]. Yokoyama et al. (2006)[3] examined the ability *Myxobolus arcticus* and *Thelohanellus hovorkai* to respond to natural and non-susceptible hosts. They compared actinospore response to mucus isolates as well as the presence of fluorescently stained sporoplasm in exposed fish. The two approaches suggested *M. arcticus* responds quickly and non-specifically to fish stimuli, whereas *T. hovorkai* responds more slowly and specifically to its natural host.

Kallert et al. (2009)[6] continued this vein of research with the model myxozoan *Myxobolus cerebralis*. They exposed Troutlodge strain rainbow trout *Oncorhynchus mykiss*, less susceptible Hofer strain rainbow trout, non-susceptible carp *Cyprinus carpio*, and a "mimic fish" cut out of agar to fluorescently stained *M. cerebralis* actinospores and compared the prevalence of tissue-bound sporoplasm. There was no difference in sporoplasm count in the three fish species, suggesting *M. cerebralis* can detect live fish, but cannot differentiate susceptible vs. non-susceptible hosts. This non-specific invasion was recently brought into question by Eszterbauer et al. (2019)[7], who compared *M. cerebralis* infection in rainbow trout, less susceptible brown trout (*Salmo trutta*) and non-susceptible gibel carp (*Carassius gibelio*) with nested PCR. More rainbow trout were infected than either of the two species (p=0.059), however more gibel carp (non-susceptible) were infected than brown trout (somewhat susceptible)

A potential application of this lack of specificity, is the use of non-susceptible "decoy" fish as a "biological filters" to reduce the parasite load for more susceptible fishes. Kallert et al. (2009)[6] explored this concept, exposing non-susceptible carp to *M. cerebralis*, and later exposing

susceptible rainbow trout in the same waters. Infection severity was decreased for exposure water which had previously contained carp. This supports the use of non-susceptible fish as a preventative measure for infection. However, it provides no insight into the nature of infection in environments of mixed fish species, which is often the case in aquaculture.

In this experiment, we used qPCR and scanning electron microscopy (SEM) to compare *M. cerebralis* infection in susceptible rainbow trout, non-susceptible goldfish (*Carassius auratus*) and zebrafish (*Danio rerio*). We compared infection in each species exposed individually and then as a mixed-species community. Individual exposures were short, ~ 1 minute, as we were interested in parasite attachment to the hosts rather than infection, and this timeframe is appropriate to observe *M. cerebralis* actinospore attachment, and the early stages of sporoplasm migration [8]. Mixed exposures were longer, ~15 minutes as we were primarily interested in attachment regardless of the stage of infection. From the literature, salmonids exposed to *Myxobolus arcticus*, a close relative of *M. cerebralis*, the maximum number of sporoplasms were present in gills at 10 minutes, then was progressively lower at 30, 60, 90, and 120 minutes[3], thus we conservatively chose 15 minutes of continuous exposure.

METHODS

Individual exposures

In 250-mL containers, we added 60,000 *M. cerebralis* actinospores and cold well water sufficient to fill the container to 50 mL. We added aeration via pipette tip bubblers[9] and allowed the containers to equilibrate to 14.4 °C (lab room temperature). Three fish were added to the container collectively. After one minute of exposure, fish were removed and killed by an overdose of MS-222. We measured the additional time it took from cessation of spore exposure to fixation. One side of gills was removed and placed in 300 μL EM fixative (2.5% glutaraldehyde, 1% paraformaldehyde, and 0.1 M Cacodylate buffer). Once all three fish had one side of gills fixed for EM, the other side of gills were removed and stored in 2 mL tubes and frozen for qPCR. Exposures and gill removal were conducted for zebrafish, rainbow trout and goldfish.

Scanning Electron Microscopy

Gills from the three fish species were stored in EM fixative for 24 hours. The samples were rinsed three times with fixative and the gill arches were separated and stored in fresh fixative. Samples were dehydrated in an ascending ethanol series up to 100 %, transferred to 100 % acetone, mounted on carbon stubs, air dried, sputter coated with a mixture of gold and palladium, and examined using a FEI QUANTA 600F environmental SEM.

Mixed exposures

In 250 mL containers, we added 180,000 *Myxobolus cerebralis* actinospores and cold well water sufficient to fill the container to 150 mL. We added pipette tip bubblers[9] and allowed the containers to equilibrate to 14.3 °C. Three zebrafish, three goldfish and three rainbow trout were added to the container collectively. In a separate container, three rainbow trout were exposed to 60,000 actinospore from the same filtered batch of actinospores. After 15 minutes of exposure, fish were removed and killed by an overdose of MS-222. Both sides of gills was removed and stored in 2-mL tubes and frozen for qPCR.

Infection quantification via qPCR

We extracted total DNA from frozen gill samples using a Qiagen DNeasy Blood and Tissue kit following the manufacturer's instructions. DNA was eluted from the column with two washes of 100 µL buffer AE. Total DNA concentration was measured with a Nanodrop spectrometer (Thermo Scientific), and we normalized total DNA concentration by dilution with molecular grade water to 150 ng/µL. DNA extracted from zebrafish gills was less concentrated than 150 ng/uL so these samples were not diluted. *M. cerebralis* DNA concentration was measured by the standard qPCR following the protocol of Kelley et al. (2004)[10].

Statistics and Data Processing

Three replicates fish from each species were included the analyses. Cq values from zebrafish gill samples were normalized by multiplying the Cq by a constant of 150 (the intended ng/uL) divided by the measured ng/uL concentration. Normality of data was checked by the Shapiro-Wilk Test. Normal variance was tested by the Bartlett's test. As a non-parametric alternative to one-way ANOVA, the Kruskal-Wallis test was used to examine differences between all treatments. We used Dunn's Test with Holm multiple testing corrections to examine pairwise differences between treatments.

RESULTS

Individual Exposure

qPCR detection levels of Mc-DNA are shown in Fig. A9. The greatest quantity of *M. cerebralis* DNA was detected in goldfish samples, though no significant differences existed between the three fish species.
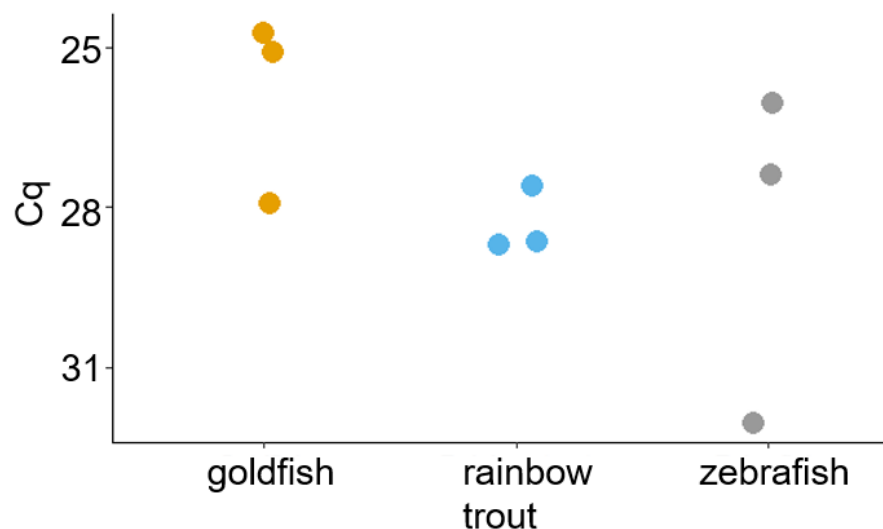

Figure A9. Quantification cycle (Cq) for *M. cerebralis* DNA detected on gills of exposed fish. Goldfish (*Carassius auratus*), rainbow trout (*Oncorhynchus mykiss*), and zebrafish (*Danio rerio*) were exposed in separate containers at the same parasite dose of 20,000 actinospores per fish.

Scanning Electron Microscopy

Scanning electron microscopy images of fish gills are displayed in Figures A10-15. In samples from all three species, lamellae were visible and not obscured by mucus. In gills from rainbow trout and goldfish, ~5 µm, holes in the gill epithelium were visible (Fig. A11-14). These were most common in rainbow trout samples, and in some cases, circular features resembling germ-cells of sporoplasm are visible within the holes (Fig. A13 and A14). No whole actinospores were observed attached to the gills. One elongated, myxozoan valve cell-like structure was attached to a rainbow trout gill lamella (Fig. A15), however its reduced size (30µm), and lack of discernible nematocysts, obfuscates its identity.
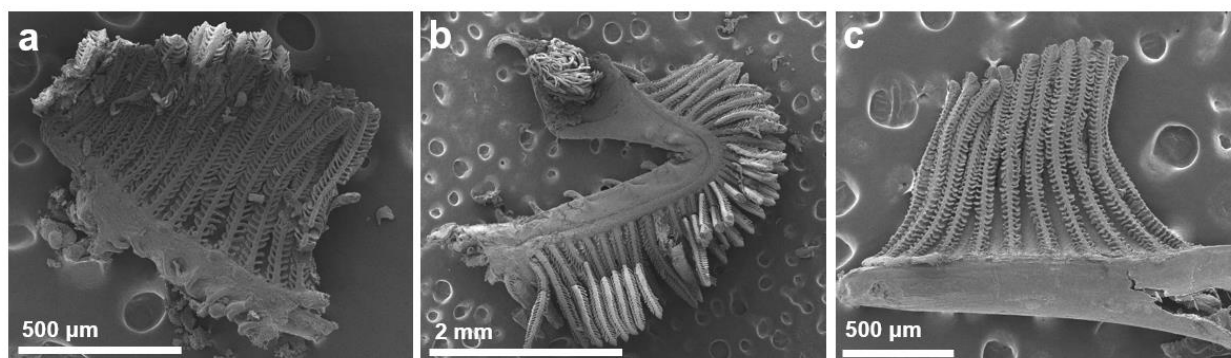

Figure A10. Scanning electron microscopy of gills excised from fish exposed to *Myxobolus cerebralis* for 1 minute, with 2-4 minutes post-exposure before fixation: a: zebrafish; b: rainbow trout; c: goldfish.
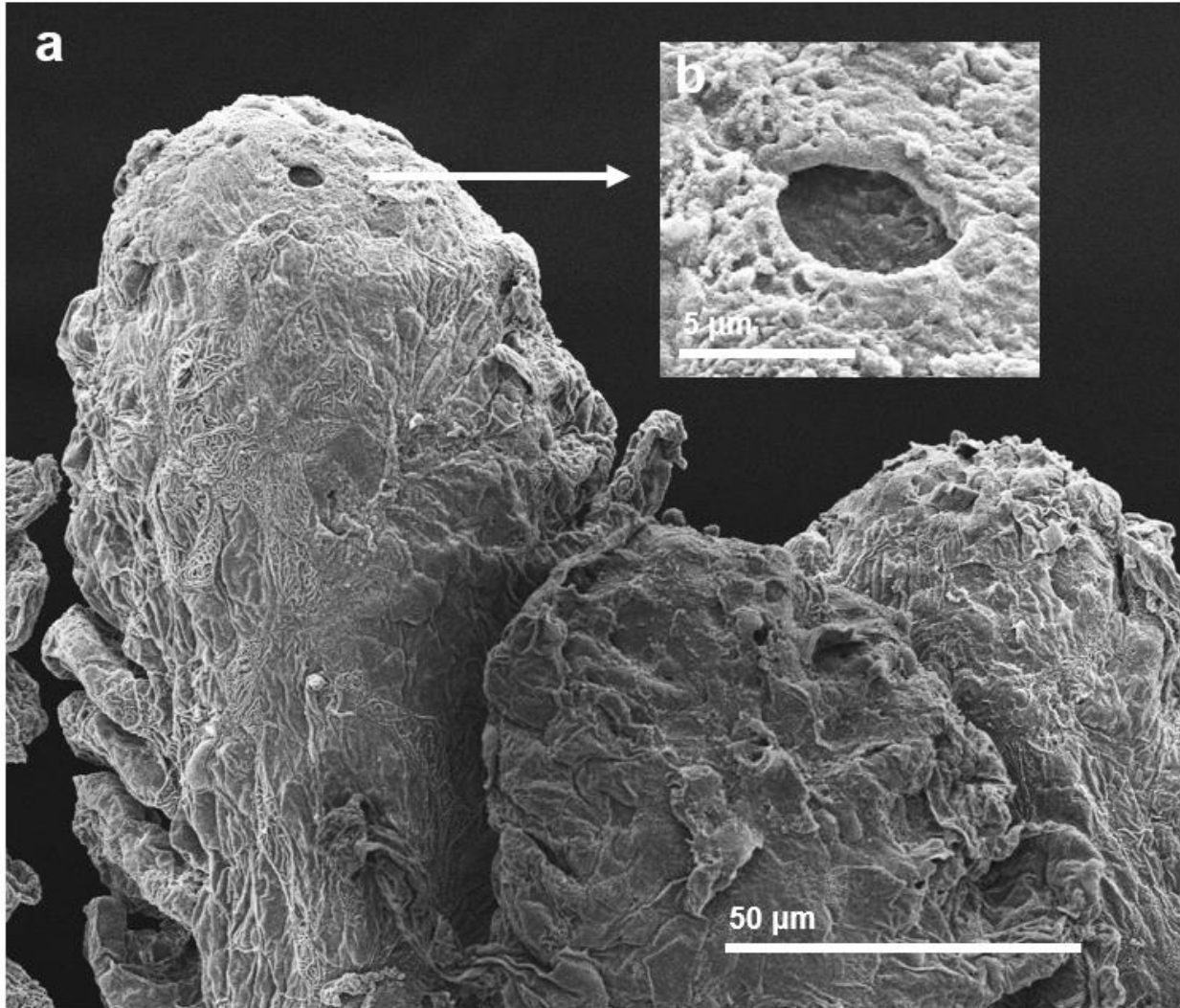
Figure A11. Scanning electron microscopy of goldfish (*Carassius auratus*) gills exposed to *Myxobolus cerebralis* actinospores for 1 minute and placed in fixative after an additional 5 minutes 55 seconds. a & b; Hole on the distal tip of a gill filament, ~5 μm in diameter, possibly caused by sporoplasm penetration.
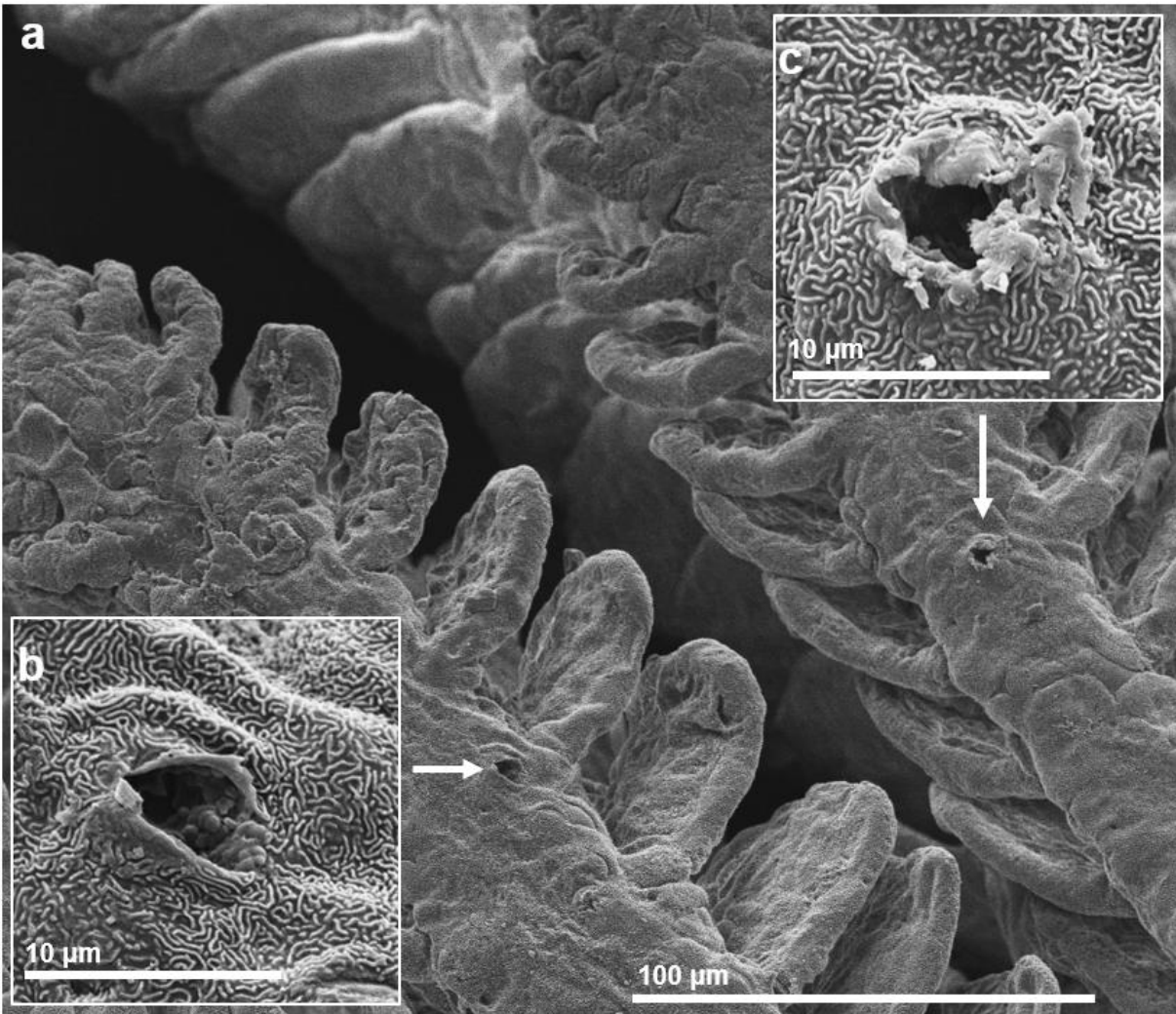
Figure A12. Scanning electron microscopy of gills from rainbow trout (*Oncorhynchus mykiss*) exposed to *Myxobolus cerebralis* actinospores for 1 minute and placed in fixative after an additional 3 minutes 7 seconds. a: detail of two gill filaments with ~5 μm holes in the interbranchial septum, potentially due to sporoplasm penetration; b & c: Higher magnification views of holes.
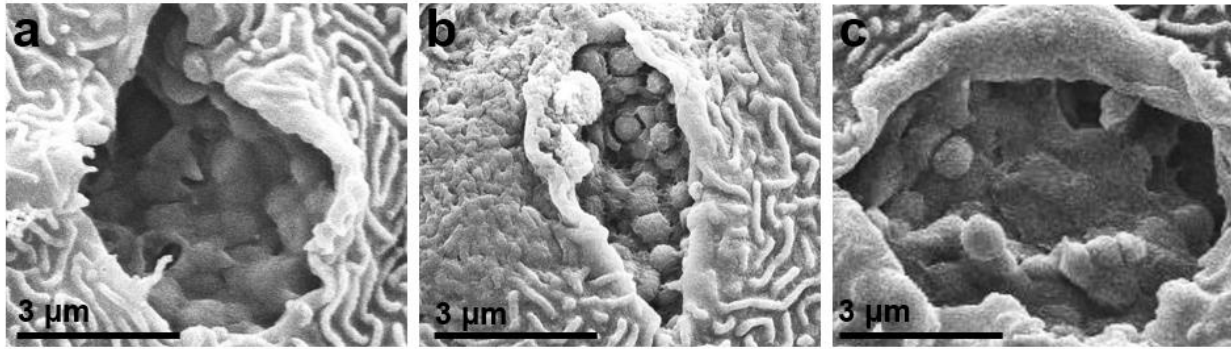
Figure A13. Scanning electron microscopy of gills from rainbow trout (*Oncorhynchus mykiss*) exposed to *Myxobolus cerebralis* actinospores for 1 minute and placed in fixative after an additional 3 minutes 7 seconds. a, b, & c: Holes in gill epithelium, possibly with embedded sporoplasm showing its spherical germ cells.
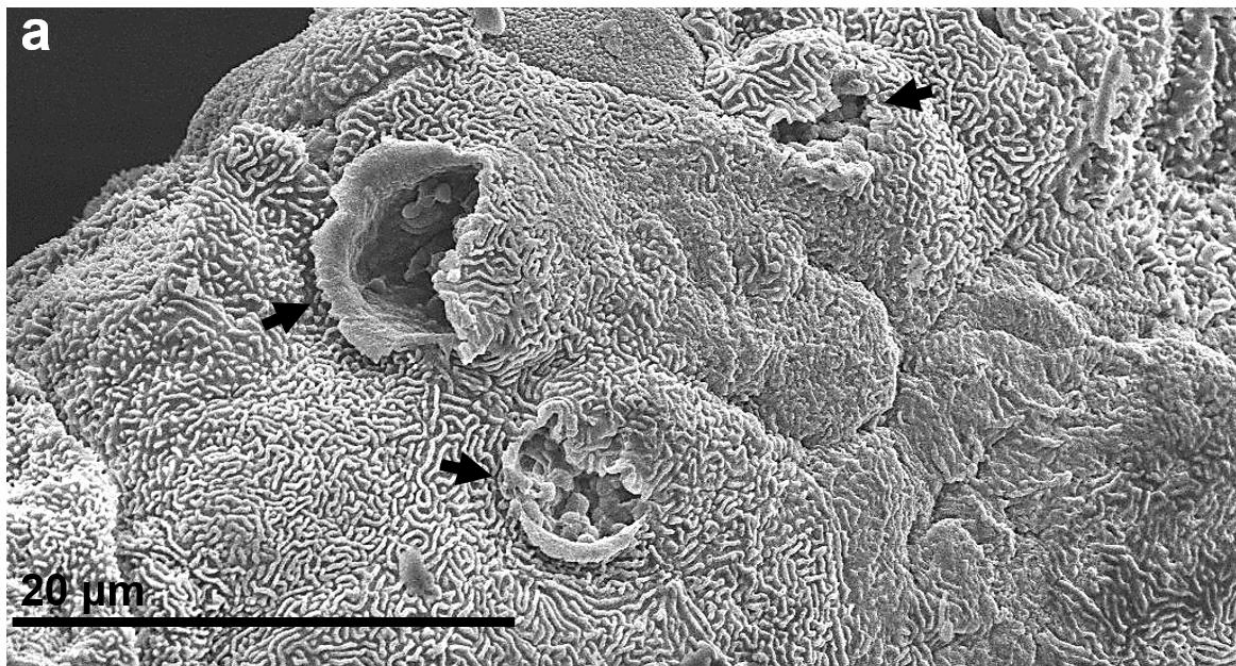

Figure A14. Scanning electron microscopy of the distal tip of a gill filament from a rainbow trout (*Oncorhynchus mykiss*) exposed to *Myxobolus cerebralis* actinospores for 1 minute and placed in fixative after an additional 3 minutes 7 seconds. Arrows indicate holes in gill epithelium, possibly with embedded sporoplasm showing spherical germ cells.
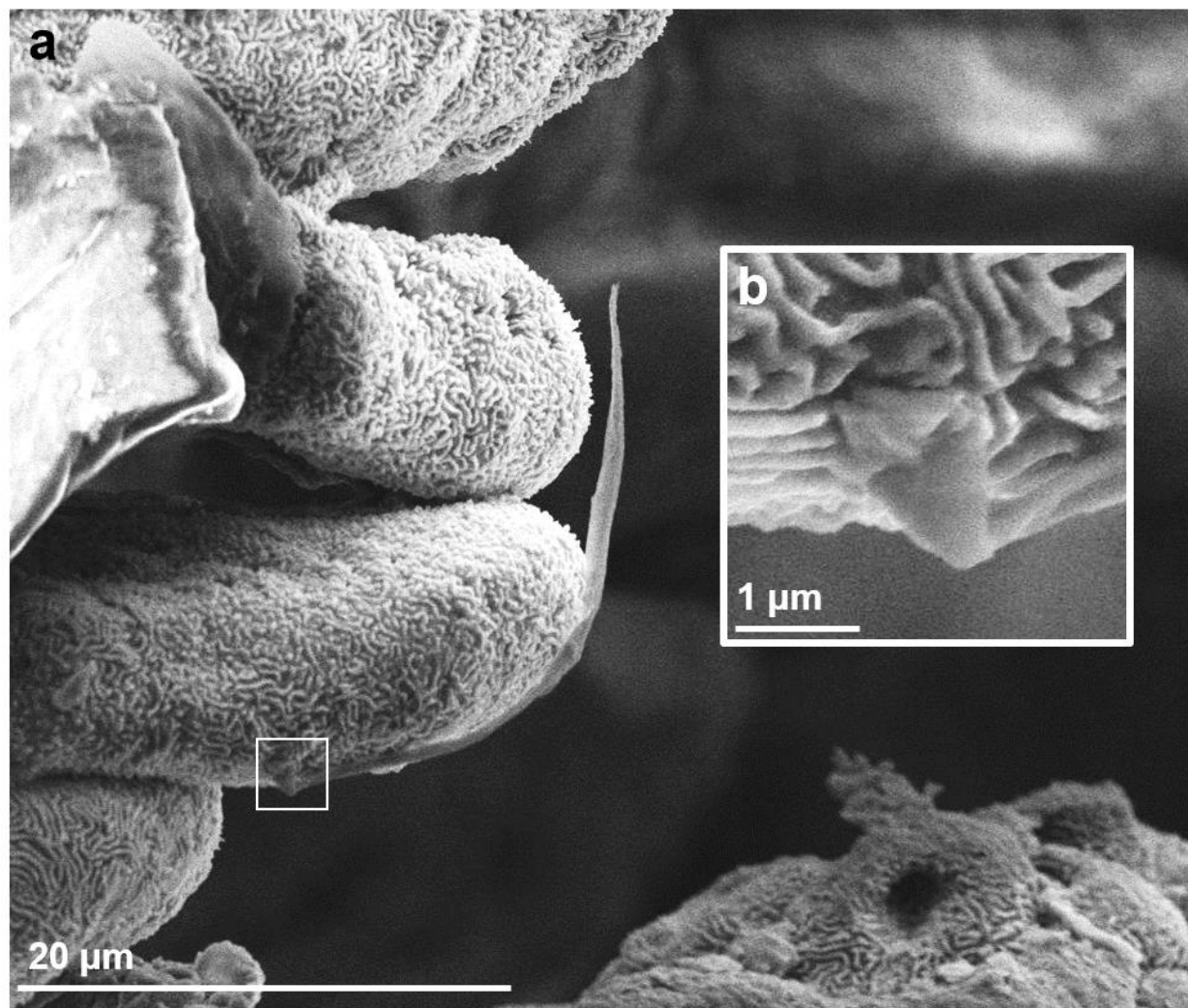
Figure A15. Scanning electron microscopy of the gill lamellae from a rainbow trout (*Oncorhynchus mykiss*) exposed to *Myxobolus cerebralis* actinospores for 1 minute and placed in fixative after an additional 3 minutes 7 seconds. a: valve cell-like structure is attached to the middle lamella. b: magnification of structure at attachment point. It is difficult to determine whether this structure is an actinospore or simply debris.

Mixed species exposure

qPCR detection levels of Mc-DNA are shown in Fig. A16. Rainbow trout from the mixed exposure had the greatest mean quantity of *M. cerebralis* DNA of the three fish species tested. No significant differences ($p<0.05$) existed between exposure groups (Kruskal-Wallis p=0.0824). The greatest differences in mean Cq existed between rainbow trout exposed alone and zebrafish

from the mixed exposure **Δ**Mean Cq= 4.7102, ~26× *M. cerebralis* DNA quantity, (p=0.1045, Dunn's test with Holm adjustment) and rainbow from the mixed exposure and rainbow trout exposed alone **Δ**Mean Cq= 1.9953, 4× *M. cerebralis* DNA quantity, (p=0.2077, Dunn's test with Holm adjustment).
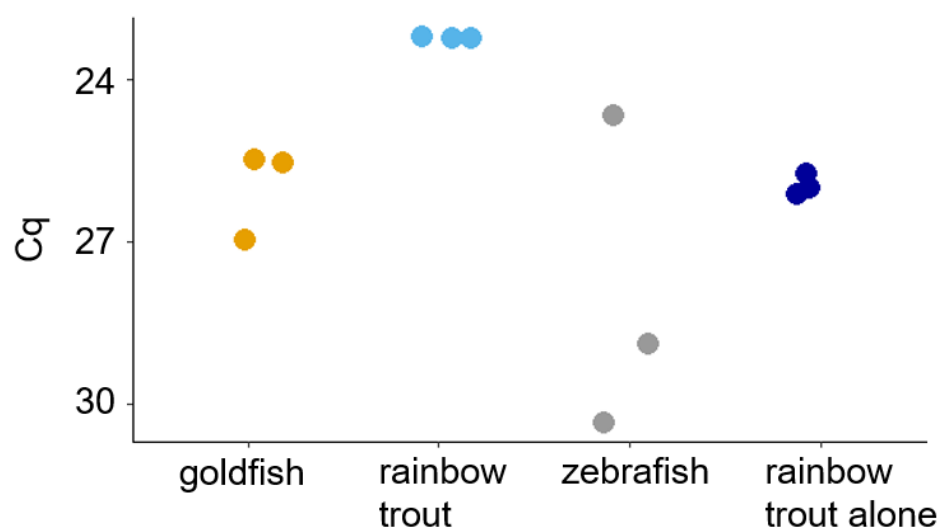

Figure A16. Quantification cycle (Cq) for *Myxobolus cerebralis* DNA detected on gills of goldfish (*Carassius auratus*), rainbow trout (*Oncorhynchus mykiss*), and zebrafish (*Danio rerio*) exposed to 180,000 actinospores (20,000 per fish) together in a single container. "Rainbow trout alone" were exposed at the same actinospore concentration in a separate container.

DISCUSSION

The myxozoan parasite *Myxobolus cerebralis*, exhibits non-specific fish detection, attaching to dead-end hosts [1–5]. The application of non-susceptible "decoy" fish as biological filters for more susceptible fish may be a method of disease reduction in aquaculture [6] and mimic an interaction already occurring in natural systems. In this experiment, we compared *M. cerebralis* infection in one susceptible and two non-susceptible fish species in individual and mixed-species exposures.

In the individual exposures, we observed no significant difference in *M. cerebralis* infection between fish species. This aligns with our understanding of *M. cerebralis*' aforementioned lack of specificity in fish detection. However, it is in disagreement with the SEM imagery, which

details many more holes in the gill epithelium of rainbow trout than goldfish or zebrafish. The holes are similar in size and the irregularity of their margins as those observed by El-Matbouli et al. (1999) in rainbow trout exposed to *M. cerebralis* and fixed after 4 minutes (Fig A17 [8].
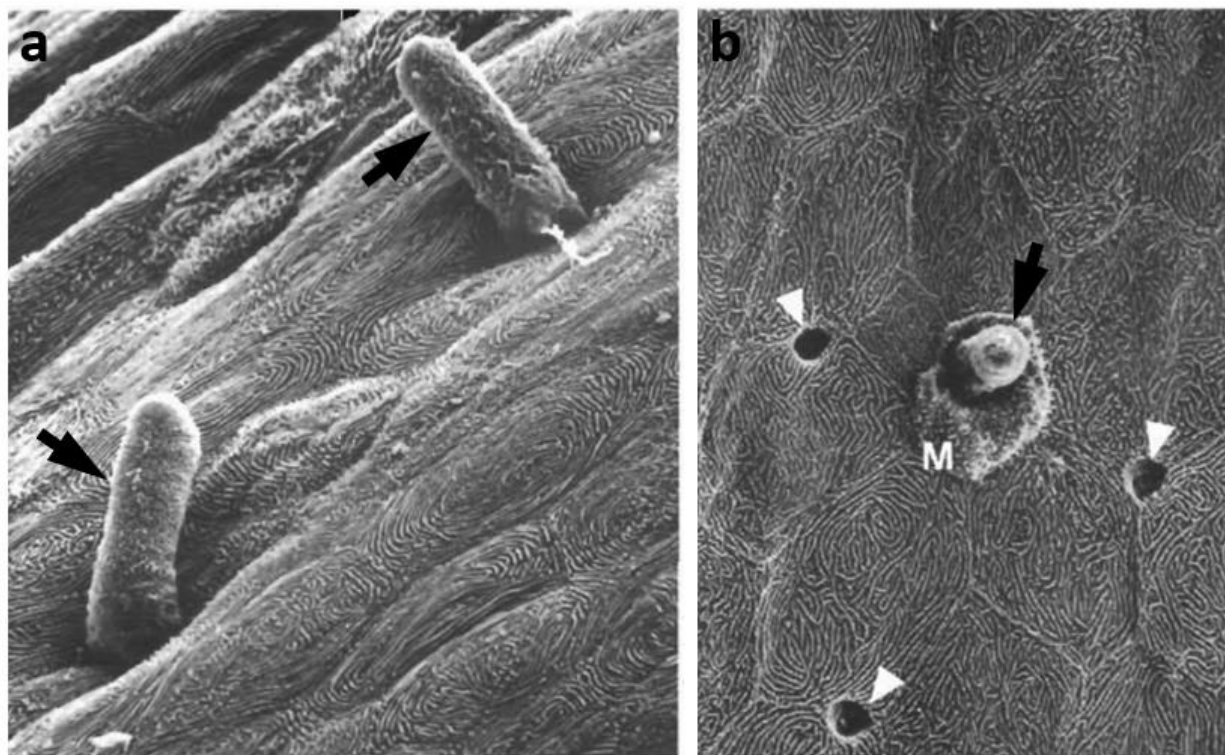

Figure A17. Scanning electron microscopy from El-Matbouli et al. 1999[8] of juvenile rainbow trout exposed to *Myxobolus cerebralis* and fixed at a: 2 minutes post-exposure and b: 4 minutes post-exposure. Black arrows indicate burrowing sporoplasm. White triangles indicate secretory openings of mucous cells, and "M" indicates tissues and mucus associated with a burrowing sporoplasm.

In the mixed exposures, which lasted 15 minutes, more *M. cerebralis* DNA was detected in rainbow trout than either goldfish or zebrafish. This contrasts with results from the shorter 1-minute individual exposures in which there was no difference. There are three possible explanations for this: 1.) There is some level of host selection by the parasite in which they discharge tubules or emit sporoplasm less readily in dead-end hosts. In an experiment comparing infection in rainbow trout, carp, goldfish, and nose (*Chondrostoma nasus*) exposed to the same sporoplasm dose of *M. cerebralis*, sporoplasms were identified by histology in rainbow trout but

not the three cyprinid species. Moreover *M. cerebralis* discharges polar tubules to a greater extent when exposed to mucus from rainbow trout than mucus from non-susceptible fish[2]. Perhaps after 1 minute, this level of host-specificity and "host-rejection" is indiscernible, but after 15 minutes, when many more parasites have had opportunities to infect the fish, it plays a much greater role. Alternatively, 2.), the population of viable mucus pores in zebrafish and goldfish became saturated with *M. cerebralis*, prior to those in rainbow trout. Likewise this effect would be indiscernible in the 1-minute individual exposures. 3.) Lastly, perhaps the mean respiration rate, which modulates the quantity of actinspores flowing past the gills, was greater for rainbow trout than goldfish or zebrafish, and differences did not emerge in the short, 1-minute exposures.

More *M. cerebralis* DNA was detected in rainbow trout exposed to *M. cerebralis* alongside goldfish and zebrafish than those exposed alone at the same dose. This difference may be attributed to the factors described above. The rainbow trout in the two exposures are the same species and are equally attractive to *M. cerebralis*, however the total pool of actinospores in the mixed-species exposure is higher (180,000 vs 60,000). If the three fish species were infected at the same intensity, we would expect the rainbow trout in the mixed exposure and the 15-minute individual exposure to receive the same infectious dose of 20,000 actinospores per 50 mL and per fish. However, if rainbow trout are infected at a greater intensity than goldfish or zebrafish, their fraction of the whole pool is greater. Alternatively, the larger volume of 150 mL vs. 50 mL or the presence of 3× more fish in the mixed-species container, may have increased the respiration rate of the rainbow trout relative to those in the individual exposure.

The results of these experiments reaffirm that *M. cerebralis* infection occurs extremely quickly, in < 3 minutes[8], and supports recent observations that *M.cerebralis* preferentially infects rainbow trout over dead-end hosts[7]. It may be interesting, in future experiments with "decoy" fish, to expose fish at a reduced parasite dose, similar to what might be found in the wild, or expose rainbow trout alone and in mixed-species exposures at the same volume and actinospore/mL concentration (not actinospore/fish) and compare infection. In future experiments seeking to visualize actinospore attachment and sporoplasm migration, it is advisable to quickly euthanize

and fix whole fish[8] or euthanize fish via decapitation and fix heads as to not overshoot the timeframe of invasion and retain recognizable actinospores on the gills.

REFERENCES

1. Yokoyama, H., Ogawa, K. & Wakabayashi, H. Some biological characteristics of actinosporeans from the oligochaete *Branchiura sowerbyi*. *Diseases of Aquatic Organisms* **17**, 223–228 (1993).
2. Yokoyama, H., Ogawa, K. & Wakabayashi, H. Chemoresponse of actinosporean spores of *Myxobolus cultus* to skin mucus of goldfish *Carassius auratus*. *Diseases of Aquatic Organisms* **21**, 7–11 (1995).
3. Yokoyama, H., Kim, J.-H. & Urawa, S. Differences in host selection of actinospores of two myxosporeans, *Myxobolus arcticus* and *Thelohanellus hovorkai*. *Journal of Parasitology* **92**, 725–729 (2006).
4. McGeorge, J., Sommerville, C. & Wootten, R. Studies of actinosporean myxozoan stages parasitic in oligochaetes from the sediments of a hatchery where Atlantic salmon harbour *Sphaerospora truttae* infection. *Diseases of Aquatic Organisms* **30**, 107–119 (1997).
5. Özer, A. & Wootten, R. Biological characteristics of some actinosporeans. *Journal of Natural History* **36**, 2199–2209 (2002).
6. Kallert, D. M., Eszterbauer, E., Grabner, D. & El-Matbouli, M. In vivo exposure of susceptible and non-susceptible fish species to *Myxobolus cerebralis* actinospores reveals non-specific invasion behaviour. *Dis. Aquat. Organ.* **84**, 123–130 (2009).
7. Eszterbauer, E., Sipos, D., Szakály, Á. & Herczeg, D. Distinctive site preference of the fish parasite (Cnidaria, Myxozoa) during host invasion. *Acta Vet. Hung.* **67**, 212–223 (2019).
8. El-Matbouli, M., Hoffmann, R. W., Schoel, H., McDowell, T. S. & Hedrick, R. P. Whirling disease: host specificity and interaction between the actinosporean stage of *Myxobolus cerebralis* and rainbow trout *Oncorhynchus mykiss*. *Diseases of Aquatic Organisms* **35**, 1–12 (1999).
9. Bjork, S. J. & Bartholomew, J. L. Invasion of *Ceratomyxa shasta* (Myxozoa) and comparison of migration to the intestine between susceptible and resistant fish hosts. *International Journal for Parasitology* **40**, 1087–1095 (2010).
10. Kelley, G. O., Zagmutt-Vergara, F. J., Leutenegger, C. M., Myklebust, K. A., Adkison, M. A., McDowell, T. S., Marty, G. D., Kahler, A. L., Bush, A. L., Gardner, I. A. & Hedrick, R. P. Evaluation of Five Diagnostic Methods for the Detection and Quantification of *Myxobolus cerebralis*. *Journal of Veterinary Diagnostic Investigation* **16**, 202–211 (2004).

APPENDIX E

IN VIVO ASSAY FOR *MYXOBOLUS CEREBRALIS* AND *CERATONOVA SHASTA* CO-
INFECTION

INTRODUCTION

The goal of this experiment was to develop a methodology for detecting *Myxobolus cerebralis*
and *Ceratonova shasta* DNA in the gills of rainbow trout after a single mixed-parasite exposure.
The mixed-fish-species exposures (Appendix D) suggested that saturation of infectable tissue
does not occur in rainbow trout, even at very high parasite densities (20,000 actinospores per fish
per 50 mL). If we expose fish to both parasites at the same time and competition for host tissue is
negligible, we can assume that the presence of one parasite will not interfere with the other's
ability to infect fish. Co-infection assays with more than one parasite will allow us to test
multiple treatments on different parasites simultaneously while maintaining the same
experimental conditions.

METHODS

To 5, 250-mL containers, we added 10,000 *M. cerebralis* and 1,000 *C. shasta* actinospores and
sufficient cold well water to make the volume in each container 50 mL. We added pipette tip
bubblers[1] to each container and allowed 5 minutes for the actinospores to homogenize.
Individually, juvenile rainbow trout were exposed in the containers for 30 minutes, netted, rinsed
with cold tap water, and killed by overdose wit MS-222. Gills were removed with scissors and
forceps and frozen in 2-mL tubes.

We extracted total DNA from each gill sample using a Qiagen DNeasy Blood and Tissue kit
following the manufacturer's recommendations. We eluted DNA from the column with two
washes of 100 µL buffer AE. Total DNA concentration was measured with a Nanodrop
spectrometer (Thermo Scientific), and total DNA concentration normalized by dilution with
molecular grade water to 150 ng/µL. *M. cerebralis* and *C. shasta* DNA concentration was

measured by the standard qPCR following the protocol of Kelley et al. (2004)[2] and Hallett and Bartholomew (2006)[3] respectively.

RESULTS

The Cq for *M. cerebralis* and *C. shasta* DNA is displayed in Figure A18. The mean Cq for *M. cerebralis* DNA was 28.5 and the mean Cq for C. shasta was 33.8. These means varied significantly (p=0.0045, Two Sample t-test), however the two treatments varied also in parasite dose, parasite DNA content, and detection efficiency thus a comparison may not be warranted. The Cq data is displayed also as a scatter plot in figure A19. The two variables had a positive, linear relationship (R = 0.84, $p = 0.072$.)
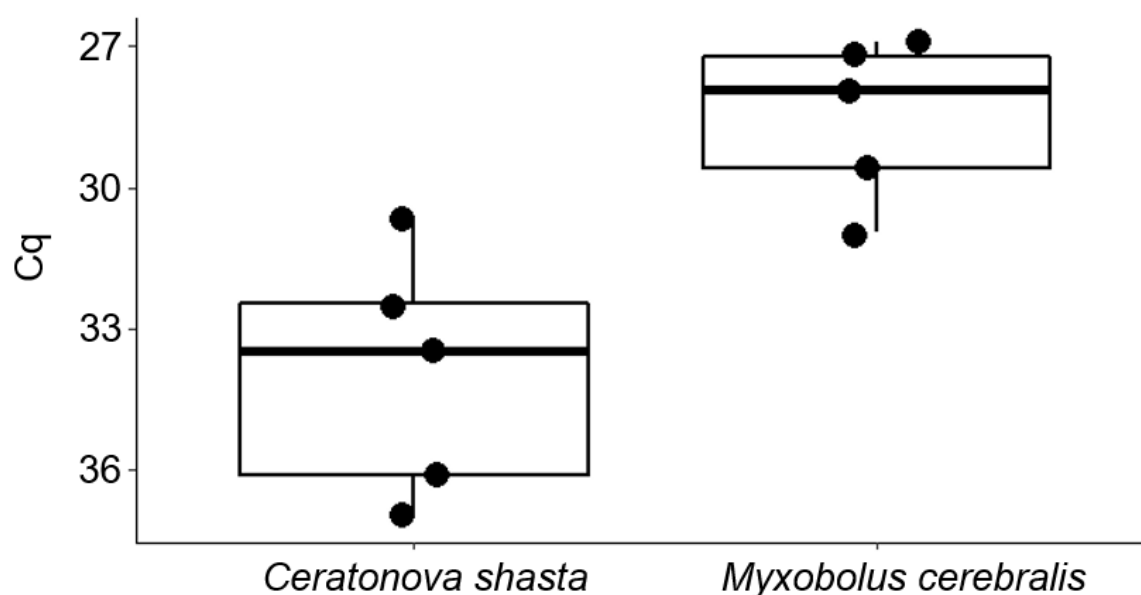

Figure A18. Box and whisker plot of quantification cycle (Cq) of *Myxobolus cerebralis* and *Ceratonova shasta* DNA detected in juvenile rainbow trout exposed individually to 10,000 *M. cerebralis* and 1,000 *C. shasta* actinospores per fish.
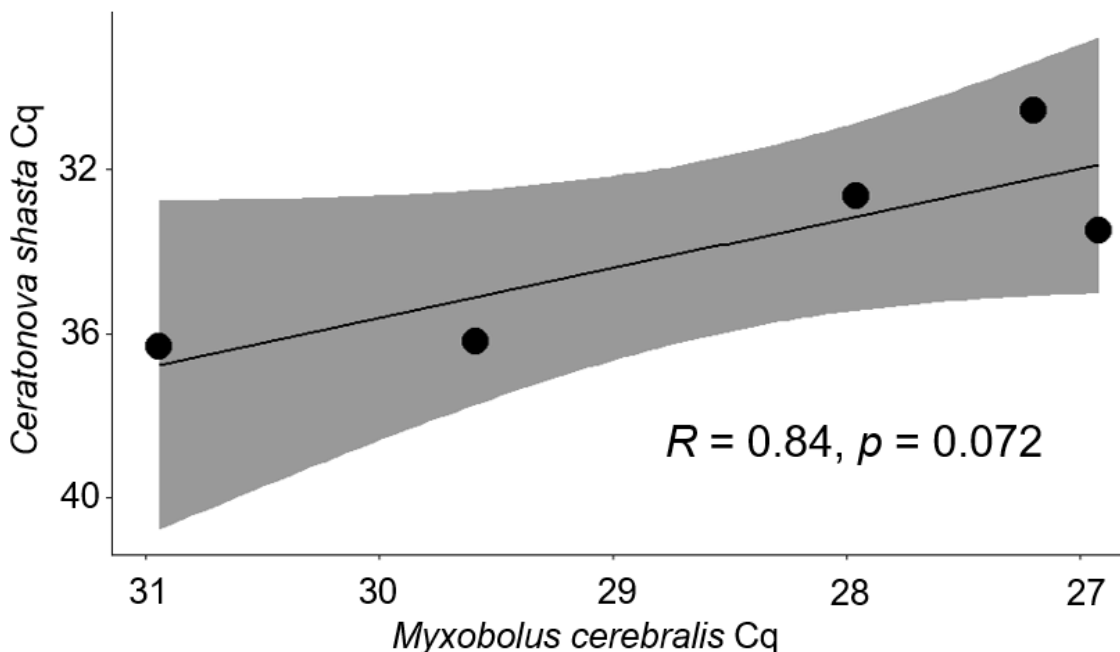
Figure A19. Scatter plot of *Myxobolus cerebralis* and *Ceratonova shasta* DNA detected in juvenile rainbow trout exposed individually to 10,000 *M. cerebralis* and 1,000 *C. shasta* actinospores per fish.

DISCUSSION

The goal of this experiment was to validate methods that would allow us to test multiple treatments on different parasites simultaneously while maintaining the same experimental conditions. In experiments with treatment aimed to inhibit infection, it will be beneficially to have high DNA concentration in untreated, positive controls. Cq values ranging from 24 to 30, will provide maximal statistical power to detect inhibition. Understanding this, we can employ *M. cerebralis* exposures of 10,000 actinospores per 50 mL per fish for 30 minutes exposures, however experiments with *C. shasta* will require higher parasite density.

An interesting, unexpected result of this experiment is that DNA concentration of *M. cerebralis* and *C. shasta* appears positively correlated (Fig. A19).This may suggest that fish which are particularly susceptible to one myxozoan parasite, are highly susceptible to others. Both *M. cerebralis* and *C. shasta* can infect fish via the gills[14]. *M. cerebralis* actinospores attach to and

invade fish via mucus pores[5] and their nematocysts can be triggered to discharge by inosine, a compound found in fish mucus[6]. Less is known about the infection dynamics of *C. shasta*, however, the positive correlation we observed, suggests that *C. shasta*'s mechanism for sensing and invasion may be similar to that of *M. cerebralis*.

Past experiments examining co-infections with myxozoan parasites have shown antagonistic relationships between the parasites, with host outcome worse in co-infected groups than single-infected groups[7,8]. This effect is thought to be mediated by host immunosuppression by one or both parasites. Past myxozoan co-infection experiments quantified infection at the point of pathology and mortality, so it remains unknown whether an antagonistic or synergistic effect could be observable in the very short time-frame (30 minutes) of our experiment. An antagonistic relationship would explain the positive correlation in *C. shasta* and *M. cerebralis* DNA that we observed (Fig A19).

Features that may make fish of the same strain more or less susceptible to infection may include enrichments in mucus production, inosine content in mucus, mucosal pore density in gills, or depletions in host innate immune activity. Alternatively, the relative enrichment of myxozoan DNA concentrations observed in some fish may simply be a product of individual behavior of increased movement and respiration. Future experiments exploring this phenomenon should utilize more replicate fish and quantitatively track movement and respiration of individuals.

REFERENCES

1. Bjork, S. J. & Bartholomew, J. L. Invasion of *Ceratomyxa shasta* (Myxozoa) and comparison of migration to the intestine between susceptible and resistant fish hosts. *Int. J. Parasitol.* **40**, 1087–1095 (2010).
2. Kelley, G. O., Zagmutt-Vergara, F. J., Leutenegger, C. M., Myklebust, K. A., Adkison, M. A., McDowell, T. S., Marty, G. D., Kahler, A. L., Bush, A. L., Gardner, I. A. & Hedrick, R. P. Evaluation of Five Diagnostic Methods for the Detection and Quantification of *Myxobolus cerebralis*. *Journal of Veterinary Diagnostic Investigation* **16**, 202–211 (2004).

3. Hallett, S. L. & Bartholomew, J. L. Application of a real-time PCR assay to detect and quantify the myxozoan parasite *Ceratomyxa shasta* in river water samples. *Dis. Aquat. Organ.* **71**, 109–118 (2006).
4. Eszterbauer, E., Sipos, D., Szakály, Á. & Herczeg, D. Distinctive site preference of the fish parasite *Myxobolus cerebralis* (Cnidaria, Myxozoa) during host invasion. *Acta Veterinaria Hungarica* vol. 67 212–223 (2019).
5. el-Matbouli, M., Hoffmann, R. W., Schoel, H., McDowell, T. S. & Hedrick, R. P. Whirling disease: host specificity and interaction between the actinosporean stage of *Myxobolus cerebralis* and rainbow trout *Oncorhynchus mykiss*. *Dis. Aquat. Organ.* **35**, 1–12 (1999).
6. Kallert, D. M., Bauer, W., Haas, W. & El-Matbouli, M. No shot in the dark: myxozoans chemically detect fresh fish. Int. J. Parasitol. 41, 271–276 (2011)
7. Kotob, M. H., Gorgoglione, B., Kumar, G., Abdelzaher, M., Saleh, M., & El-Matbouli, M. *Tetracapsuloides bryosalmonae* and *Myxobolus cerebralis* co-infections on pathology in rainbow trout. Parasit. Vectors 10, 442 (2017).
8. Densmore, C. L., Ottinger, C. A., Blazer, V. S., Iwanowicz, L. R. & Smith, D. R. Immunomodulation and Disease Resistance in Post yearling Rainbow Trout Infected with *Myxobolus cerebralis*, the Causative Agent of Whirling Disease. Journal of Aquatic Animal Health vol. 16 73–82 (2004).

APPENDIX F

METHOD FOR ISOLATING MYXOZOAN SPORES FOR SCANNING ELECTRON MICROSCOPY

Preparation of clean, Myxobolus cerebralis actinospores with fired nematocysts

From infected worms in clean sand (see Chapter 2: Source of *M. cerebralis* Actinospores), we filtered water from a 72 hour exposure to 1/10th its original volume on a 20 μm filter. The residue was moved to a 50 mL tube and allowed to settle for ~10 minutes at 4°C . We removed 6 × 1.7-mL tubes of clear supernatant and centrifuged all at max speed (18,213 × G) for 3 minutes. The supernatant was discarded, and the pellets were combined and resuspended in 1 mL dechlorinated tap water. This was allowed to settle for ~10 minutes at 4°C. Aliquots of 250 μL supernatant were moved to 0.5-mL tubes nested in empty 2-mL tubes and centrifuged at max speed (18,213 × G) for 5 minutes. The supernatant was removed, and the pellets were combined. We added 4 μL 0.1M potassium chloride to induce nematocyst discharge, and then 100 μL EM fixative consisting of 2.5% glutaraldehyde, 1% paraformaldehyde, and 0.1 M cacodylate buffer. Fixed spores were visualized at 200× magnification with a compound microscope in a ventilation hood, to ascertain spore concentration before being submitted for scanning electron microscopy processing at OSU's Electron Microscopy Center.

Preparation of cleaved, Ceratonova shasta myxospores

C. shasta myxospores were obtained from laboratory-infected rainbow trout and purified by centrifugation at 113 × G for 1 minute. The supernatant was discarded. The pellet was resuspended by flicking and 10 μL was added to two 0.5-mL tubes. We added 90 μL dechlorinated tap water to each tube and centrifuged again at 113 × G for 1 minute to pellet. The supernatant was discarded. We added 4 μL 0.1 M NaOH to one of the tubes to cause polar capsules to split open, and then 100 μL EM fixative to each. Fixed spores were visualized at 200× magnification with a compound microscope in a ventilation hood, to ascertain spore concentration before being submitted for scanning electron microscopy processing at OSU's Electron Microscopy Center.
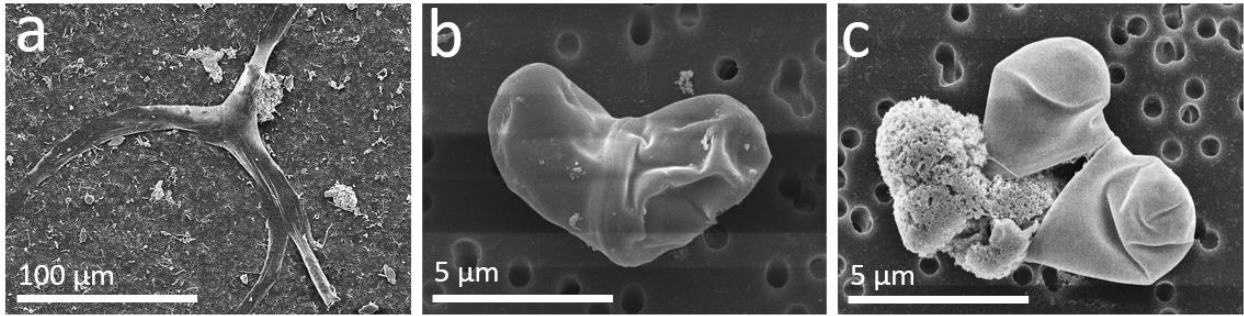
Figure A20. Scanning electron microscopy of myxozoan spores. a: *Myxobolus cerebralis* actinospore. Valve cells are flattened against the slide while the polar end containing nematocysts and sporoplasm remains elevated. For discharged tubules, see Fig. 1.8. b: *Ceratonova shasta* myxospore. c: *C. shasta* myxospore treated with NaOH. The two valve cells have cleaved, and the spore contents are extruded.
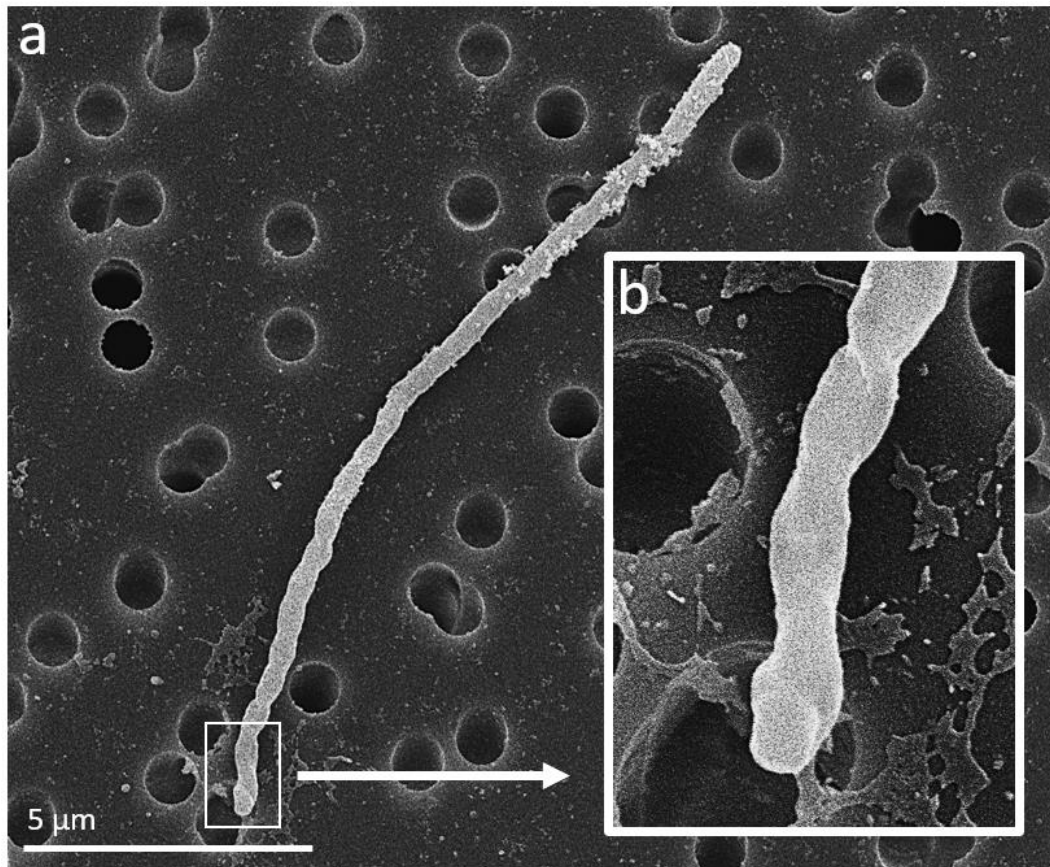

Figure A21. a: Polar tubule released from cleaved *Ceratonova shasta* myxospore. b: Inset of tubule tip. Tubule appears helical with a sealed tip.